INVESTIGATIONS IN BETA-RAY DOSIMETRY USING ^{32}P AND STUDIES ON THE STOPPING POWER OF LIQUID WATER.

Thesis
submitted by

M. McInally
B.Sc. (Edinburgh)

for the Degree of
Doctor of Philosophy

University of Edinburgh
May, 1955.

CONTENTS.

PREFACE.

The investigations described in this thesis were carried out under the supervision of Professor N. Feather and Mr. J. Dainty.

The research described in the first part was carried out at the Medical Research Council Radiobiological Unit at Harwell. Dr. G.J. Neary proposed the problem and suggested the general plan of the investigations described in Chapter V. He was also helpful in discussing and criticising the analysis given in Chapter IV. The main findings of this investigation have been reported in the British Journal of Radiology (26, (1953), 539). The author wishes to thank Dr. Neary for his helpful advice and stimulating criticism. He also wishes to thank Dr. Loutit of the above unit for granting him facilities to prosecute this research and the technical staff for their assistance.

The second part of this work though begun at Harwell has for the most part been carried out at the Department of Natural Philosophy of Edinburgh University. The progress of this work has been helped by discussions with Mr. J. Dainty, Dr. G.J. Neary, Dr.B.F. Bayman, Dr. N. Miller, Dr. L.H. Gray, Dr. J.W. Boag and Professor N. Feather. Mr. Headridge and his staff

have been very helpful in finding solutions to many difficult technical problems.

P A R T O N E.

INVESTIGATIONS IN BETA-RAY DOSIMETRY USING ^{32}P.

CHAPTER I.

INTRODUCTION.

The investigation of the effects produced by external irradiation with β-rays is of importance in radiobiology and especially in work on radiation protection. To carry out surface irradiation of animals for this purpose, a convenient method is to place the animals in an enclosure having β-active walls. A suitable material for constructing such an enclosure is phosphorus-Bakelite, a homogeneous mixture of roughly equal parts by weight of red phosphorus and Bakelite. Its properties are described by Bizzell et al. (1). On activation of this material in a thermal neutron flux the isotope ^{32}P is formed, which emits β-radiation of mean energy 0.69 MeV, and high specific activities are readily obtained. In an enclosure of radioactive phosphorus-Bakelite, called for convenience a ^{32}P box, the thickness of the walls usually exceeds the range of ^{32}P β-radiation. The construction of various ^{32}P boxes is described by Raper et al. (2) and details of the ^{32}P box used in the present experiments are given by Neary and Young (3).

The theoretical and experimental investigation described here is concerned with the surface dosage received by various masses of soft tissue of simple

shape when placed in a ^{32}P box. In particular, the effects due to backscattered radiation are examined in detail.

In the following chapters the general problem is first discussed and a simple method is described for deriving surface dosage rates (Chapter II). The method is only approximate and limited in its applications and to correct it and extend it to more general conditions, data on the backscattered radiation produced by ^{32}P β-radiation are required. The experiments carried out to provide this information are described in Chapter III. A detailed analysis of the problem of surface dosage follows in Chapter IV and equations are derived for finding the surface dosage in many systems of interest. Finally, the experiments by which the theory was tested are described in Chapter V.

CHAPTER II.

ELEMENTARY METHOD FOR DERIVING SURFACE DOSAGE.

When tissue is irradiated with β-rays, the dose rate is defined as the energy absorbed per second per unit mass of the tissue at the point under consideration. The dose rate is usually derived from measurements of the ionisation rate in a small air cavity placed at the point considered. Thus for such a cavity if J is the ionisation rate, expressed as the number of ion pairs produced per second per cc of air at N.T.P., W the average energy expended by a β-particle in producing one ion pair in air, ρ the ratio of the linear stopping power of tissue to that of air at N.T.P. and d the tissue density, then the dose rate, E, the energy absorbed per second per gm. of tissue, is according to the Bragg-Gray relation (Gray (4), (5) and (6))

$$E = \frac{JW}{d}\rho \qquad (1).$$

This equation applies equally well to points on the surface as well as in the interior of a tissue mass.

The dose rate E may be expressed in ergs/gm./sec. or since this unit is small in rad/sec., one rad representing an energy dissipation of 100 ergs/gm. For convenience in clinical work β-ray dose rates

are often expressed in rep/sec., one rep representing a dose of 93.1 ergs/gm. If D is the dose rate in rep/sec. and J is expressed in e.s.u. per sec. per cc of the cavity and if it is assumed that W = 32.5 electron volts and that the electronic density and electronic stopping power of soft tissue are the same as those of water then

$$D = \rho_e J \qquad (2)$$

where ρ_e is the electronic stopping power of water relative to air and is about 1.01 for the β-rays emitted by radium, according to Neary (7).

In the theory and experiments to follow it is convenient to discuss the problems for the most part in terms of J, the ionisation rate. The ionisation rate bears a fixed ratio to the dose rate and where necessary the latter can be found from equation (1) or (2).

Elementary Theory.

When a mass of soft tissue is placed in a ^{32}P box, i.e. an enclosure whose walls are of radioactive phosphorus-Bakelite, it is often difficult to measure the surface ionisation rate and hence dosage rate at a given point on the mass. On the other hand it is comparatively easy to measure $J_{4\pi}$, the ionisation rate in the empty ^{32}P box when air absorption has

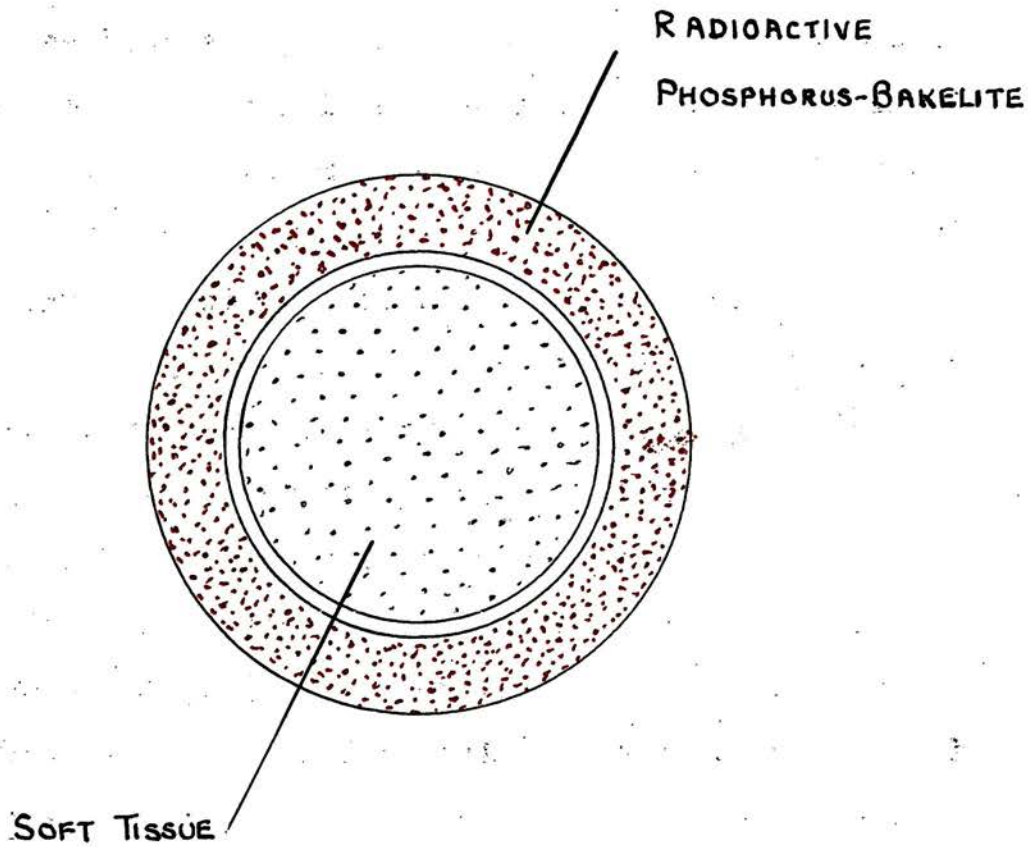

Fig. 1.

been corrected for. It is therefore of interest to find out under what conditions $J_{2\pi}$, the surface ionisation rate at a point on the tissue mass when air absorption has been corrected for, can be derived from $J_{4\pi}$.

Consider a system (Fig. 1) in which a large sphere of soft tissue is placed centrally in a spherical ^{32}P box, a very thin air film separating the two. Initially the inner sphere is supposed replaced by an exactly similar one of phosphorus-Bakelite. If the latter were given the same specific β-activity as the enclosure, then since absorption in the air film is negligible, the ionisation rate on the surface of the sphere would be equal to $J_{4\pi}$, the ionisation rate (corrected for air absorption) in the empty ^{32}P box. Further this surface ionisation rate would be due equally to the inner sphere and the enclosure. It follows that when the inner sphere is not radioactive the surface ionisation rate $J_{2\pi}$ will be equal to $\frac{1}{2}J_{4\pi}$. If the backscattered radiation produced in soft tissue by β-rays is the same as that for phosphorus-Bakelite then when the inner sphere is of soft tissue the surface ionisation rate will be the same. So for the system considered (Fig. 1)

$$J_{2\pi} = 0.500\ J_{4\pi} \qquad (3).$$

This equation is discussed briefly by Raper et

al. (2). It is argued that a point on the surface of any large object in a ^{32}P box receives radiation over a solid angle of 2π and hence the surface ionisation rate is $\frac{1}{2}J_{4\pi}$. It is stated that the equation is only approximate because of β-ray scattering, but no further analysis is made.

Returning to the argument above it is clear, in the first place, that equation (3) will require modification if the backscattered radiations from soft tissue and phosphorus-Bakelite differ significantly.

Secondly, if the inner sphere of soft tissue is made appreciably smaller than the ^{32}P box while still being large compared with the range of ^{32}P β-radiation in soft tissue, it is doubtful if equation (3) will still apply. Since the tissue sphere no longer acts as a complete shield, preventing β-rays from one part of the box reaching another part by a direct path, the radiation received at a point on the tissue sphere will be supplemented by radiation emitted by one part of the wall and backscattered by another.

Thirdly, if the radius of the inner sphere is made comparable with the range of ^{32}P β-radiation in soft tissue, then the inner sphere will be partially transparent to β-radiation and the surface

ionisation rate will be increased.

To treat the first two effects in detail and find the modifications required in equation (3) requires data on the properties of the backscattered radiation produced by ^{32}P β-rays. The experiments to fulfil this need are described next and following this the theoretical discussion is resumed.

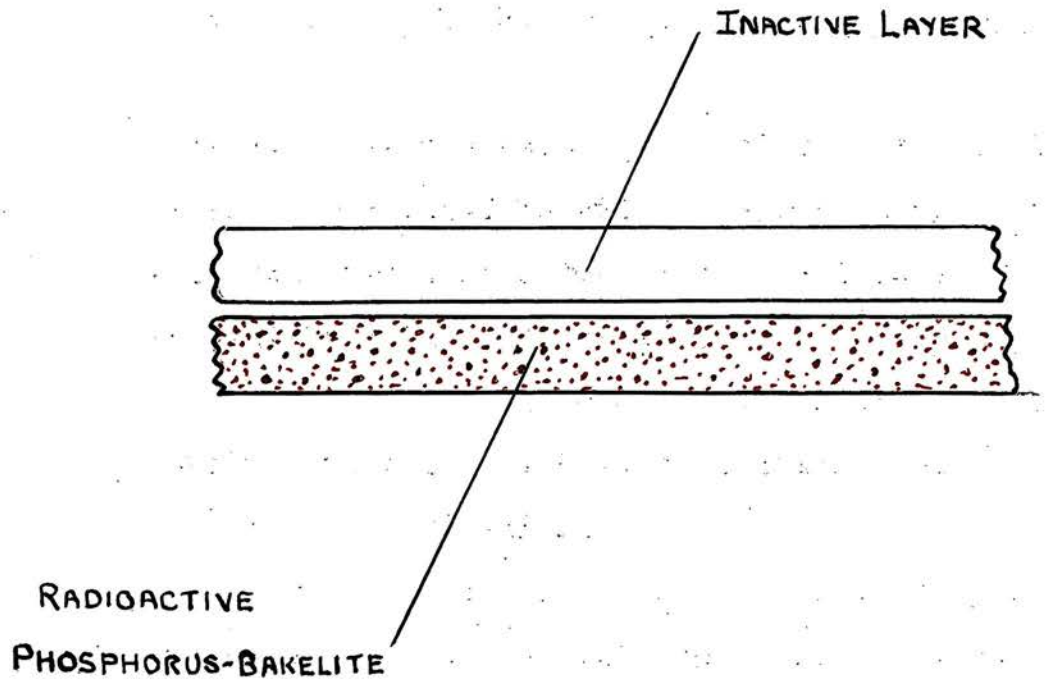

Fig. 2.

CHAPTER III.

EXPERIMENTS ON BACKSCATTERED BETA-RADIATION.

If a thin air film separates a thick β-active plaque of phosphorus-Bakelite of large area from a thick layer of inactive material of large area (Fig. 2), the ionisation rate J_t at the centre of the film may be split into two components:

(1) the ionisation rate J_f due to forward radiation, i.e. to β-rays making their first traversal of the air film and

(2) the ionisation rate due to β-rays backscattered one or more times, i.e. making their second or higher order traversal of the air film. This component is proportional to J_f and will be denoted by RJ_f where R is called the total backscatter coefficient.

Hence $$J_t = J_f(1 + R) \qquad (4).$$

Sometimes it is convenient to analyse the ionisation rate caused by backscattered radiation into a series of components. The ionisation rate of the n^{th} component is due to β-rays making their $(n + 1)^{th}$ traversal of the air film. When the inactive layer (Fig. 2) is of phosphorus-Bakelite, the total backscatter coefficient is denoted by R_1. If the ionisation rate due to the first component of the backscattered radiation is $r_1 J_f$ where r_1 is called the

single backscatter coefficient, it seems plausible to take the ionisation rate due to the n^{th} component as $r_1{}^n J_f$. Summing all the components we obtain

$$R_1 = \frac{r_1}{1 - r_1} \qquad (5).$$

If the inactive layer is not of phosphorus-Bakelite but of another material of total backscatter coefficient R_2 and has a single backscatter coefficient r_2, then since the β-rays are backscattered alternately by the phosphorus-Bakelite and by the inactive material, it follows by summing the series of components that

$$R_2 = \frac{1 + r_2}{1 - r_1 r_2} - 1 \qquad (6).$$

Experiments were carried out to determine (1) the relative values of (1 + R) for various materials, (2) the absorption coefficient of the backscattered radiation, (3) the values of R and r for various materials. The results are needed to develop the theory of surface ionisation rates in a ^{32}P box but the accuracy required is only moderate.

Relative values of (1 + R).

In the first experiments a small coin-shaped ionisation chamber was inserted between a β-plaque of phosphorus-Bakelite (5.2 x 7.7 cm.) and a thick plaque (12.5 x 10.0 cm.) of the material under test,

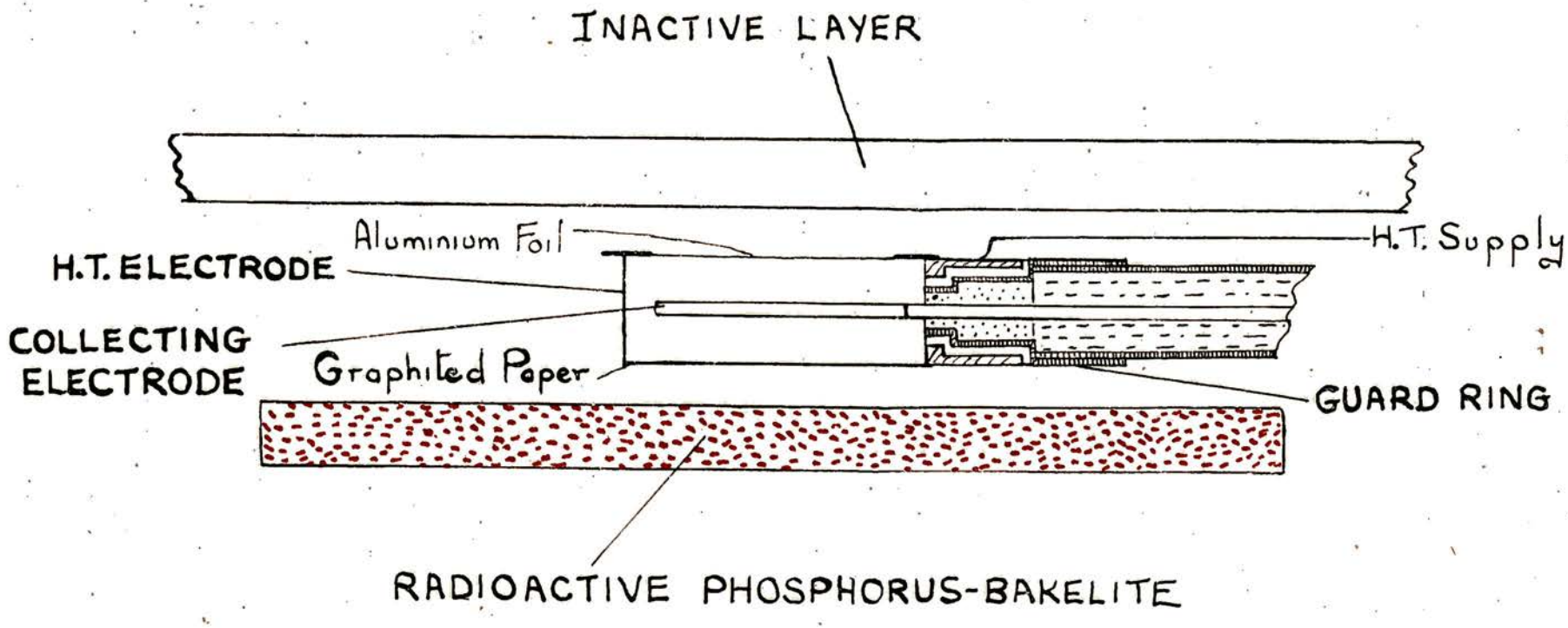

Fig. 3. Apparatus used to investigate backscatter from various materials.

called the backscatterer (Fig. 3). The ionisation chamber (height 0.90 and diameter 2.3 cm.) was designed to be as transparent as possible to the β-radiation. It was made from graphited paper (8.8 mg./cm.^{2}) except for the side facing the backscatterer, which was made from a disc of very thin aluminium foil (0.25 mg./cm.^{2}) of diameter 1.9 cm., surrounded by a rim of graphited paper (8.8 mg./cm.^{2}) of width 0.4 cm. The central collecting electrode was a thin cylinder of aluminium foil of radius 0.5 mm. and thickness 5 mg./cm.^{2}. This electrode was fitted to a standard chamber stem (radius 0.45 cm.), equipped with a guard ring and a lead carrying the H.T. supply to the outer electrode.

The ionisation currents were measured with a Townsend balance system using a Lindemann electrometer as the null detector. The high ionisation rates at the surface of the plaque - of the order of 500 e.s.u./cc./hr. - allowed accurate measurements to be made. Frequent tests were made by plotting chamber current : voltage curves to ensure that complete ion collection was obtained and that no ion multiplication occurred. Because of the fragile nature of the chamber, frequent checks were necessary to ensure that no distortion had occurred and this was done by measuring the chamber current when the chamber was returned to a fixed position between a

β-plaque and a backscatterer at a fixed distance apart.

For the measurements of the relative values of (1 + R) a sheet of acrylic resin (Perspex) was taken as the standard. The ionisation rate in the chamber was read for a variety of values of h_1, the distance from the chamber mid-point to the plaque and h_2, the distance from the mid-point to the backscatterer, both for the material under test and for the standard. It was found that the ratio of the ionisation rates varied linearly with h_1 and h_2 for values of h_2 ranging from 0.60 cm. to 1.50 cm., and for values of h_1 from 0.60 to 1.00 cm., and therefore an extrapolation process was permissible to find the ratio of total ionisation rates at $h_2 = 0$, $h_1 = 0$. It was found that on extrapolating the experimental ratios for a fixed value of h_1 and variable h_2 that the values corresponding to $h_2 = 0$ hardly changed as h_1 was varied. The total extrapolation factor for aluminium was 1.035 and for lead 1.10, both measured from the lowest values of h_1 and h_2 used.

The extrapolated value of the ratio of total ionisation rates gives the value that would be obtained in the ideal system of a thin air film separating a plaque and backscatterer of large area, but a small correction is necessary for the backscatter

TABLE 1

RELATIVE VALUES OF (1 + R)

Material	1 + R
Acrylic Resin	1.000
Aluminium	1.137
Copper	1.290
Lead	1.510

TABLE 2

RELATIVE VALUES OF (1 + R)

Material	Relative Total Ionisation Rate at $h_1 = h_2 = 0.85$ cm.	1 + R
Polythene	0.982	0.970
Polystyrene	0.994	0.990
Acrylic Resin	1.000	1.000
Tissue Phantom Material	1.000	1.000
Soft Tissue	1.021	1.033
Phosphorus-Bakelite	1.046	1.067
Aluminium	1.088	1.137
Copper	1.205	1.290
Lead	1.383	1.510

Note: All values in Tables 1 and 2 are uncorrected for chamber backscatter.

contribution from the chamber itself and this is made later (p.23).

The full extrapolation process was carried out for three materials relative to acrylic resin and the uncorrected values of (1 + R) relative to that for acrylic resin are shown in Table 1.

The total ionisation rates were then measured for a variety of materials for a fixed value of h_1 = 0.85 cm. and h_2 = 0.85 cm., and the corrections required to give the relative values of (1 + R) were derived from the known corrections for the three materials of Table 1. The relative ionisation rates and the values of (1 + R), uncorrected for chamber backscatter, are given in Table 2.

The acrylic resin and polythene used were I.C.I. commercial products, and the polystyrene was made by B.D.X. The tissue phantom material was Mix D, as described by Jones and Raine (8). The material chosen to simulate soft tissue was an agar gel, containing 1% by weight of agar. The layer of sulphide and oxide on the lead backscatterer was carefully removed.

In a supplementary experiment the phosphorus-Bakelite plaque was covered with an aluminium absorber (428 mg./cm.^{2}) which reduced the ionisation chamber current to 3% of its previous value. The

TABLE 3

EFFECT OF ALUMINIUM ABSORBER.

Material	Relative Values of (1 + R)	
	Bare Plaque	Al Filter
Acrylic Resin	1.000	1.00
Aluminium	1.137	1.12
Copper	1.290	1.32
Lead	1.510	1.65

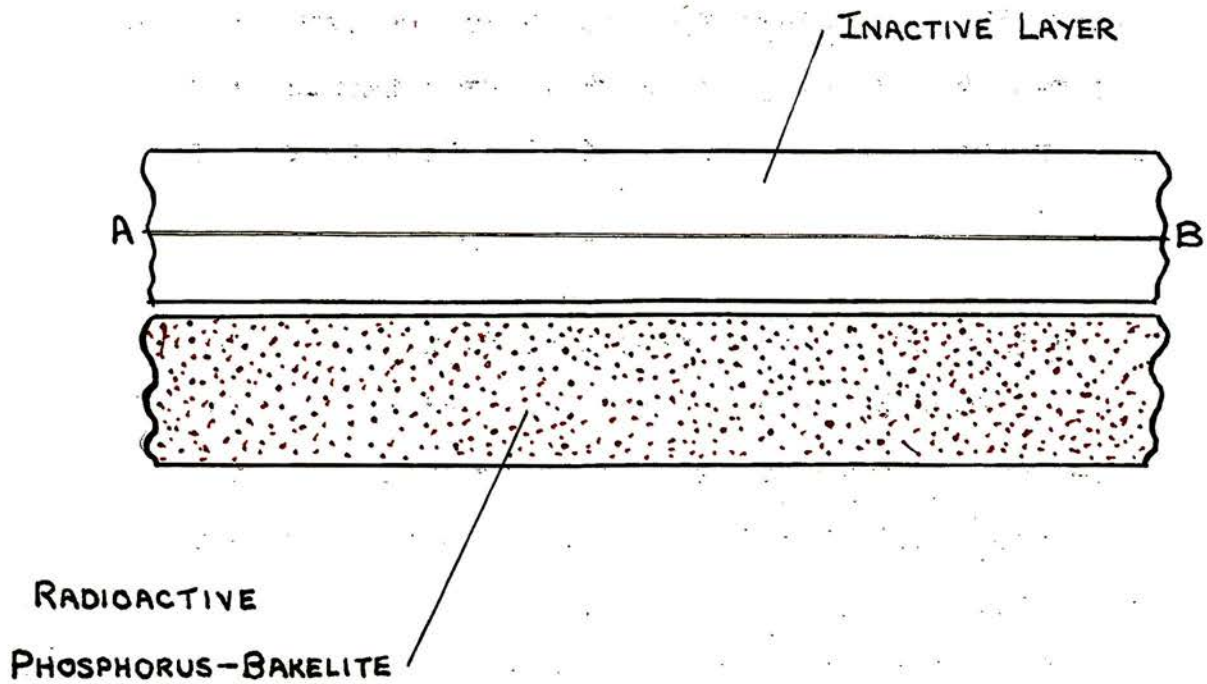

AB is a layer of thickness dm mg./cm.^{2} separated by a layer of thickness m mg./cm.^{2} from the air gap.

Fig. 4.

relative values of (1 + R) were determined by the same method as before for aluminium, copper and lead. The results (Table 3) show that for aluminium and copper the relative values of (1 + R) change very little.

Absorption of Backscattered Radiation.

To derive the absolute values of (1 + R) it is necessary to investigate the absorption of back-scattered radiation in materials composed of light elements.

Consider a system (Fig. 4) consisting of a β-plaque of phosphorus-Bakelite of infinite area separated by a thin air film from a thick layer of backscattering material. It is assumed:-

(1) that the ionisation rate produced by forward radiation in the material decreases exponentially so that at a depth of m mg./cm.^{2} the ionisation rate due to forward radiation may be written as $J_f e^{-\mu m}$ where μ is the absorption coefficient of the forward radiation,

(2) that the ionisation rate produced by the β-radiation backscattered by a thin layer AB of thickness dm mg./cm.^{2} at this depth is $kJ_f e^{-\mu m}$ dm at AB, and

(3) that the ionisation rate produced by the

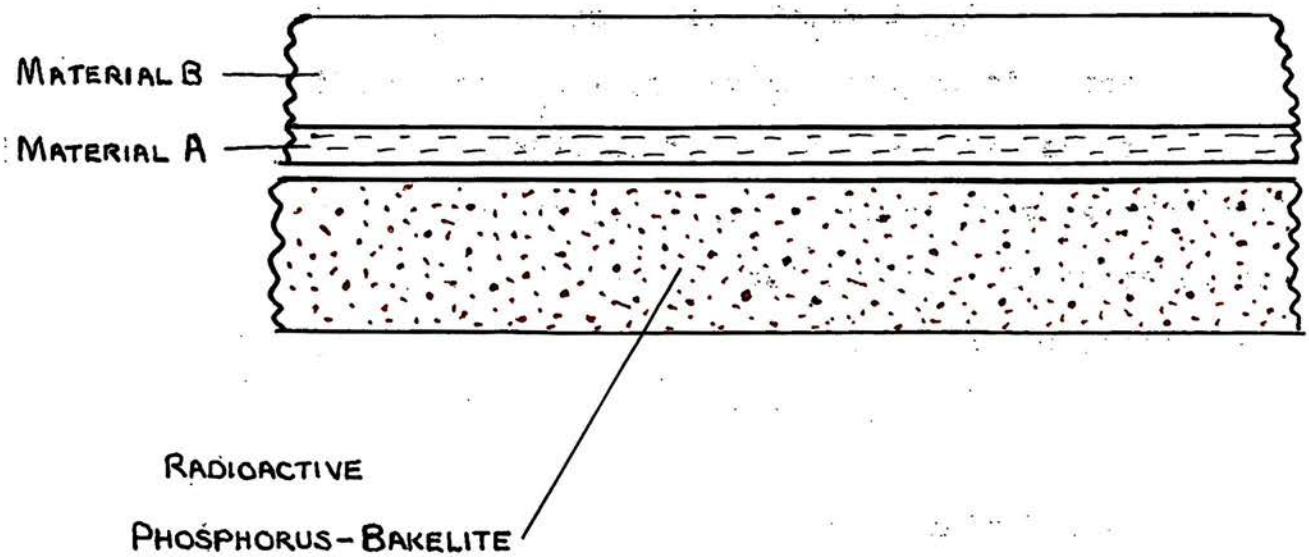

Fig. 5.

β-radiation backscattered from AB falls off exponentially so that its contribution to the total ionisation rate in the air film is

$$dJ_b = kJ_f e^{-\mu m} . e^{-\mu' m} dm \qquad (7)$$

where μ' is called the absorption coefficient for the backscattered β-radiation.

Integrating over the whole thickness of the backscatterer to find the ionisation rate J_b due to the backscatterer, we obtain

$$J_b = \frac{kJ_f}{\mu + \mu'} \qquad (8).$$

But by the definition of R

$$J_b = RJ_f.$$

$$\therefore k = (\mu + \mu')R \qquad (9).$$

If a composite backscatterer (Fig. 5) is now used, consisting of m_1 mgm./cm.^{2} of material A covering a thick layer of another material B, the ionisation rate in the air film may now be found. The contribution due to backscatter from A, denoted by j_1, is

$$J_1 = \int_0^{m_1} R_1 (\mu_1 + \mu_1') J_f e^{-(\mu_1 + \mu_1')m} dm$$

where suffix one is used for the constants appropriate to A and suffix two is used for those of B.

$$\therefore J_1 = R_1 J_f (1 - e^{-(\mu_1 + \mu_1')m_1}) \qquad (10).$$

The contribution made by the thick layer of B is

$$J_2 = \int_{m_1}^{\infty} R_2 (\mu_2 + \mu_2') J_f e^{-(\mu_1 + \mu_1')m_1} e^{-(\mu_2 + \mu_2')m} dm$$

assuming that the backscattered radiation from B has also absorption coefficient μ_1' in material A.

$$\therefore J_2 = R_2 J_f e^{-(\mu_1 + \mu_1')m_1} \qquad (11).$$

Hence the ionisation rate due to the total back-scattered radiation is

$$J_b = J_f \left[R_1 \left(1 - e^{-(\mu_1 + \mu_1')m_1} \right) + R_2 e^{-(\mu_1 + \mu_1')m_1} \right] \qquad (12).$$

The total ionisation rate including forward radiation is

$$J_t = J_f \left[1 + R_1 \left(1 - e^{-(\mu_1 + \mu_1')m_1} \right) + R_2 e^{-(\mu_1 + \mu_1')m_1} \right] \qquad (13).$$

But for a complete backscatterer of material A the total ionisation rate is

$$J_1 = J_f(1 + R_1)$$

and for material B the total ionisation rate is

$$J_2 = J_f(1 + R_2).$$

Substituting these values in equation (13) we find

$$\frac{J_t - J_1}{J_2 - J_1} = e^{-(\mu_1 + \mu_1')m_1} \qquad (14).$$

Thus by measuring J_t for various values of m_1 it is possible to derive the value of $(\mu_1 + \mu_1')$ and since μ_1 can be readily measured the value of μ_1' can be found. While equation (14) is derived for a system of infinite area, a reasonable approximation to the value of $(\mu_1 + \mu_1')$ will be obtained with a system of moderate area if the ionisation rates are determined over the central region of the air film.

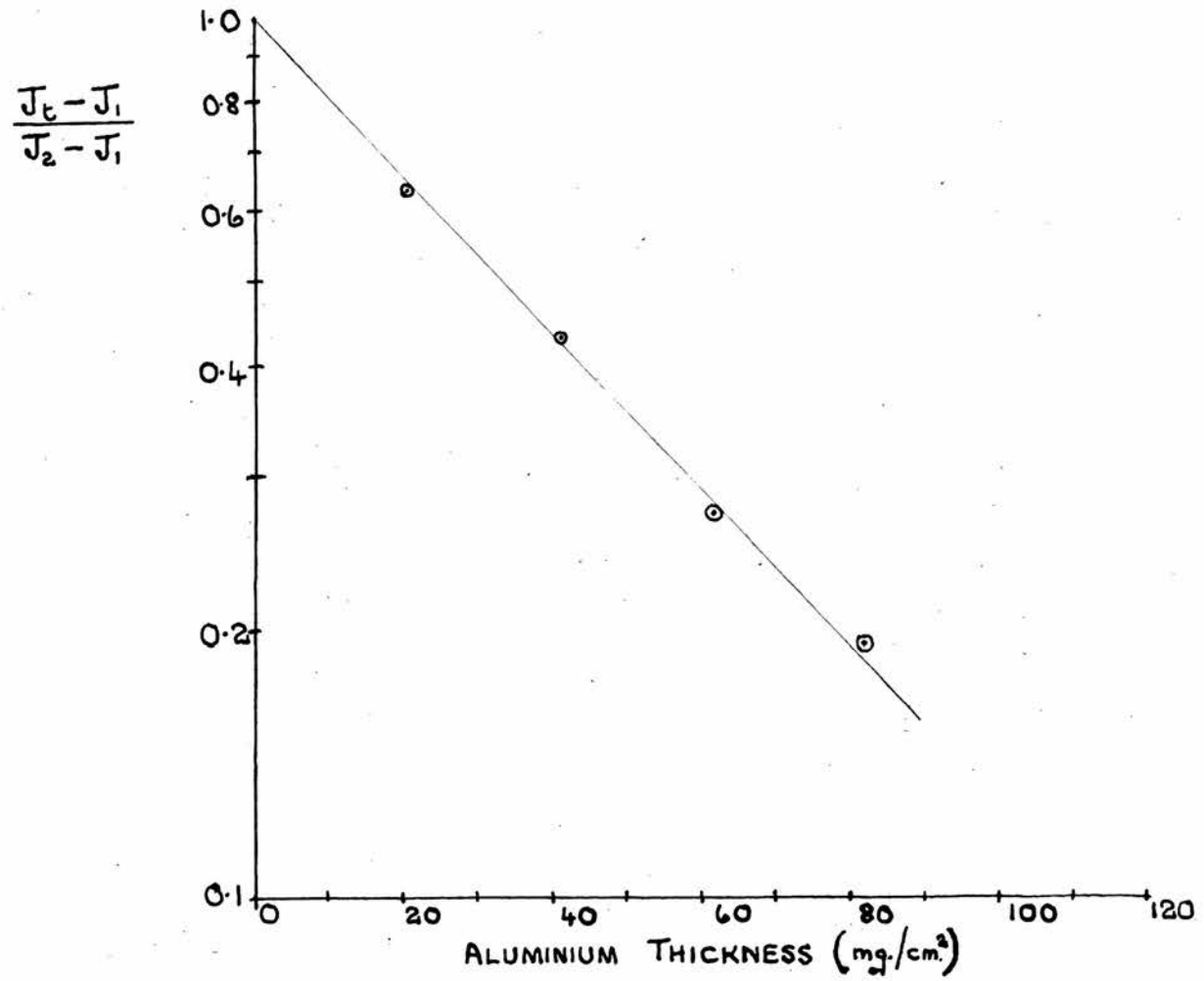

FIG. 6. Curve showing how total ionisation rate decreases as aluminium layers are added to a lead backscatterer.

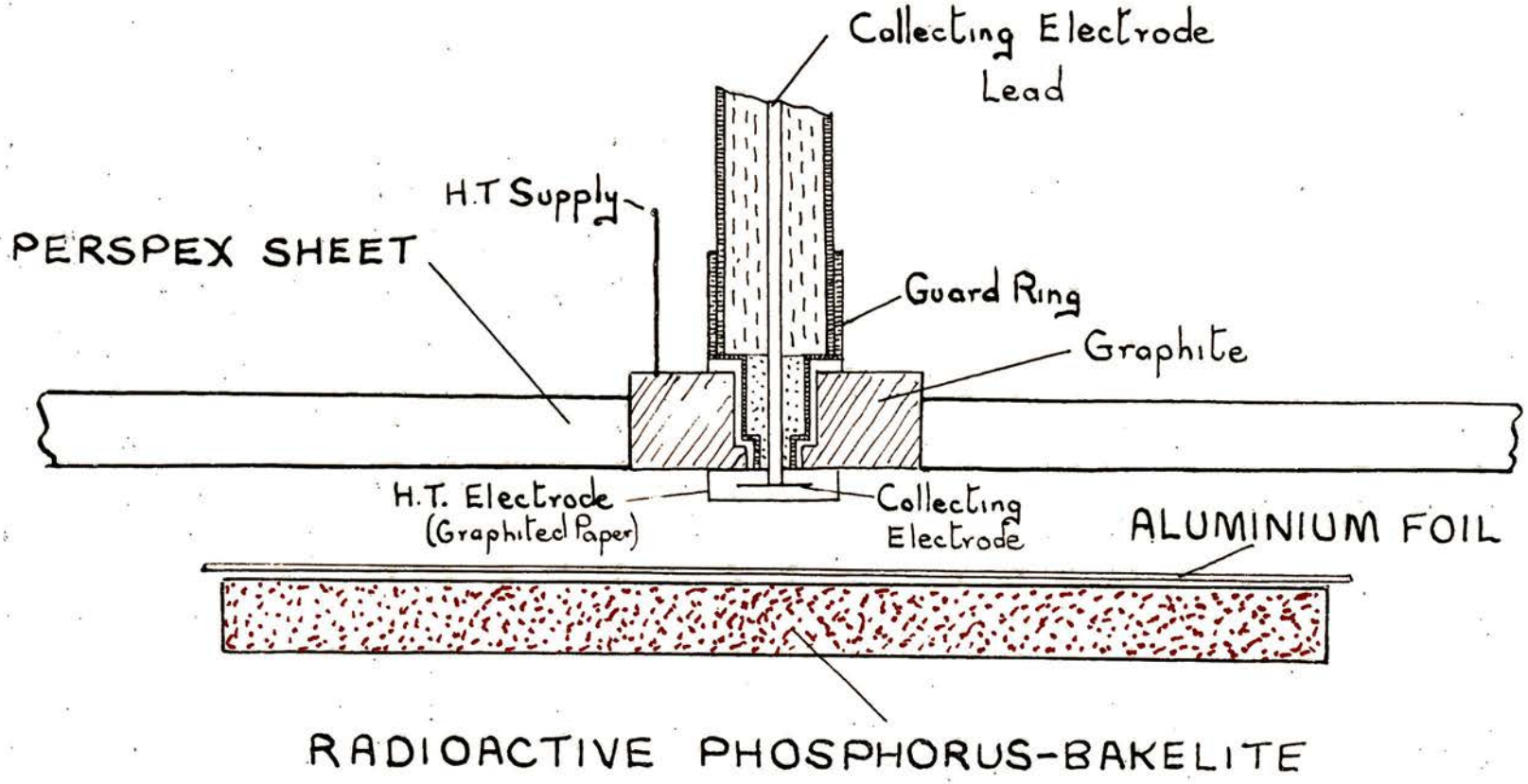

Fig. 7. Apparatus used to measure absorption of ^{32}P β-radiation in aluminium.

Note: β-ray ionisation chamber is the "2π" ionisation chamber fully described on p. 52.

The same apparatus (Fig. 3) was used as in the experiment to determine the relative values of (1 + R), the mid-point of the coin-shaped chamber being 0.65 cm. from the plaque and 0.90 cm. from the composite backscatterer. Lead was used as material B and aluminium as material A in order to obtain a reasonable difference in the total ionisation rates. Measurements were made of the total ionisation rate when foils of aluminium, of 20.5 mg/cm.^{2} thickness, were used to cover the lead. The values of $\frac{J_t - J_1}{J_2 - J_1}$ were calculated, their logarithms plotted against the values of aluminium thickness (Fig. 6), and the value of $(\mu_1 + \mu_1')$ found. A small correction (2%) was made for the fact that with a finite spacing of the plaque and backscatterer a slightly lower value of $(\mu_1 + \mu_1')$ is obtained due to the difference in the extrapolation factors for lead and aluminium.

It was found that

$$(\mu_1 + \mu_1') = 0.0214 \pm 0.0006 \text{ cm.}^2/\text{mg.}$$

In the experiment carried out to find the value of μ_1, a small β-ray ionisation chamber of shallow depth (Fig. 7) was placed with its base flush with a large sheet of acrylic resin at a height of 0.8 cm. above a β-plaque of phosphorus-Bakelite. Readings of the chamber current were made with different thicknesses of aluminium on the plaque, and from the

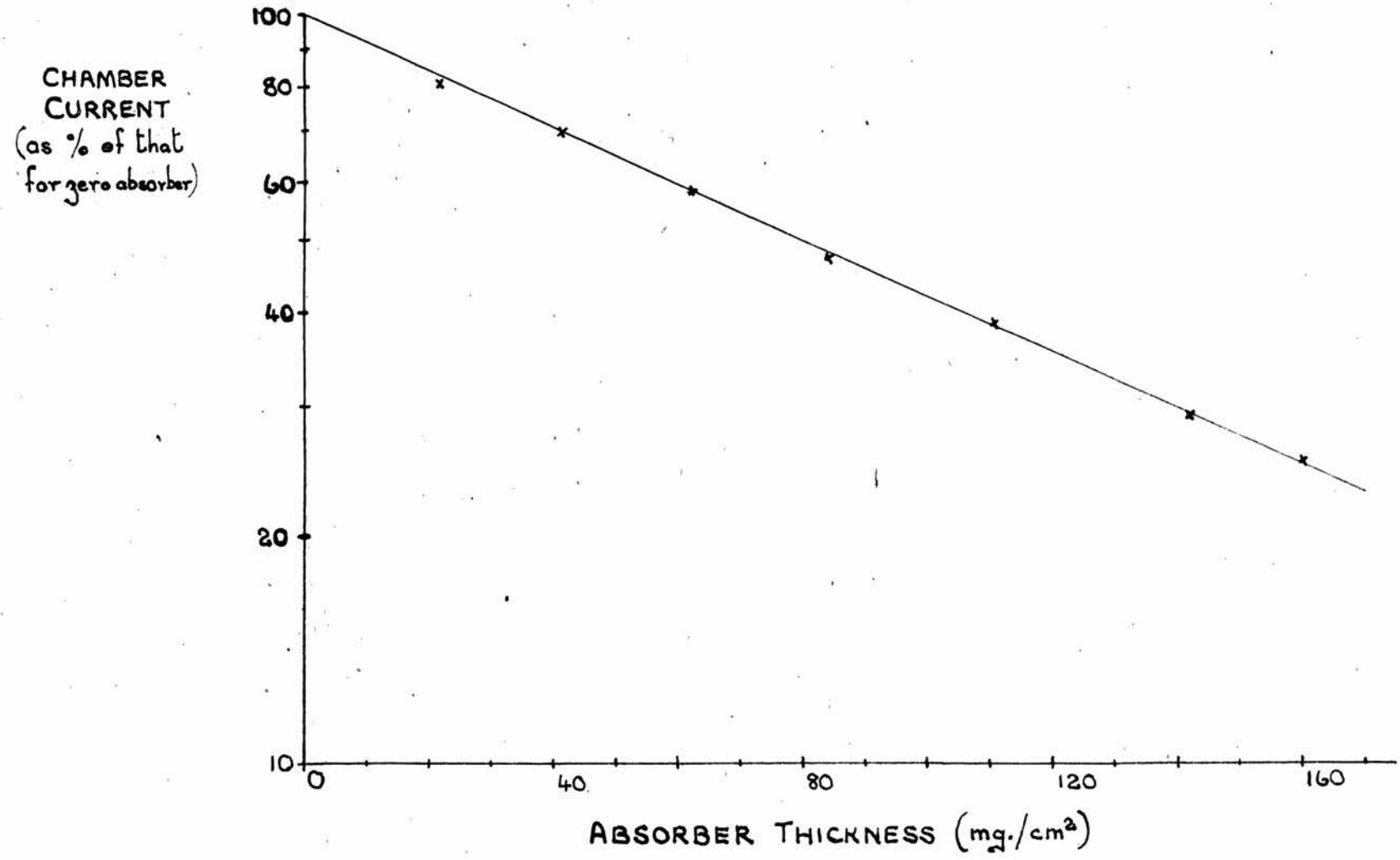

FIG. 8. Absorption in aluminium of β-radiation from Phosphorus-Bakelite plaque.

results (Fig. 8) it was concluded that the absorption obeyed the exponential law. A small correction (1%) was made to cover the slight increase in the back-scatter when aluminium foils were placed on the plaque and it was found that for aluminium

$$\mu_1 = 0.0088 \pm 0.0003 \text{ cm.}^2/\text{mg.}$$

and that hence

$$\mu_1' = 0.0126 \pm 0.0007 \text{ cm.}^2/\text{mg.}$$

The value of μ_1' derived is sufficiently accurate since it is used only for making small corrections in the experiment to follow. From this result it appears that the ionisation due to the back-scattered radiation from a thin layer is reduced to half its initial value when the radiation traverses a layer of 55 mg./cm.^{2} of material.

Determination of R.

(a) Ionisation Measurements.

In a previous experiment the relative values of (1 + R) were found for various materials and hence, if R is determined for any one material, the values of R for all the materials can be derived.

If the total ionisation rate at the centre of the surface of a β-plaque of phosphorus-Bakelite of large area, separated by a thin air film from an overlying thick layer of acrylic resin, is denoted by J_p, and if the total ionisation rate at the same

point when there is only air above the β-plaque is denoted by J_a, air backscatter being corrected for, then since J_a is the ionisation rate due solely to forward β-radiation

$$\frac{J_p}{J_a} = (1 + R) \qquad (15)$$

where R is the total backscatter coefficient for acrylic resin.

The same apparatus (Fig. 3) was used as in the experiment to determine the relative values of (1 + R). To determine J_p, the chamber current was measured with the chamber at various distances from the β-plaque and the overlying sheet of acrylic resin. By an extrapolation process the chamber current and hence the value of J_p were found for an infinitely small air gap. The correction required for backscatter from the components of the ionisation chamber is negligible since the materials used in the chamber had much the same total backscatter coefficient as acrylic resin, and although a small chamber effect exists for finite spacings of the plaque and the acrylic resin sheet it disappears in the extrapolation process.

The ionisation rate at the surface of the plaque with no backscatterer present was measured. The plaque was exposed in a large room, of height and width exceeding 30 feet, with only the ionisation

chamber and its stem above it. Readings of the chamber current were taken at various heights above the plaque and by extrapolation the chamber current and the ionisation rate at the surface of the plaque were found. This ionisation rate still requires correction for the backscatter due to the chamber and the air but denoting the uncorrected value by J_a' it was found that

$$\frac{J_p}{J_a'} = 1.162.$$

(b) Air and Chamber Corrections.

In calculating the corrections for air and chamber backscatter, it is permissible to introduce some approximations. The air correction was assessed by calculating the value of the ionisation rate at the centre of the plaque due to the backscattered radiation from the air. The first simplification introduced is to replace the rectangular plaque by a circular one of equal area. If the ionisation rate due to forward β-radiation is J_f at the centre of the surface of the plaque (radius a) then assuming that the plaque surface obeys the cosine law of emission the ionisation rate J_h due to forward β-radiation at height h above the centre of the plaque is

$$J_h = J_f\left(1 - \frac{h}{(h^2 + a^2)^{\frac{1}{2}}}\right) \qquad (16)$$

when air absorption is neglected. When air absorption is taken into account and μ_l is the linear absorption coefficient then

$$J_h = J_f e^{-\mu_l h}\left(1 - \frac{h}{(h^2 + a^2)^{\frac{1}{2}}}\right) \qquad (17).$$

The forward ionisation rate at height h cm. is less at points distant from the centre. The variation of J_f is difficult to express in analytical form but a simplification may be introduced by which the forward ionisation rate is regarded as remaining constant at the value J_h over a circle of radius r and is zero outside. The radius r is given by

$$J_h . \pi r^2 = J_f \pi a^2 \qquad (18).$$

This implies that in the absence of air absorption the integrated ionisation rate remains the same at all heights.

For a thin layer of air of thickness δ m at height h cm. above a β-plaque of infinite area, the ionisation rate at the surface of the plaque due to radiation backscattered from this layer is

$$J_b = (\mu_l + \mu_l')RJ_f e^{-(\mu_l + \mu_l')h}\,\delta m$$

where μ_l' is the linear absorption coefficient of the backscattered radiation and R is the total backscatter coefficient for air.

For the β-plaque of radius a, it is assumed that the ionisation rate along the central line of the system due to the backscattered radiation

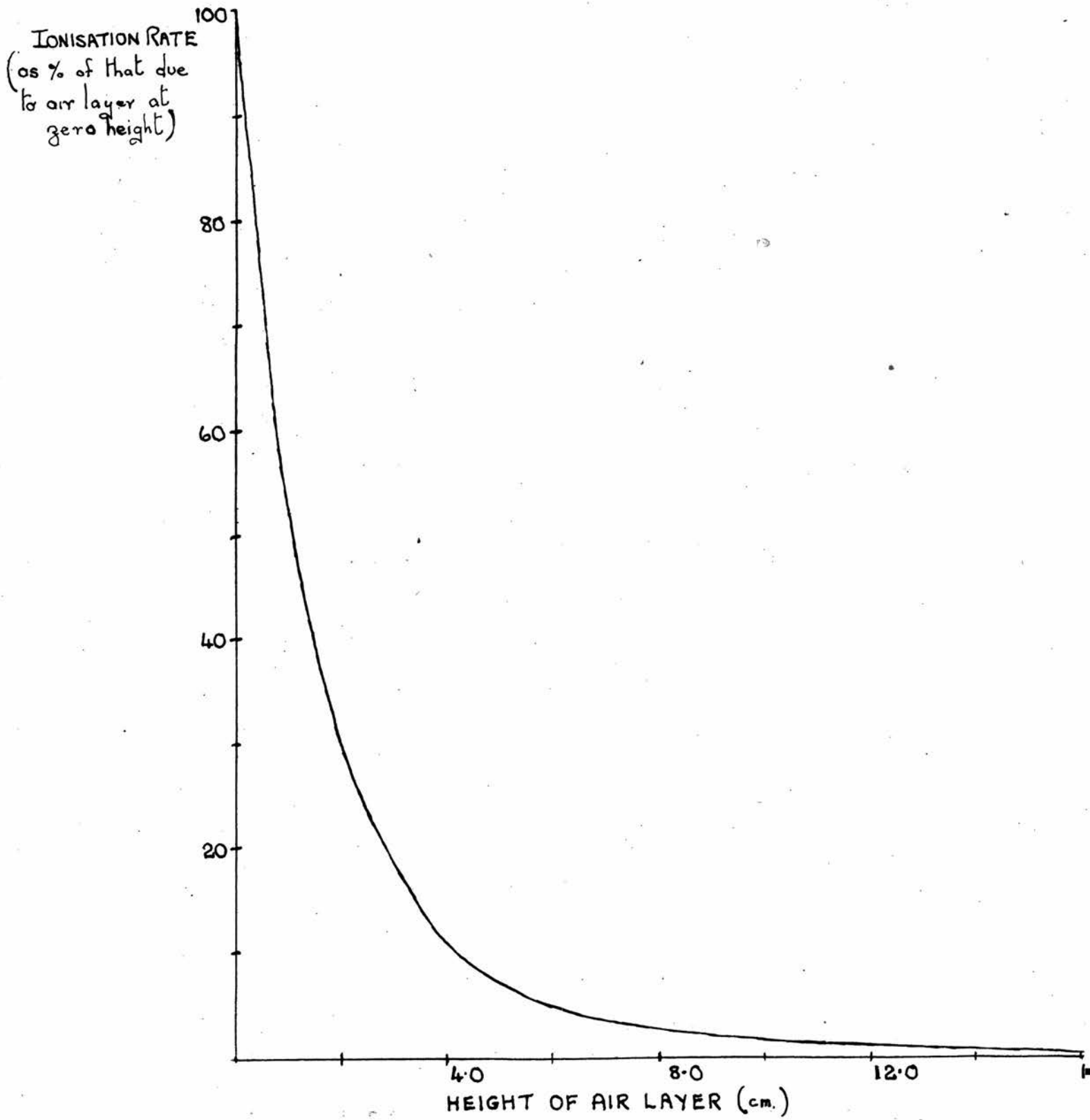

FIG. 9. Graph showing how the relative ionisation rate due to backscatter from an air layer decreases as the height of the layer increases.

decreases according to a law similar to that for forward β-radiation (equation (11)). Hence the contribution to the ionisation rate at the centre of the plaque by a thin layer of air at height h cm. is

$$\delta J_b = (\mu_l + \mu_l') R J_f \left(1 - \frac{h}{(h^2+a^2)^{\frac{1}{2}}}\right)\left(1 - \frac{h}{(h^2+r^2)^{\frac{1}{2}}}\right) e^{-(\mu_l + \mu_l')h} S_m \quad \ldots\ldots (19)$$

This equation was used to compute the total ionisation rate due to the radiation backscattered from the air. Since the value of R was required and to derive this from equation (15) the air correction is required, a method of successive approximations was necessary. The values of μ_l and μ_l' were derived from the measured mass absorption coefficients for aluminium. The rapid decrease in the contributions made to the ionisation rate as the height of the layer is increased is shown in Fig. 9; it is mainly due to the rapid decrease in the factor $(1 - \frac{h}{(h^2 + a^2)^{\frac{1}{2}}})$.

At the temperature and pressure of the air during the measurement of J_a', the ionisation rate due to the air backscatter was found to be

$$J_b = 0.013 J_f.$$

The correction required for the chamber backscatter was made in a similar way. The parts of the chamber were regarded as radiators of backscattered radiation and the ionisation rates produced by them in the chamber were calculated. The contributions

TABLE 4

IONISATION RATE DUE TO CHAMBER COMPONENTS.

Component	Ionisation Rate (relative to that for forward radiation)
Circular Wall	0.0059
Stem	0.0088
Collecting Electrode	0.0022
Top Wall	0.0033

made by the four components - the circular wall of the chamber, the ionisation stem, the collecting electrode and the top wall of the chamber are given in Table 4. The sum of the contributions was $0.0202J_f$.

(c) Final value of R.

$$\text{Since } J_a' = J_a + 0.013J_a + 0.0202J_a$$

$$\text{and } \frac{J_p}{J_a'} = 1.162$$

$$\therefore \frac{J_p}{J_a} = 1.197$$

and $\therefore (1 + R) = 1.197$ for acrylic resin. The experimental error is estimated at $\pm$ 0.02 and so we finally obtain

$$R = 0.20 \pm 0.02.$$

Final results.

The relative values of (1 + R) can now be corrected for the small backscatter produced by the chamber. To do this it is necessary to calculate the ionisation rate produced by this backscatter and the reduction in the ionisation rate for the material under investigation, caused by the absorption in the chamber. The correction as seen from Table 5 is small for most materials and even for lead amounts to only 2.5%. From the corrected values of (1 + R) the

TABLE 5

BACKSCATTER FROM VARIOUS MATERIALS.

Material	Relative Values of (1 + R)		R	r
	Uncorrected	Corrected		
Acrylic Resin	1.00	1.00	.20	.16
Polythene	0.97	0.97	.16	.13
Polystyrene	0.99	0.99	.19	.15
Tissue Phantom Material	1.00	1.00	.20	.16
Soft Tissue	1.033	1.035	.24	.19
50% Phosphorus-Bakelite	1.067	1.070	.28	.22
Aluminium	1.137	1.145	.37	.28
Copper	1.290	1.310	.57	.42
Lead	1.510	1.545	.85	.61

values of R and r can be derived and are given in Table 5.

The standard error in the relative values of (1 + R) is estimated to be less than $\pm$ 0.01 for substances of mean atomic number lower than aluminium. For lead the error is estimated at $\pm$ 0.045 and for copper $\pm$ 0.02. The values of R and r carry a standard error of $\pm$ 10%.

The results given in Table 5 are in general agreement with those of Neary (7) obtained under similar conditions but using the β-radiation from radium applicators.

Most investigations on the backscattered radiation produced by β-radiation have been carried out with end-window counters. Usually the increases in counting rate obtained when a thin source of ^{32}P is backed by various materials have been measured. The results of such experiments, as reported by Zumwalt (9), Burtt (10) and Yaffe and Justus (11), exhibit an increase in backscatter with increasing atomic number similar to that found here.

When a β-ray ionisation chamber of conventional design, i.e. having a solid base and a shallow collecting volume, is used to find the dose rate in tissue for ^{32}P applicators, the results of Table 5 may be used to correct the readings when the base

material differs significantly from soft tissue, e.g. aluminium.

Note. In a published account of part of this work (McInally and Neary (12)) the value of r for soft tissue is erroneously given as 0.20 instead of the correct value 0.19.

CHAPTER IV.

THEORETICAL DERIVATION OF SURFACE DOSAGE RATES.

It is now possible to correct and extend the method, given on p. 5, for finding the surface ionisation rate and hence the dosage rate for a mass of soft tissue placed in a ^{32}P box. Three factors will be considered in turn:

(a) the modification in equation (3), (p. 6), required by the difference in backscatter from soft tissue and phosphorus-Bakelite

(b) the effect of having a finite air gap between the tissue mass and the ^{32}P box, and

(c) the effect of making the dimensions of the tissue mass comparable with the range of ^{32}P β-radiation in soft tissue.

The theory is first developed for systems having spherical geometry and then the applicability of the results to other systems, including that used in the experimental tests, is discussed. Usually explicit reference is made only to the surface ionisation rate, but this bears a fixed ratio to the surface dosage rate (p. 5).

Modification of Elementary Theory.

The surface ionisation rate $J_{2\pi}$ for a large sphere of soft tissue placed centrally in a closely-

fitting spherical ^{32}P box was considered previously (p. 5). It was shown that, if the inner sphere was replaced by one of inactive phosphorus-Bakelite, the surface ionisation rate was equal to half $J_{4\pi}$, the corrected ionisation rate in the empty ^{32}P box. In the absence of information on the difference in backscatter from soft tissue and phosphorus-Bakelite, it was concluded that the ionisation rate on an inner sphere of soft tissue would be the same.

But from the results given in Table 5 (p.24), when a thick plaque of β-active phosphorus-Bakelite of large area is separated by a thin air film from an overlying thick layer of material, the ionisation rate at the centre of the film for a layer of soft tissue is 0.966 of that for a layer of phosphorus-Bakelite. A similar decrease will hold for the present system and hence on the surface of a large sphere of soft tissue in a closely-fitting ^{32}P box the surface ionisation rate is

$$J_{2\pi} = 0.48_3 J_{4\pi} \qquad (20).$$

Effect of Finite Air Gap.

Consider a spherical mass of soft tissue (Fig. 10), placed centrally in a ^{32}P box of spherical shape, the radius of the tissue sphere, a, being less than that of the ^{32}P box, b, but still large compared with

radiation from the inner sphere is emitted from a surface of $4\pi a^2$ and is received and backscattered by a surface of area $4\pi b^2$. Hence the ionisation rate at the inner sphere produced by this backscattered radiation, being proportional to $\frac{a^2}{b^2}$, is negligible for the present system. The decrease due to this effect is annulled by an increase due to β-radiation emitted by the outer sphere and backscattered by the walls of the outer sphere before reaching the inner sphere. In effect, the outer sphere is thus responsible for more than half of the surface ionisation rate on the inner sphere. Therefore, when the inner sphere is not radioactive, the ionisation rate at its surface is greater than half $J_{4\pi}$. A similar effect will occur when the inner sphere is of soft tissue.

To derive the actual increases, the inner sphere is first considered to be of radioactive phosphorus-Bakelite. Let r_1 denote the single backscatter coefficient and R_1 the total backscatter coefficient for phosphorus-Bakelite (p. 9). The surface ionisation rate on the inner sphere may be divided into three components. The first, J_x', is due to β-radiation from the inner sphere itself and as may be seen from the case of a closely-fitting spherical ^{32}P box

$$2J_x'(1 + R_1) = J_{4\pi}$$

$$\therefore \quad J_x' = \tfrac{1}{2}J_{4\pi}(1 - r_1) \qquad (21).$$

that

$$J_{2\pi} = 0.48_3 J_{4\pi} \qquad (20).$$

Thus there is a considerable increase (23%) in the surface ionisation rate and hence dose rate when the air gap separating the sphere and enclosure is large.

The intermediate case may be investigated by introducing some simplifying assumptions. It is assumed that when a flux F of β-rays is incident on a surface a backscattered flux rF is produced. This is assumed to hold whether or not the incident flux is isotropic. The backscattered flux is assumed to be emitted according to the cosine law. The ionisation rate at a point is proportional to the flux at the point, and the constant of proportionality is taken to be independent of the number of backscattering processes which the flux has undergone.

These assumptions are not strictly valid. Neary (7) has shown that for β-radiation incident mainly normally the amount of backscatter is less than for an isotropic beam, but the error introduced by disregarding this is believed to be small. Further the constant of proportionality relating ionisation rate and flux increases as the mean energy of the flux falls. The error introduced is small since the contribution made to the surface ionisation rate by radiation which has undergone more than two back-

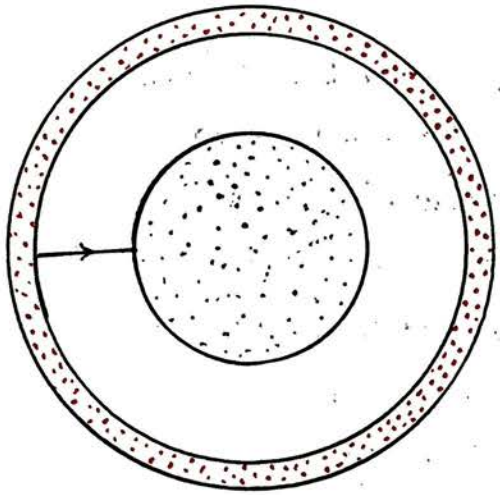

GROUP 1 β-rays reaching inner sphere without being backscattered by outer sphere.

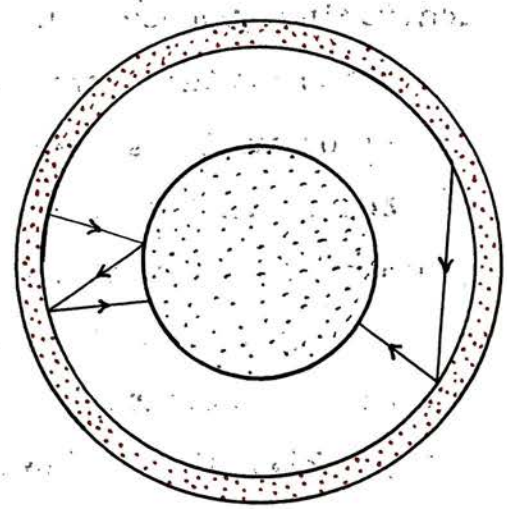

GROUP 2. β-rays reaching inner sphere after being backscattered once by outer sphere

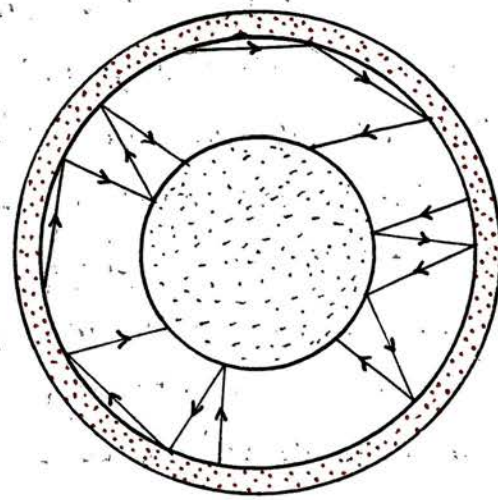

GROUP 3. β-rays reaching inner sphere after being backscattered twice by outer sphere.

FIG 11 METHOD OF GROUPING THE VARIOUS FLUXES OF BETA-RAYS FALLING ON INNER SPHERE.

scattering processes is small.

The surface ionisation rate, $J_{2\pi}$, on the tissue sphere of radius a, centrally placed in a spherical ^{32}P box of radius b, is due to β-radiation which impinges directly or has suffered one or more back-scattering processes by the inner sphere or enclosure. The various streams of β-rays may be divided into groups (Fig. 11). The first group includes all β-rays which reach the tissue sphere without being backscattered by phosphorus-Bakelite. The second group includes all those which have been backscattered once by the phosphorus-Bakelite. It includes β-rays backscattered once by soft tissue and then once by phosphorus-Bakelite as well as those reaching the inner sphere for the first time after being back-scattered by phosphorus-Bakelite. The n^{th} group includes all those which have been backscattered $(n - 1)$ times by the phosphorus-Bakelite.

Each element of area dS of the outer sphere is taken to emit a flux $f.\cos\theta.dS$ per unit solid angle at an angle θ to the normal of the element. Unit area thus emits a total flux πf over a solid angle of 2π. The incident flux per unit area of the tissue sphere due to the primary flux from the whole of the outer sphere is isotropic and of magnitude πf. The ionisation rate produced by this flux together with the first-order backscattered radiation it produces is

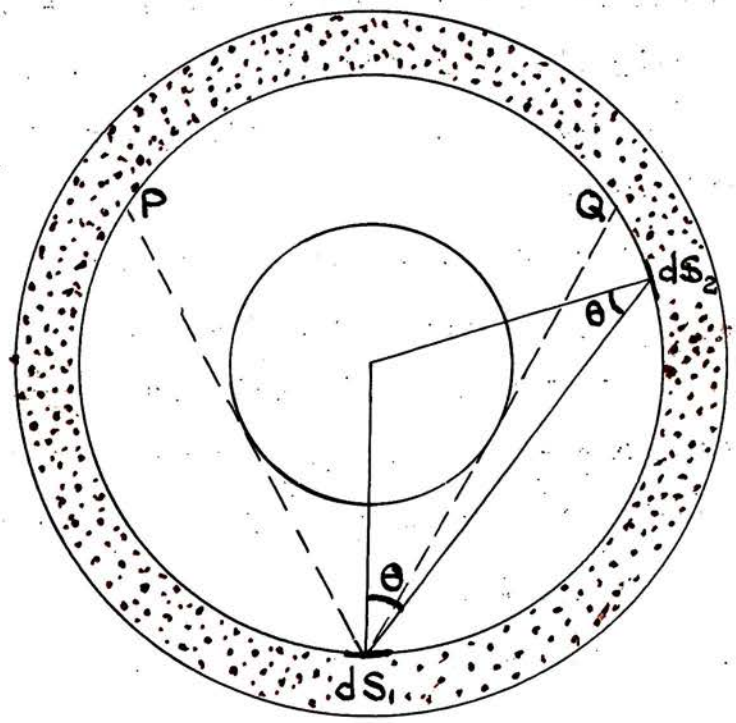

Radius of sphere of soft tissue = a

Radius of ^{32}P box = b.

Fig. 12.

$$j_1 = \pi kf(1 + r_2) \qquad (28)$$

where k is a constant, being the ionisation rate produced by unit isotropic flux without backscatter. Equation (28) thus gives the contribution made by the first group of β-rays.

The primary flux of β-rays on the tissue sphere produces a total backscattered flux of $4\pi a^2.\pi f r_2$, and this falls on the outer sphere of total area $4\pi b^2$, thus causing each element dS of the outer sphere to produce a backscattered flux $r_1 r_2.\frac{a^2}{b^2}.f \cos\theta \, dS$ per unit solid angle at angle θ to the normal of the element. Due to this, a flux per unit area of amount

$$\pi f r_1 r_2 \frac{a^2}{b^2} \qquad (29)$$

falls on the tissue sphere, this being the first component of the second group.

There is a further component due to β-radiation which is backscattered once by the phosphorus-Bakelite before reaching the tissue sphere for the first time. An element of the outer sphere dS_1 (Fig. 12) receives from another element dS_2 an amount of primary flux given by

$$f \cos\theta \, d\omega_1 dS_2, \qquad (30)$$

where $d\omega_1$ is the solid angle which dS_1 subtends at dS_2 and θ is the angle of emission. The total incident flux of this kind received by dS_1 is given by

summing over the whole sphere except for the region PQ (Fig. 12) which is screened by the inner sphere.

Since

$$d\omega_1 = \frac{dS_1 \cos\theta}{x^2}$$

where x is the length of the line joining dS_1 and dS_2, we can rewrite the primary flux received by dS_1 from dS_2 as $f \cos\theta\, d\omega_2 dS_1$, where $d\omega_2$ is the solid angle which dS_2 subtends at dS_1. The contribution made by the area of the sphere which lies between angle θ and $\theta + d\theta$ is thus

$$2\pi f \sin\theta \cos\theta\, d\theta\, dS_1$$

and therefore we find that the total incident flux

$$= \int_{\sin^{-1}\frac{a}{b}}^{\pi/2} 2\pi f \sin\theta \cos\theta\, d\theta\, dS_1$$

$$= \pi f dS_1 (1 - \frac{a^2}{b^2}) \qquad (31).$$

This flux is backscattered and the backscatter forms the second component of the second group. The flux which is incident per unit area of the tissue sphere due to this component is $\pi r_1 f(1 - \frac{a^2}{b^2})$. The first component produces a flux $\pi f r_1 r_2 \frac{a^2}{b^2}$ and thus we obtain for the ionisation rate at the inner sphere due to the second group

$$j_2 = (1 + r_2)\pi k f \left[r_1 r_2 \frac{a^2}{b^2} + r_1 (1 - \frac{a^2}{b^2}) \right] \qquad (32)$$

or

$$\left.\begin{aligned} j_2 &= M j_1 \\ \text{where } M &= r_1 r_2 \frac{a^2}{b^2} + r_1\left(1 - \frac{a^2}{b^2}\right) \end{aligned}\right\} \qquad (33).$$

The flux of the third group is evaluated similarly. It has four components (Fig. 11):

(1) β-rays which have not been backscattered by soft tissue.

(2) β-rays backscattered alternately by soft tissue and phosphorus-Bakelite.

(3) β-rays backscattered first by soft tissue and then twice by phosphorus-Bakelite.

(4) β-rays backscattered first by phosphorus-Bakelite then by tissue and lastly by phosphorus-Bakelite.

It is found that the total incident flux per unit area of the inner sphere is $\pi f\left(r_1 r_2 \frac{a^2}{b^2} + r_1\left(1 - \frac{a^2}{b^2}\right)\right)^2$ for this third group. Thus the ionisation rate produced on the tissue sphere is

$$j_3 = M^2 j_1 \qquad (34).$$

For the n^{th} group the ionisation rate is

$$j_n = M^{(n-1)} j_1 \qquad (35).$$

Summing for the infinite series of groups we find that the total surface ionisation rate on the tissue sphere is

$$\begin{aligned} J_{2\pi} &= \frac{j_1}{1 - M} \\ &= \frac{(1 + r_2)\pi k f}{1 - M} \end{aligned} \qquad (36).$$

Equation (36) will also apply to an inner sphere of inactive phosphorus-Bakelite if we put $r_2 = r_1$. If we consider a system in which an inner sphere of inactive phosphorus-Bakelite is enclosed in a closely-fitting ^{32}P box then, since $M \rightarrow r_1^2$,

$$J_{2\pi} = \frac{\pi kf}{1 - r_1} \qquad (37).$$

But $$J_{2\pi} = \tfrac{1}{2} . J_{4\pi}$$

$$\therefore \pi kf = \tfrac{1}{2} J_{4\pi}(1 - r_1) \qquad (38).$$

Returning to the general equation (36) and substituting for πkf we find

$$J_{2\pi} = \tfrac{1}{2} \frac{J_{4\pi}(1 + r_2)(1 - r_1)}{(1 - M)} \qquad (39).$$

Substituting for M from equation (33) and rearranging the expression we finally obtain

$$J_{2\pi} = \tfrac{1}{2} J_{4\pi} \frac{(1 + r_2)}{1 + r_1 \frac{a^2}{b^2}(1 - r_2)} \qquad (40).$$

This equation includes the two special cases discussed before:

(1) when $a \rightarrow b$

$$J_{2\pi} = \tfrac{1}{2} J_{4\pi} \frac{(1 + r_2)(1 - r_1)}{1 - r_1 r_2}$$

$$= \tfrac{1}{2} J_{4\pi} \frac{(1 + R_2)}{(1 + R_1)}$$

which is equation (20) (p. 27)

(2) when $\frac{a}{b} \rightarrow 0$

$$J_{2\pi} = \tfrac{1}{2} J_{4\pi}(1 + r_2)$$

which is equation (27) (p. 30).

From equation (40) it is deduced that equation (27) will hold to within 1% if $\frac{a}{b} < 0.22$ and hence the solid angle subtended by the tissue sphere at a point on the outer sphere is less than $0.024 \cdot 2\pi$. Thus, when the air gap is more than 3.5 times the radius of the tissue sphere, the surface ionisation rate on the tissue sphere is within 1% of that obtained with a very large air gap. Further when $\frac{a}{b} = 0.71$ the surface ionisation rate is

$$J_{2\pi} = 0.539 J_{4\pi} \qquad (41)$$

giving half the maximum increase in surface ionisation rate attained.

Effect of Transmitted Radiation.

When a tissue sphere whose dimensions are comparable with the range of ^{32}P β-radiation in soft tissue is placed centrally in a spherical ^{32}P box, an increase in surface ionisation rate is caused by β-rays which are partially transmitted by the tissue.

Consider first that the tissue sphere lies in a closely-fitting ^{32}P box. The tissue sphere is now replaced by one of phosphorus-Bakelite. If this inner sphere is considered to have the same specific activity as the ^{32}P box then the surface ionisation rate on the inner sphere is $J_{4\pi}$. But it is not due equally to the inner sphere and the ^{32}P box, in

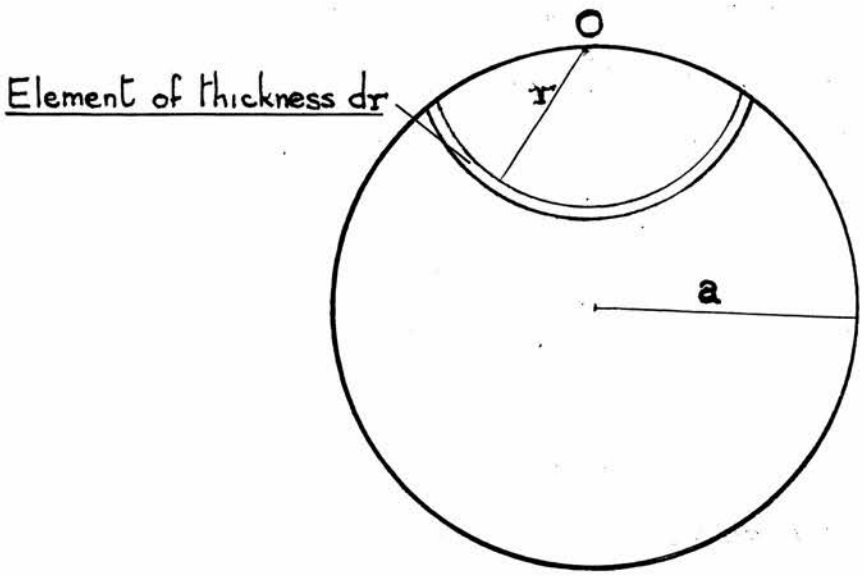

FIG. 13.

contrast to a system of large radius.

The surface ionisation rate due to the inner sphere itself may be derived approximately by making some simple assumptions about the absorption of β-radiation in materials composed of light elements. It is assumed here that the β-radiation is exponentially absorbed with a linear absorption coefficient μ up to the range d_o, beyond which no radiation penetrates. Thus the ionisation rate dJ' produced in a minute air cavity by a volume element dv at distance r is given by

$$\left.\begin{aligned} dJ' &= \frac{Ce^{-\mu r}dv}{r^2}, \quad r < d_o \\ &= 0 \qquad\qquad r \geqslant d_o \end{aligned}\right\} \qquad (42)$$

where C is some constant. Loevinger (13) and (14) has suggested more rigorous equations to supplant equations (42), but the latter are sufficiently accurate for the present purpose.

For a radioactive sphere of phosphorus-Bakelite of radius a (Fig. 13), the surface ionisation rate at the point O due to β-radiation from material lying between distance r and r + dr from O is

$$dJ' = \frac{Ce^{-\mu r}dv}{r^2}.$$

Since $$dv = 2\pi r^2(1 - \frac{r}{2a})dr$$

$$\therefore\ dJ' = 2\,C(1 - \frac{r}{2a})e^{-\mu r}dr \qquad (43).$$

When $2a < d_o$, by integrating over the whole sphere

we find that the surface ionisation rate is

$$J' = \int_0^{2a} 2\pi C(1 - \frac{r}{2a})e^{-\mu r}dr$$

$$= \frac{2\pi C}{\mu}\left[1 - \frac{(1 - e^{-2a\mu})}{2a\mu}\right] \qquad (44).$$

When $2a \geqslant d_o$

$$J' = \int_0^{d_o} 2\ C(1 - \frac{r}{2a})e^{-\mu r}dr$$

$$= \frac{2\pi C}{\mu}\ (1 - \frac{1}{2a\mu}) \qquad (45).$$

For a sphere of very large radius

$$J' = \frac{2\pi C}{\mu} = \frac{J_{4\pi}}{2}.$$

Substituting for C in equations (44) and (45), we find

$$\left.\begin{aligned} J' &= \tfrac{1}{2}J_{4\pi}(1 - \frac{1 - e^{-2a\mu}}{2a}) \text{ for } 2a < d_o \\ &= \tfrac{1}{2}J_{4\pi}(1 - \frac{1}{2a\mu}) \qquad \text{for } 2a \geqslant d_o \end{aligned}\right\} \quad (46).$$

These equations show to what extent the inner sphere fails to provide half the ionisation rate at its surface, when it is enclosed in a closely-fitting ^{32}P box. The deficiency is of course made good by the β-radiation partially transmitted by the inner sphere. Hence, when the inner sphere is not radioactive, its surface ionisation rate is

$$\left.\begin{aligned} J_{2\pi} &= \tfrac{1}{2}J_{4\pi}(1 + \frac{1 - e^{-2a\mu}}{2a}) \text{ for } 2a < d_o \\ &= \tfrac{1}{2}J_{4\pi}(1 + \frac{1}{2a\mu}) \qquad \text{for } 2a \geqslant d_o \end{aligned}\right\} \quad (47).$$

When the inner sphere is of soft tissue and not

TABLE 6

RELATIVE SURFACE IONISATION RATES

FOR TISSUE SPHERES IN

CLOSELY-FITTING ^{32}P BOXES.

Radius of Sphere cm.	Relative Surface Ionisation Rate
0.1	1.473
0.2	1.279
0.5	1.115
1.0	1.057
2.0	1.029
4.0	1.014
6.0	1.009_5

of phosphorus-Bakelite, these equations must be modified and the values of μ and d_o for soft tissue used. The first term $\frac{1}{2}J_{4\pi}$ must be multiplied by the factor $\frac{1 + R_2}{1 + R_1}$ but the second term, which refers to transmitted β-radiation, will be unchanged. The assumption is made that the backscatter coefficients appropriate to a system of very large radius may be used. This is only approximately true and in fact the backscatter coefficients must be slightly less. By carrying out a calculation, similar to that above, for the backscattered radiation produced in the inner sphere, it can be shown that the backscattering coefficients should be multiplied by a factor

$$1 - \frac{1 - e^{-2a(\mu + \mu')}}{2a(\mu + \mu')} \qquad (48)$$

where μ' is the absorption coefficient for backscattered radiation. Since the correction involved is small, it is permissible to write $\mu' = \mu$ and the factor becomes

$$(1 - \frac{1 - e^{-4a\mu}}{4a\mu}) \qquad (49).$$

The surface ionisation rates for tissue spheres of various sizes in closely-fitting ^{32}P boxes are given in Table 6. The value used for μ is 8.7 cm.$^{-1}$, corresponding to a half-value layer of 80 mg/cm.^{2} and d_o is taken as 0.80 cm. For tissue spheres of radius 6 cm. or greater the increase in surface ionisation rate is less than 1%.

and to extend the applications of these equations to other systems.

Extension of Results.

For a large sphere of soft tissue placed in a closely-fitting ^{32}P box the surface ionisation rate is

$$J_{2\pi} = 0.48_3 J_{4\pi} \qquad (20).$$

This result holds tc an accuracy of 1% for a sphere of radius exceeding 6 cm. For smaller radii, transmitted β-radiation has to be taken into account. The equation will also apply to other systems in which the air gap is minute. The usual kind of ^{32}P box has rectangular sides and for a closely-fitting tissue phantom the surface ionisation rate will be given by this equation, except for points affected by transmitted β-radiation. Transmitted radiation will be negligible at points further than 7 mm. from the edges of the tissue phantom.

When the air gap in a spherical system is large there is a considerable increase in the surface ionisation rate of the tissue sphere. It becomes

$$J_{2\pi} = 0.59_5 J_{4\pi} \qquad (27)$$

as long as transmitted β-radiation is negligible. The value is accurate to 1% provided the air gap exceeds 3.5 times the radius of the inner sphere, i.e.

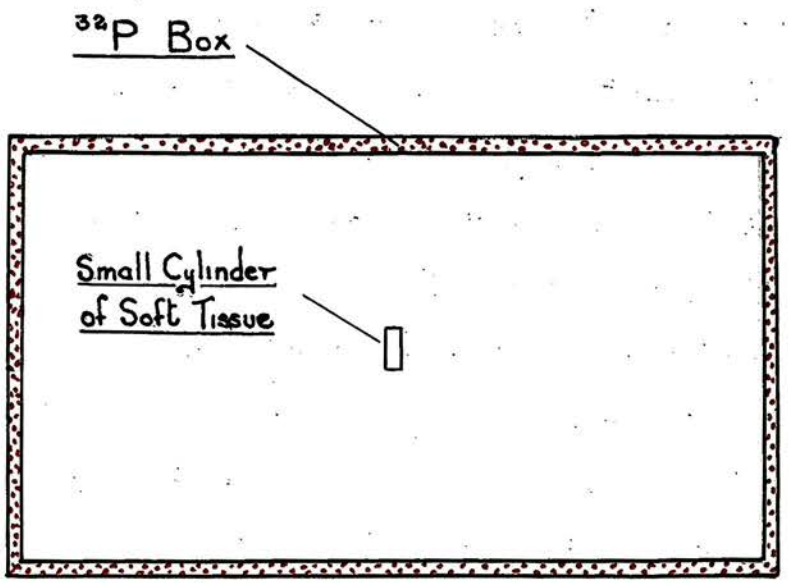

FIG. 14. Small cylindrical mass of soft tissue at centre of a ^{32}P box with rectangular sides.

when the solid angle which the inner sphere subtends at any point on the ^{32}P box does not exceed 0.024.2π. The equation will be valid for any small tissue mass in any shape of ^{32}P box under similar conditions. It is essential that the solid angle subtended by the tissue mass at a point on the ^{32}P box should not exceed 0.024.2 , that transmitted β-radiation should be negligible at the point considered, and that the point should not be screened by any surrounding part. As an example the system used in the experimental tests may be considered. A small cylindrical tissue phantom (Fig. 14) is placed centrally in a large ^{32}P box with rectangular sides. On the flat ends of the cylinder at points further than 7 mm. from the edges the surface ionisation rate will be given by equation (27).

Lastly the effects of transmitted β-radiation may be estimated by the same method as for systems having spherical geometry. Thus for a small sphere of soft tissue in a large ^{32}P box of any shape, equation (40) with r_2 replaced by expression (50) will be valid.

Summary.

If a mass of soft tissue of simple shape is exposed in a ^{32}P box, the surface ionisation rate $J_{2\pi}$

and hence the surface dosage rate can be derived from $J_{4\pi}$, the ionisation rate in the empty box. Three factors have to be considered: (1) the difference in backscatter from soft tissue and phosphorus-Bakelite (2) the size of the air gap between the tissue mass and the box and (3) the transmission of β-radiation through the tissue mass. For points on a tissue mass unaffected by transmitted radiation, the surface ionisation rate in a closely-fitting ^{32}P box, when air absorption is corrected for, is

$$J_{2\pi} = 0.483 J_{4\pi}.$$

When the air gap is not negligible an increase in surface ionisation rate results. For a large air gap the ionisation rate at points unaffected by transmitted radiation is, when air absorption is corrected for,

$$J_{2\pi} = 0.595 J_{4\pi}.$$

The effects of transmitted radiation are negligible for points on an object where the radii of curvature exceed 6 cm. For a tissue sphere of radius 1.0 cm. the values of $J_{2\pi}$ are increased by 6% by transmitted β-radiation and the increase rises steeply for spheres of smaller radii.

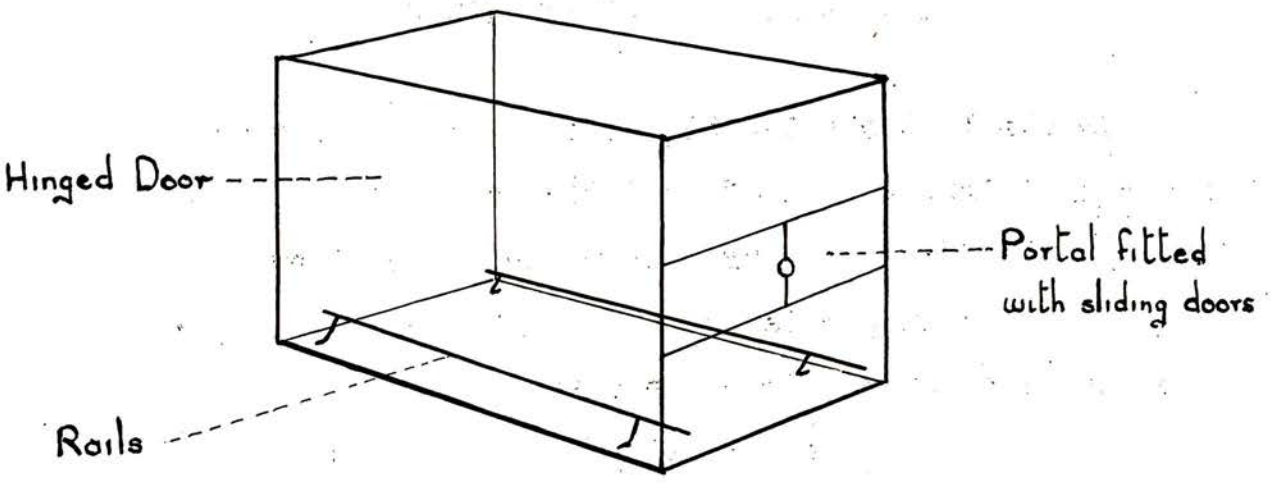

SCHEMATIC DIAGRAM OF ^{32}P BOX

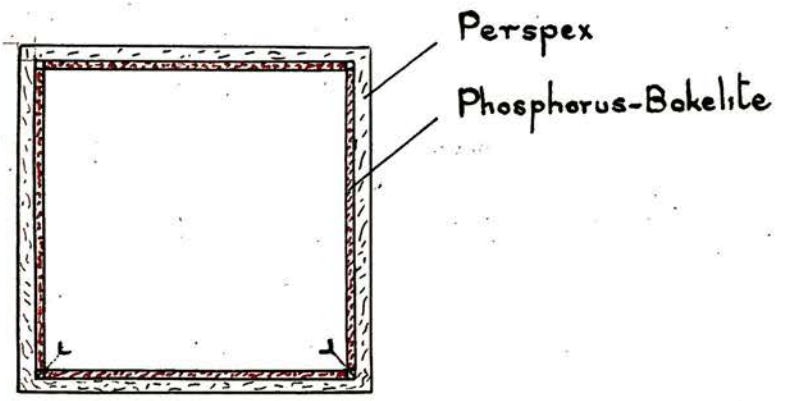

SECTION THROUGH BOX

FIG. 15

CHAPTER V.

EXPERIMENTAL INVESTIGATIONS.

In the last chapter it was shown that, when a small cylindrical mass of soft tissue is placed centrally in a large ^{32}P box with rectangular sides, the surface ionisation rate $J_{2\pi}$ on the flat ends at points greater than 0.7 cm. from the edges is given by

$$J_{2\pi} = 0.595 J_{4\pi} \qquad (27)$$

where $J_{4\pi}$ is the ionisation rate in the empty ^{32}P box. It is assumed that both ionisation rates are corrected for air absorption.

The object of the experimental investigation described here was primarily to test this equation. At the same time a test was made of the equation predicting the ionisation rate $J_{2\pi}$ on the surface of a tissue phantom of rectangular sides in a closely-fitting ^{32}P box, namely

$$J_{2\pi} = 0.483 J_{4\pi} \qquad (20).$$

^{32}P Box.

The ^{32}P box used was designed by Neary and Young (3). It had rectangular sides and its internal size was 38.6 x 21.6 x 21.6 cm. It was built from phosphorus-Bakelite plaques, each of area 7.7 x 5.2

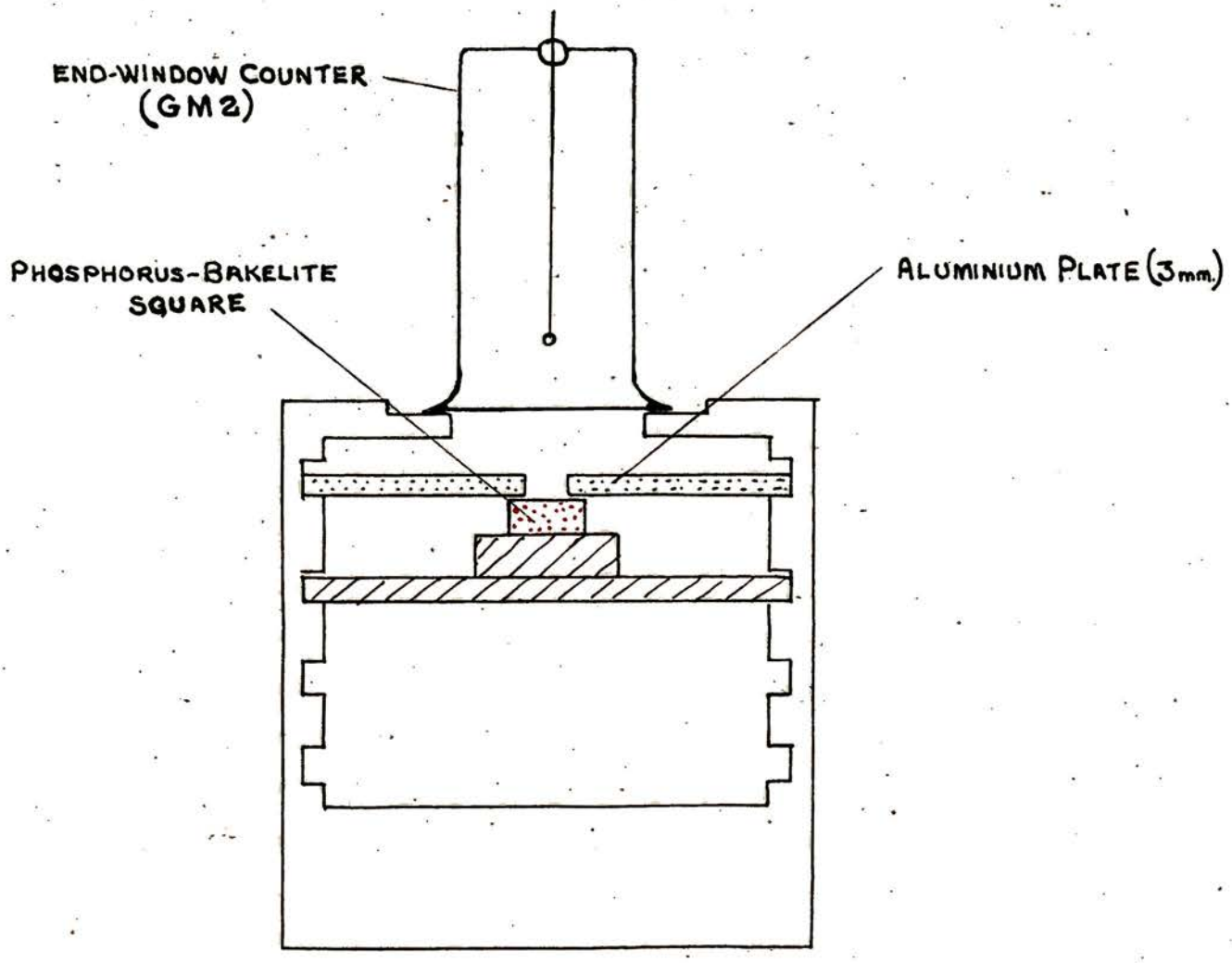

FIG. 16. Apparatus used to compare β-ray emission from intact and filed faces of Phosphorus-Bakelite squares.

cm. and thickness 0.45 cm., the plaques being fitted to the walls of a thick Perspex box (Fig. 15). At the front of the box there was a small portal fitted with sliding doors, which was useful for inserting small ionisation chambers into the box. The rear end of the box was fitted with a hinged door so that large tissue phantoms could be inserted into the box. The floor of the box carried two thin rails which were used to support the phantoms.

Test on Phosphorus-Bakelite.

In the manufacture of phosphorus-Bakelite it is possible that the layers near the surface may be given a concentration of phosphorus appreciably different from that in the interior. If this occurs then the theory given previously will no longer be strictly applicable.

To test for any surface layer effect five squares of phosphorus-Bakelite of 1 cm. side were used. One face of each square was left intact while from the opposite face a weighed amount of material was removed by filing. The squares were then activated together in a thermal neutron flux and after sufficient time had elapsed to ensure that any extraneous activities were negligible, each square was assayed in a counter assembly (Fig. 16). The narrow aperture of the diaphragm covering the samples ensured

TABLE 7

TEST ON PHOSPHORUS-BAKELITE.

Sample	Layer Removed mg./cm.^{2}	Counts Recorded (3 min. period) Intact Face	Filed Face	% Increase (with filed face)
1	2.9	10,835	10,874	+ 0.35
2	31.1	9,690	10,200	+ 5.3
3	30.3	10,325	10,325	-
4	55.1	9,972	9,871	- 1.0
5	11.1	10,224	10,120	- 1.0

that the β-radiation was received from a well-defined area. The counting rates were determined both for the intact and filed faces, the results being given in Table 7.

From the results the mean counting rate over the filed faces is 0.7% greater than for the intact faces. If a surface layer of 10 mg./cm.^{2} possessed no phosphorus, then the filed face would show an increase in counting rate of 10% over the intact face. It seems safe to conclude that with the phosphorus-Bakelite used the surface layers were not significantly enriched or deficient in phosphorus.

Ionisation Current Measurements.

Before describing the ionisation chambers used in the experiments, it is convenient to comment briefly on the current measuring system. As in the experiments in Chapter II a Townsend balance method was used with a Lindemann electrometer as the null detector. The instrument was fitted with three Townsend capacitors: (1) a small air gap condenser of 39.6 pF, (2) a small Plastapack condenser of 2117 pF and (3) a large Plastapack condenser of 54800 pF. The Plastapack condensers were subjected to stringent tests as regards leakage but no defect was found. The values of the capacities were measured with a de Sauty bridge, using a small air condenser of 10.76 pF

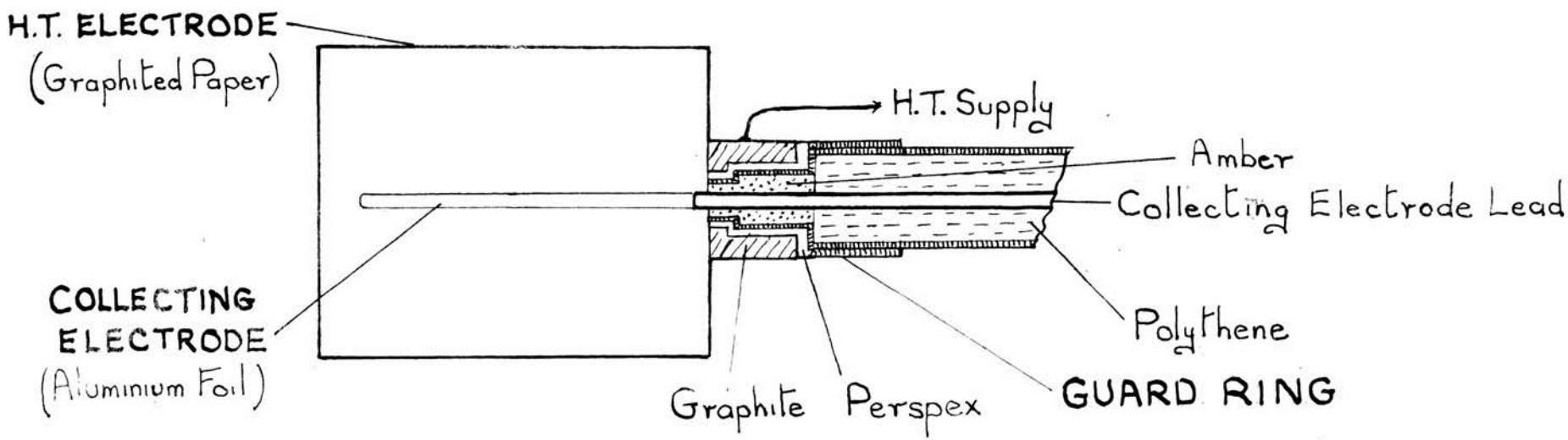

Fig. 17. "4π" Ionisation Chamber.

(N.P.L. calibration) as standard. The values were checked by measuring the same ionisation currents with different condensers and agreement to within $\pm$ 0.5% was obtained.

Using these condensers it was possible to measure currents ranging from 3×10^{-8} amp. to 10^{-12} amp. with high accuracy. Throughout the experiments the equipment gave trouble-free service.

Measurements of $J_{4\pi}$.

The ionisation chambers used to measure $J_{4\pi}$, the ionisation rate in the empty ^{32}P box, were designed to be as transparent as possible to ^{32}P β-radiation and at the same time to be sufficiently robust to ensure that they were not easily distorted. A cylinder of thin graphited paper (radius 1.2 cm., length 3 cm.) was used as the high voltage electrode with a coaxial collecting electrode and guard ring (Fig. 17). Two chambers were used, the first with a paper thickness of 11.5 mg./cm.^{2} and the second of 8.7 mg./cm.^{2}. In both chambers the central collecting electrode was a cylinder of aluminium foil (0.1 cm. in diameter, 2.4 mg./cm.^{2} thickness), which was mounted on the 1 mm. high projection of the aluminium wire used in the ionisation chamber stem.

Several corrections had to be applied to derive the value of $J_{4\pi}$ from the readings of chamber current.

These covered:

(1) absorption of the β-radiation by the air

(2) absorption of the β-radiation by the chamber walls

(3) shielding of the collecting volume by the chamber base

(4) shielding by the central electrode

(5) shielding by the rails on the floor of the ^{32}P box.

The first two corrections were determined experimentally. This is desirable since β-ray absorption curves depend on the relative dispositions of the source, absorber and detector. To find the correction factor for air absorption, a light aluminium frame (17.6 x 18.0 x 35.5 cm.) was used to support boxes of paper of various thickness, the 4π chamber being placed at the centre of the ^{32}P box. The reduction in chamber current, allowing for the reduction due to the aluminium frame, was measured for various thicknesses of paper and the mean path of the β-radiation in the paper was calculated. The mean air path was then worked out and the air absorption found. At 20°C, 760 mm. Hg pressure, a correction factor of 1.11 was found to be needed.

The wall absorption was corrected for by finding the reduction in chamber current produced when the

TABLE 8

CORRECTIONS TO READINGS

OF 4π CHAMBERS.

Effect	Correction Factor	
	Chamber 1 (11.7 mg./cm.^{2})	Chamber 2 (8.7 mg./cm.^{2})
Air Absorption	1.11	1.11
Wall Absorption	1.075	1.06
Base Shielding	1.023	1.023
Electrode Shielding	1.005	1.005
Rail Shielding	1.02	1.02
Total	1.25	1.23

chamber was enclosed in closely-fitting paper hoods of various thicknesses. The correction factor was found to be 1.075 for the ionisation chamber of 11.5 mg./cm.^{2} wall thickness and 1.06 for that of 8.7 mg./cm.^{2}.

The other corrections, which were small, were calculated (Table 8) and the total correction factor was found to be 1.25 for the first chamber (11.5 mg./cm.^{2}) and 1.23 for the second (8.7 mg./cm.^{2}).

The collecting volume of an ionisation chamber is less than its geometrical volume since a small amount of the ionisation is always collected by the guard ring. To find the collecting volume here, the ionisation chamber was enclosed in an aluminium cylinder of 3.0 mm. wall thickness and the chamber currents were measured when a radium needle of known strength (194 mg. - N.P.L. calibration) was placed at measured distances from the ionisation chamber.

According to Gray (4) and (5), the ionisation rate at 1 cm. distance from 1 mg. of radium filtered by 0.5 mm. platinum is 8.4 e.s.u./cc./hr. for an air-wall chamber (the walls of the chamber being thick enough to ensure "equilibrium" electron emission and wall absorption being corrected for). For an aluminium chamber the ionisation rate is increased, being multiplied by a factor 1.07. In the present system a factor of 1.06 was used since part of the ionisation

TABLE 9

DETERMINATIONS OF $J_{4\pi}$.

Chamber	Time	$J_{4\pi}$ e.s.u./cc./hr.	Extrapolated $J_{4\pi}$ e.s.u./cc./hr.
1	13.00 hrs. 11th Sept.	16,050	1060
2	9.00 hrs. 4th Nov.	1,230	1060
2	15.00 hrs. 7th Nov.	1,052	1065

Note: Standard time to which readings of $J_{4\pi}$ are extrapolated is 10.00 hrs. 7th Nov.

rate in the chamber was due to secondary electrons generated by the γ-rays in the paper wall of the chamber. It was necessary to employ fairly large spacings between the radium needle and the ionisation chamber to minimise the variation in γ-ray intensity over the chamber volume. The final value for uniform intensity was derived by extrapolating the curve of id^2 against d where i was the chamber current and d was the distance from the centre of the needle to the centre of the chamber.

When ionisation chambers are employed to measure high ionisation rates, the effective collecting field is reduced by the large space charges which form (Boag (15) and (16)). This effect was observed here and at the peak ionisation rate of 13,000 e.s.u./cc./hr. it was found that the voltage required to obtain complete collection of the ions was 1300 volts.

Three determinations of $J_{4\pi}$, the ionisation rate in the empty ^{32}P box were made. In each experiment the value of the chamber current was measured both before and after the volume calibration. The experiments were made over a period of two months and the values were extrapolated to a standard time using a half-life for ^{32}P of 14.5 d. (Lockett and Thomas (17)). There was remarkably close agreement in the results (Table 9). The chief sources of error were in the estimation of the chamber volume (2%), the

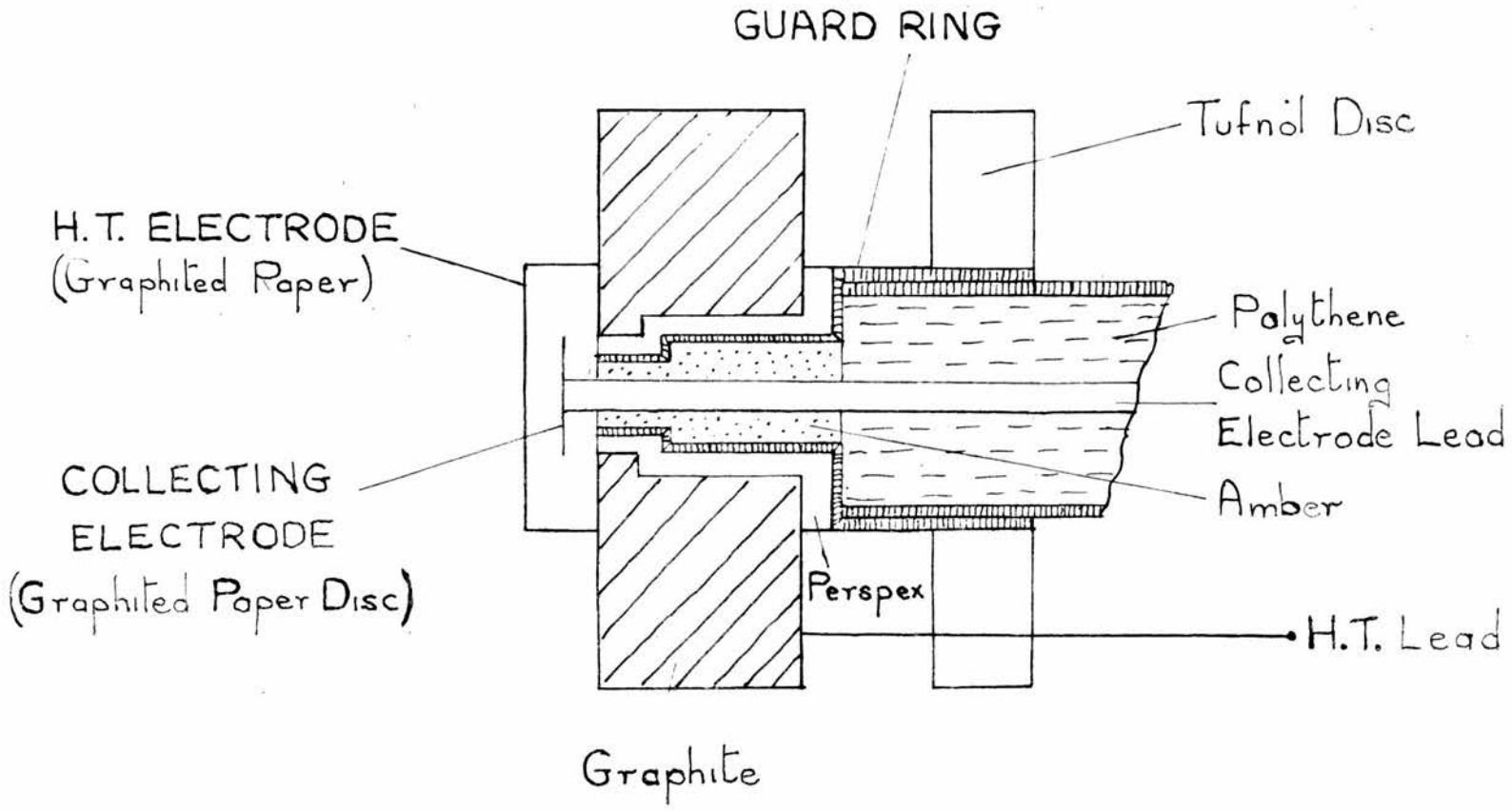

Fig. 18. "2π" Ionisation Chamber.

measurement of the current (1%) and in the determination of the chamber corrections (1%). A standard error of 2.5% in the final result accrued from these. Thus from Table 9 it was found that at the standard time and at S.T.P.

$$J_{4\pi} = 1060 \pm 25 \text{ e.s.u./cc./hr.}$$

2π Ionisation Chamber.

The 2π ionisation chamber (Fig. 18), which was used to measure surface ionisation rates, had a cylindrical collecting volume of small thickness. The high voltage electrode was a cylinder (0.90 cm. diameter, 0.24 cm. height) of thin graphited paper, the flat top being of thickness 3.5 mg./cm.^{2} and the circular wall 5.8 mg./cm.^{2}. This was supported by a solid base of diameter 2.03 cm. The base was of graphite (0.70 cm. thickness) except for the small central portion which carried the guard ring and the central electrode wire together with the intervening insulators of amber and Perspex. The Tufnol disc behind the graphite base was merely used to support the wire carrying the H.T. supply to the graphite. The collecting electrode was the small projection of the aluminium wire from the chamber stem. This was of height 0.12 cm. and of radius 0.045 cm., and was fitted with a thin disc of graphited paper (radius 0.2 cm., thickness 3.0 mg./cm.^{2}). In early

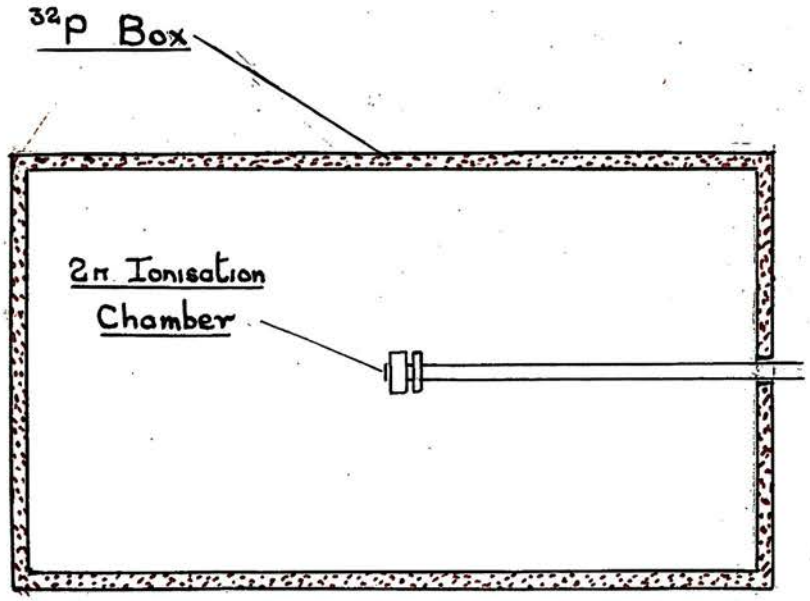

FIG. 19. Small Cylinder System.

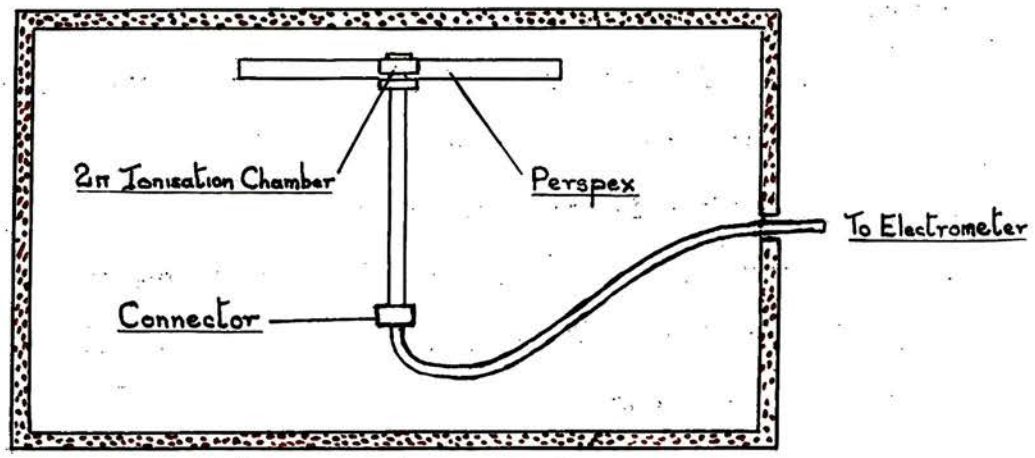

FIG. 20. Large Plane System.

experiments, when this disc was not used, it was found that the current readings were variable due to substantial ion collection on the amber insulator. When the disc was introduced this difficulty disappeared. When ionisation chambers with shallow collecting volumes are used, the current readings are sometimes erroneous due to ion multiplication. To guard against this effect and to ensure that complete ion collection was obtained, chamber current: collecting voltage curves were taken for each determination of ionisation rate.

The 2π ionisation chamber was used in two ways. In the first it was used alone (Fig. 19) and the readings of chamber current were used to find the value of $J_{2\pi}$, the surface ionisation rate, at the centre of the flat end of a cylinder of soft tissue of the same dimensions as the graphite cylinder. This system will be called the small cylinder system. In the second system (Fig. 20), the ionisation chamber was fitted so that its base lay flush or just above a thick square sheet of acrylic resin (17.2 x 17.2 x 1.0 cm.). The readings of chamber current were used to derive the value of $J_{2\pi}$ at the centre of the surface of a plane of soft tissue of the same dimensions as the sheet of acrylic resin. This system will be called the large plane system.

The corrections needed to derive the values of $J_{2\pi}$ from the chamber currents differed for the two systems and for different positions of these systems in the ^{32}P box. As with the 4π ionisation chambers, corrections were required for air and wall absorption and these were experimentally determined in the same way. It was found difficult to determine the air absorption correction for the large plane system when it lay close to the walls of the ^{32}P box. This was chiefly because of the large differences in path length of the β-rays reaching the chamber. The corrections for the small cylinder system at the centre of the ^{32}P box and for the large plane system at 1.65 cm. from the centre of one of the long sides of the ^{32}P box are given in Table 10. The correction for wall absorption includes a correction for the small absorption effect due to the paper disc on the central electrode. The correction for the shielding effect of the aluminium needle of the collecting electrode was calculated.

Two special corrections were necessary. The first arose because the chamber measured the ionisation rate at the mid-point of the chamber volume and not at the mid-point of the base as required. At the mid-point of the chamber volume the ionisation rate is greater than at the base since radiation can

reach the point over a solid angle greater than 2π. The correction required to give the ionisation rate at the base is given to a close approximation by the inverse ratio of the solid angle over which radiation is received at the mid-point to that over which it is received at the base (2π). In calculating the former solid angle allowance was made for the partial penetration of the β-rays through the edge of the graphite disc (small cylinder system) or the acrylic resin sheet (large plane system). The correction factor for the small cylinder system was 0.89 and for the large plane system 0.987.

The second correction arose because the back-scatter coefficient for soft tissue is slightly greater than for the base of the chamber. A correction factor of 1.02 was used.

The volume calibration of the 2π ionisation chamber was made in the same way as for the 4π ionisation chamber, but here the chamber was enclosed by a graphite cap of 3 mm. wall thickness. It was assumed that the ionisation rate inside a carbon chamber at a fixed distance from a radium source enclosed in 0.5 mm. platinum is 0.99 times that inside an air-wall chamber at the same distance (wall absorption being corrected for and the walls being thick enough to ensure "equilibrium" electronic

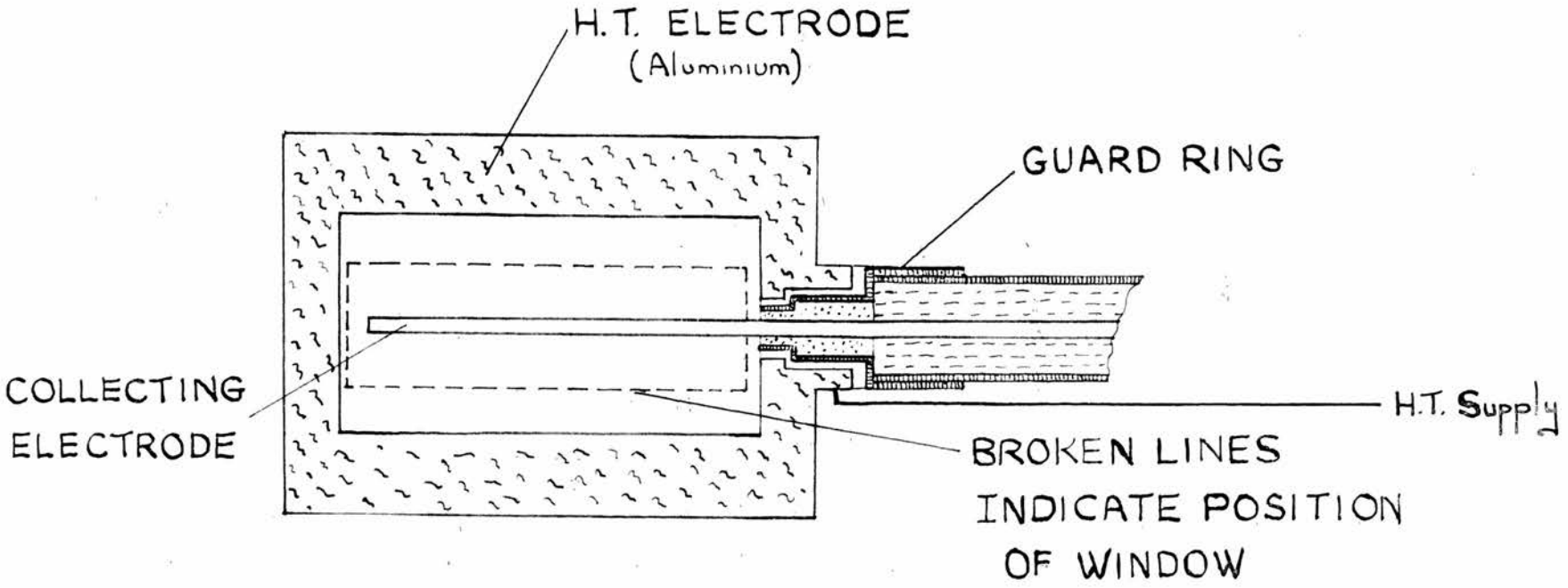

Fig. 21. Special ionisation chamber used to test uniformity of activation of walls of ^{32}P box.

emission in both cases).

Uniformity of Box.

Before describing the actual measurements of $J_{2\pi}$ for the two systems, it is convenient to digress and discuss the experimental tests on the uniformity of activity of the surface of the ^{32}P box.

In the first test a special ionisation chamber was used to survey the long sides of the box. The chamber (Fig. 21) had a cylindrical high voltage electrode with a coaxial collecting electrode and guard ring and was in general design similar to the 4π ionisation chambers. But this chamber was designed to be directional in its response. The high voltage electrode was a thick aluminium cylinder (4.0 cm. length, 1.4 cm. radius and 6 mm. wall thickness) and β-radiation was received only through a long narrow window, this being a slit of 0.9 cm. width, 3.0 cm. length covered with a thin aluminium foil (1.0 mg./cm.^{2}). The chamber thus received radiation only over a fairly small angle at right angles to its axis. The chamber was placed with its axis along the longitudinal axis of the ^{32}P box and was turned round to face the four sides in turn while readings of chamber current were taken. The readings were repeated at various distances along the axis of

TABLE 11

DETERMINATIONS OF $J_{2\pi}$

FOR LARGE PLANE SYSTEM.

Time	$J_{2\pi}$ e.s.u./cc./hr.	Extrapolated $J_{2\pi}$ e.s.u./cc./hr.
10.00 hrs. 3rd Oct.	2,715	512
13.00 hrs. 8th Oct.	2,090	502
15.00 hrs. 31st Oct.	704	513

Note: Standard time to which readings of $J_{2\pi}$ are extrapolated is 10.00 hrs. 7th Nov.

of the box.

The measurements of $J_{2\pi}$ for the large plane system (Fig. 20) were made using a light aluminium frame to support the large sheet of acrylic resin and the 2π ionisation chamber at a small distance from the centre of a long side of the ^{32}P box. The frame was inserted into the box through the hinged end and because of the intense beam of β-radiation which emerged through the open door, it was necessary to use remote-handling tools. To avoid damage to the delicate walls of the ionisation chamber in the insertion process, the spacing between the acrylic resin sheet and the walls of the ^{32}P box was not reduced below 1.65 cm.

Readings of chamber current were taken with the ionisation chamber facing the centres of the right-hand and left-hand long sides of the box. Before and after each reading the ionisation chamber was removed from the large plane system and placed alone at the centre of the ^{32}P box, where its current was read. In this way it was possible to detect any distortion of the chamber brought about by the insertion process.

Three separate determinations of $J_{2\pi}$ were made using the correction factors given in Table 10. The results (given in Table 11) extrapolated to the standard time agreed closely and it was concluded

that the surface ionisation rate at the centre of a large sheet of tissue of the same size as the sheet of acrylic resin at a distance of 1.65 cm. from the centres of the long sides of the ^{32}P box was

$$J_{2\pi} = 509 \pm 13 \text{ e.s.u./cc./hr.}$$

The experimental error was due chiefly to three causes: the determination of the correction factors (2%), the volume calibration (1.5%) and the measurement of currents (1%).

At first sight it might appear that the above value of $J_{2\pi}$ would also hold for a plane of tissue infinitely close to the walls. But as can be seen from Fig. 20 it is still possible with the above arrangement for a small amount of β-radiation from the rest of the box to be received and backscattered by the wall immediately opposite the ionisation chamber. It seems reasonable to suppose that the correction factor required to the above value of $J_{2\pi}$ will be proportional to the solid angle over which radiation from the rest of the box is received by the wall just opposite the 2π ionisation chamber. To determine the correction factor the solid angle was reduced by using an enlarged plane (34.6 x 17.2 cm.) in the large plane system and readings of $J_{2\pi}$ with the enlarged and normal plane were taken. With the normal plane a point on the wall just opposite

the ionisation chamber receives β-radiation over a solid angle of $0.185.2\pi$ and with the large plane over a solid angle of $0.130.2\pi$. The decrease in $J_{2\pi}$ brought about by using the enlarged plane was determined as $(1.4 \pm 0.8)\%$, and it was concluded that for zero solid angle the decrease would be $(4.7 \pm 2.8)\%$. Hence the correction factor by which the value of $J_{2\pi}$ for 1.65 cm. spacing must be multiplied is 0.95 ± 0.03. Therefore it was concluded that the ionisation rate at the centre of a large sheet of tissue placed infinitely close to the walls of the ^{32}P box would be

$$J_{2\pi} = 485 \pm 20 \text{ e.s.u./cc./hr.}$$

Final Results and Discussion.

A comparison can now be made of the experimental results and the theoretical predictions. It was found that at the standard time

$$J_{4\pi} = 1060 \pm 25 \text{ e.s.u./cc./hr.}$$

The value of $J_{2\pi}$ was found for two cases. In the first it was found that at the centre of the flat end of a small cylinder of tissue at the centre of the ^{32}P box

$$J_{2\pi} = 619 \pm 15 \text{ e.s.u./cc./hr.}$$

and $$\therefore J_{2\pi} = (0.58_3 \pm 0.02)J_{4\pi}.$$

The predicted value from equation (27) was, allowing for a small error (2%) in the constants,

$$J_{2\pi} = (0.59_5 \pm 0.01)J_{4\pi}$$

showing satisfactory agreement. From the measurements with the large plane system it was found that the ionisation rate on the surface of a large plane of tissue placed infinitely close to the walls of the ^{32}P box was

$$J_{2\pi} = 485 \pm 20 \text{ e.s.u./cc./hr.}$$

and $$\therefore J_{2\pi} = (0.46 \pm 0.02)J_{4\pi}.$$

The predicted value from equation (20 was

$$J_{2\pi} = (0.48_3 \pm 0.005)J_{4\pi}.$$

Here the difference lies just at the extremes of the standard errors, and the possibility arises that the difference may be a real one. But in view of the difficulties surrounding accurate measurements of surface ionisation rates, it is reasonable to suppose that the difference is due to experimental errors.

On the whole the results are in reasonable agreement with the theoretical predictions. They confirm that there is a large increase in surface ionisation rate and hence dosage rate when the air gap between the tissue mass and the walls of the ^{32}P box is large. They also show that the actual dose rates at points on tissue phantoms of simple shape where radiation transmitted through the tissue is negligible may be derived with fair accuracy ($\pm$ 5%) from measurements of the ionisation rate inside the empty ^{32}P box.

REFERENCES.

(1) Bizzell O.M., Burnett W.T. (Jr.), Tompkins P.C., and Wish L., Nucleonics 8, 17, (1951).

(2) Raper J.R., Zirkle R.E., and Barnes K.R., Effects of External Beta Radiation, (1951), Chapter I. (McGraw Hill Book Co. Inc.).

(3) Neary G.J., and Young M.E.J., J. Brit. Radiol. 27, 195 (1954).

(4) Gray L.H., Proc. Roy. Soc. A 156, 578, (1936).

(5) Gray L.H., J. Brit. Radiol. 10, 600, (1937).

(6) Gray L.H., J. Brit. Radiol. 22, 677 (1949).

(7) Neary G.J., J. Brit. Radiol. 19, 357, (1946).

(8) Jones D.E.A., and Raine H.C., J. Brit. Radiol. 22, 549, (1949).

(9) Zumwalt L.R., U.S. Atomic Energy Commission Declassified Document, MDDC 1346, (1947).

(10) Burtt B.P., Nucleonics 5, 28, (1949).

(11) Yaffe L., and Justus K.M., J. Chem. Soc. 5 Suppl. 2, 341, (1949).

(12) McInally M., and Neary G.J., J. Brit. Radiol., 26, 539, (1953).

(13) Loevinger R., Science 112, 530, (1950).

(14) Loevinger R., Radiology 62, 74, (1954).

(15) Boag J.W., J. Brit. Radiol. 23, 601, (1950).

(16) Boag J.W., J. Brit. Radiol. 25, 649, (1952).

(17) Lockett E.E., and Thomas R.H., Nucleonics 11, 14, (1953).

P A R T T W O.

STUDIES ON
THE STOPPING POWER OF LIQUID WATER.

CHAPTER I.

INTRODUCTION.

With the growth of radiobiology and radiation chemistry in recent years, there has been renewed interest in the question of whether liquid water shows any significant anomaly as regards its stopping power for α-particles. According to Bragg's law, the stopping power of a given atom is unaffected by its chemical attachment to other atoms and by the phase - gaseous, liquid or solid - in which the atom is present, and hence the stopping power of a substance may be derived when its composition and the stopping powers of its constituent atoms are known.

There are two quantities generally employed in the discussion of the validity of this law. The first is the molecular stopping power, s, of a substance at a particular α-particle energy, sometimes called the differential molecular stopping power. This is defined as the stopping power of one molecule of the substance relative to that of the average atom of air. The second quantity is the integral molecular stopping power, S, of the substance and is defined as the ratio of the range of a given α-particle in air to its range in the substance, the range in air being expressed as the number of atoms per unit area in the thickness of air traversed and the range in the

substance as the number of molecules per unit area.

If we denote the absolute stopping power of the average air atom at a particular α-particle energy as s_a and the absolute stopping power of one molecule of the substance as s_x then the molecular stopping power of the substance is

$$s = \frac{s_x}{s_a} \qquad (1).$$

The integral molecular stopping power of the substance for an α-particle of energy E is then

$$S = \frac{\int_0^E \frac{1}{s_a} dE}{\int_0^E \frac{1}{s_x} dE} \qquad (2).$$

If s_a and s_x vary in exactly the same way with energy then s and S will be equal. The Bragg law is often assumed to hold for both s and S, but it would appear more likely to apply to s and discrepancies in the value of S might be expected due to different variations of s with energy for the constituent atoms of a substance.

In an extensive review of the experimental evidence available in 1944, Gray (1) concluded that the integral molecular stopping powers of polyatomic gases for α-particles of energy 5.3 MeV to 8.8 MeV could be derived to an accuracy of $\pm$ 2% from their constituent atoms using the Bragg law. The evidence for the validity of the law for solid materials is not so extensive but measurements on mica by

Bennett (2), on polythene by Wilkinson (3) and on polystyrene by Ellis, Rossi and Failla (4), reveal no anomalies greater than ± 3%. Recent measurements by Phelps, Heubner and Hutchinson (5) on the stopping powers of various organic materials at an α-particle energy of 6.0 MeV reveal small anomalies which are less than 4.5%.

The question of whether the Bragg law applies to liquid water has been the subject of several investigations but conflicting results have been obtained. An early experiment by Michl (6) gave a range for Po α-particles 20% less than would be expected from the ranges in hydrogen and oxygen, indicating that the integral molecular stopping power of liquid water is 20% greater than the prediction of the Bragg law. Another early experiment by Philipp (7) revealed a similar anomaly for the range of RaC' α-particles. More recently, Appleyard (8) found that the molecular stopping power for α-particles at an energy of approximately 4.5 MeV is 15% greater than expected. On the other hand measurements of the ranges of the α-particles of Po and RaC' by de Carvalho and Yagoda (9) reveal anomalies of much smaller amount, namely 3% for Po α-particles and 4% for RaC' α-particles. Recent measurements by Ellis, Rossi and Failla (10), reveal no difference in stopping power for Po α-particles

between water in the liquid phase and in the vapour phase. It may be added that Förster (11) found a small anomaly (3%) for the molecular stopping power of water vapour for α-particles of mean energy about 4.0 MeV but this is of the opposite sign from those reported for liquid water. Appleyard (12) found that the range of Po α-particles in water vapour agrees with the prediction of the Bragg law.

The present investigation was planned to find the molecular stopping power of liquid water at an α-particle energy of about 6 MeV. It was at first hoped to do this by using a small cell with a thin layer of liquid water enclosed by two thin windows and finding the air equivalent of the cell with and without the water layer. This method was found impracticable due to the ease with which the water layer was distorted and due to the difficulty in obtaining a uniform water layer. Instead it was decided to use an agar gel containing a high percentage of water in place of ordinary water, and this artifice proved successful. An agar gel containing 2.5% by weight of agar is surprisingly rigid and a layer of the gel has the same air equivalent to an accuracy of 0.5% as a layer of equal mass thickness of water even if the molecular stopping power of water is anomalous to the extent of 15%. In the present experiments a thin layer of this gel was enclosed in

thin mica covers to form a mica-agar sandwich and the air equivalent of the layer of gel was found by determining the air equivalents of the sandwich with and without the gel present. The measurements were made with a source of ThC' α-particles. A calibrated β-ray thickness gauge using a source of ^{35}S was used to measure the mass thickness of the agar layer. From the two measurements the thickness of gel equivalent in stopping power to 1 cm. of dry air at 15°C and 76.0 cm. Hg pressure was found and hence the stopping power of one molecule of water relative to the average atom of air was derived.

The β-ray thickness gauge and the construction of the mica-agar sandwiches are described in Chapter II. In Chapter III the application of the β-ray gauge to the measurement of the thickness of a layer of agar gel in a mica-agar sandwich is described and details are given of the methods by which the calibration was made. Finally in Chapter IV the method of determining the air equivalent of the layer of agar gel and the experimental measurements from which the molecular stopping power of liquid water was deduced are described.

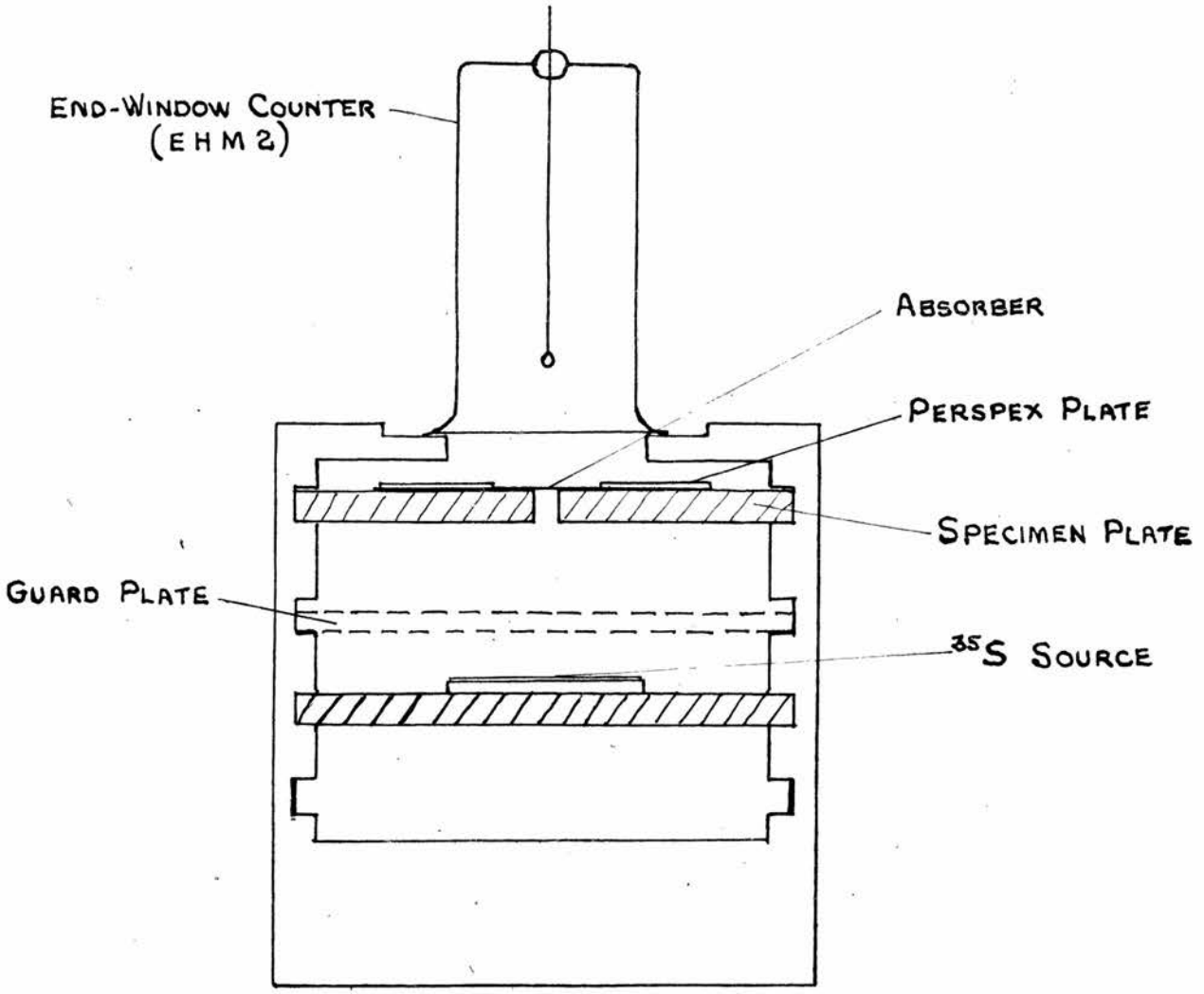

FIG. 1.

Construction of β-ray thickness gauge.

CHAPTER II.

BETA-RAY THICKNESS GAUGE AND CONSTRUCTION OF MICA-AGAR SANDWICHES.

β-ray Thickness Gauge.

It is convenient to describe first the β-ray thickness gauge as this was employed for a variety of purposes during the investigation. The application of the gauge to the measurement of the thickness of a layer of agar gel enclosed in mica covers is described in Chapter III.

The radioactive isotope of sulphur, ^{35}S, forms a suitable source for a β-ray thickness gauge for the measurement of thin films of the order of 5 mg./cm.^{2} thickness, since it emits only β-radiation of maximum energy 0.167 MeV and in a suitable geometrical system has an absorption coefficient of roughly 0.28 cm.^{2}/mg. corresponding to a half-value layer of 2.5 mg./cm.^{2}. It has the advantage of a reasonably long half-life, 87.1 days, and a source once prepared can be used over a period of several months.

The gauge used (Fig. 1) consisted of a thick source of ^{35}S placed below an end-window Geiger-Muller counter with the absorber under measurement inserted between the source and the counter. The counter was an EHM2 tube of internal diameter 2.54 cm. with a mica end-window of 2.1 mg./cm.^{2} thickness,

and was mounted on a standard counting stand inside a square lead castle. The source was a disc of blotting paper of 14.0 mg./cm.^{2} thickness and 2.5 cm. diameter, impregnated with ^{35}S and fixed by adhesive to a thin aluminium disc which was mounted on a standard plate. The plate was inserted on the third shelf of the counting stand so that the paper disc lay 3.5 cm. from the counter window. The impregnation of the paper disc with ^{35}S was carried out by adding some drops of a dilute solution of carrier-free ^{35}S and allowing the disc to dry. In order to fix the ^{35}S to the paper, a few drops of amyl acetate to which a trace of Durofix adhesive had been added were placed on the paper disc and the disc finally dried. The specimen plate, on which the absorbers under measurement were placed, was a brass plate of 4.2 mm. thickness and had a central hole of 3.0 mm. diameter. It was mounted on the first shelf below the counter so that its top surface was 0.80 cm. from the counter window. Both the source plate and the specimen plate were specially made to give very close fits in their respective shelves. The second shelf was used to carry a guard plate, which was inserted before the specimen plate was withdrawn, to prevent the counter being subjected to an intense beam of β-radiation.

The source strength was adjusted to give a counting rate of roughly 13,000 counts per minute

Fig. 2. Calibration curves with ^{35}S thickness gauge.

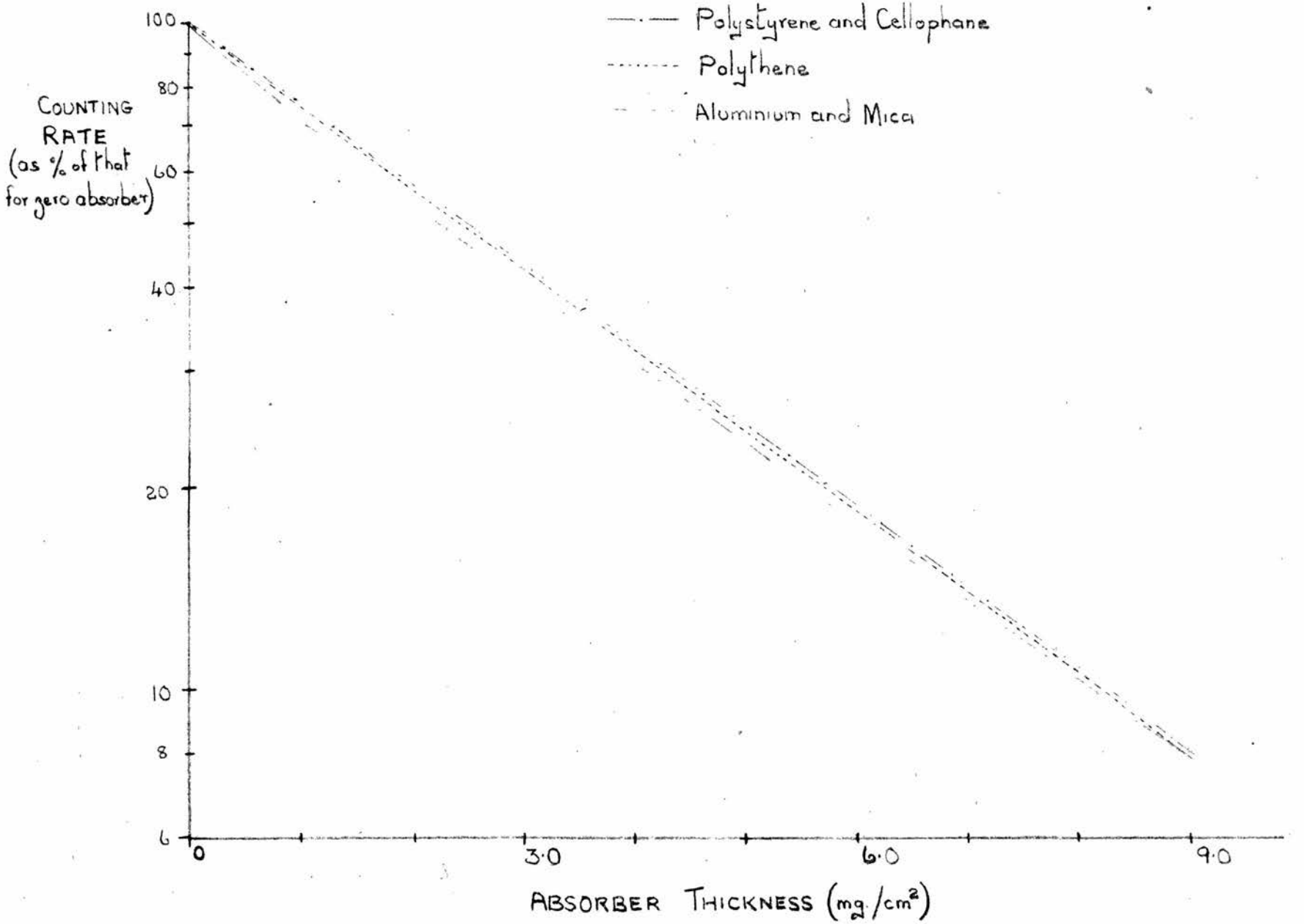

with no absorber on the specimen plate. In carrying out measurements it was found that a small Perspex plate of 1.0 mm. thickness with a central aperture of 1.5 cm. diameter, which could be screwed down on top of the specimen plate, was useful for keeping flat certain absorbers such as cellophane which tend to curl. Careful measurements with and without the Perspex plate in position showed that the addition of the Perspex plate produced no change in counting rate to an accuracy of $\pm$ 0.3%.

A β-ray thickness gauge must of course be calibrated for any particular material before use. Calibration curves for aluminium, mica, polystyrene, cellophane and polythene are shown in Figure 2. The method employed in obtaining these curves was to prepare small sheets of the materials of area roughly 3.0 x 3.0 cm. and determine their average mass thickness by weighing them and measuring their areas. Each sheet was measured with the β-ray thickness gauge at nine points, the sheet being divided into nine squares, and if the sheet was uniform to within a few per cent., the mean of the readings was taken as corresponding to the average thickness of the sheet.

All readings of counting rate require correction for losses due to the dead-time of the counter and for the background counting rate. Frequent

readings of the zero-absorber counting rate are necessary since small changes may occur. In addition to the effect of temperature variations on the counter, there is another effect due to the long air path, 3.5 cm., between the source and the counter. At 15°C and a pressure of 76.0 cm. Hg the thickness of the air between the source and counter is 4.3 mg./cm.^{2}, and a change of 1% in the absolute temperature or the pressure changes the zero-absorber counting rate by roughly 1%.

The calibration curves show that mica and aluminium give quite different curves from those obtained with the other materials. It is possible to obtain approximately the same curve for all five materials up to thicknesses of 5 mg./cm.^{2} by placing a fixed screen of 3 mg./cm.^{2} of mica over the aperture of the specimen plate, but in the present investigation this additional screen was not used.

The accuracy conveniently obtainable in the measurement of an absorber of unknown thickness with a β-ray gauge of the present type is of the order of $\pm$ 1.0%. There are two determinations of counting rate to be made, one with the absorber present and one with it absent, and these are always subject to a statistical error due to the random variations in the disintegration rate of a radioactive substance. If the calibration curve is assumed exponential and the

half-value layer m_o has been determined to high accuracy, then if Δr denotes the statistical error in r, the ratio of the counting rate for the absorber to that for zero absorber, the standard error Δm in the determination of m, the mass thickness of the absorber, is given by

$$\left(\frac{\Delta m}{m}\right) = \frac{m_o}{m \log_e 2}\left(\frac{\Delta r}{r}\right) \qquad (3).$$

Therefore for a gauge having a zero-absorber counting rate of 10,000 counts/min., a measurement accurate to ± 1% for an absorber approximately equal to the half-value layer requires a counting period of 4 minutes for the absorber reading and a counting period of 2 minutes for the zero-absorber reading. This is on the assumption that no other sources of error affect the measurement. In practice the calibration curve is difficult to determine to an accuracy better than 1.0%, and an allowance must be made for this.

The salient advantages of the gauge are its simplicity and the fact that it measures the thickness of an absorber over a small area. It is extremely useful for testing the uniformity of absorbers. Its applications in the present investigation are described in the course of the report.

Mica-Agar Sandwiches.

In the determination of the stopping power of water the measurements were made on a thin layer of

agar gel enclosed in mica covers, i.e. a mica-agar sandwich. The sandwiches had mica covers ranging from 1.65 to 2.3 mg./cm.^{2} and the thickness of agar gel used varied from 1.9 mg./cm.^{2} to 3.7 mg./cm.^{2}. Each sandwich had mica covers of nearly equal thickness. The pieces of sandwich used were squares of 1.5 cm. side and these were mounted inside a small brass holder with a central aperture of 5.0 mm. diameter (Fig. 3).

Each small piece of sandwich was cut from a selected area of a large sheet of the order of 8.0 x 8.0 cm. in area. The mica sheets used in the large sandwiches were all obtained from the same piece of Bengal Ruby mica, this mica being of the muscovite group. A given sheet of mica was split into two sheets by using a very fine tungsten needle to make the initial split and then completing the separation by inserting a small piece of moistened cardboard to force the sheets apart. With this technique it was possible to obtain thin sheets almost free from scratches. In all about two hundred thin sheets of thickness ranging from 1.65 to 2.3 mg./cm.^{2} were prepared. The β-ray thickness gauge was used to measure the sheets, an accurate calibration being made beforehand.

The agar gel was made with powdered agar supplied by the Oxo Laboratories. Agar is made from seaweed

CHAPTER III.

MEASUREMENT OF THICKNESS OF AGAR GEL LAYERS.

Method.

The major difficulty in this investigation was the accurate measurement of the thickness of the agar gel layers in the mica-agar sandwiches. The possibility of measuring the thickness with an optical microscope was explored but due to the difficulty of locating the surfaces of the layer, the possibility of errors due to the birefringence of mica and the difficulty of obtaining a suitable microscope, it was decided to seek some other method.

The device chosen was the β-ray thickness gauge, the method being to place the mica-agar sandwich on the specimen plate and find the ratio of the counting rate for the complete sandwich to that obtained with the agar gel absent. The method seemed sufficiently sensitive for layers of agar gel of thickness 1.5 to 3.5 mg./cm.^{2} and the sole difficulty was establishing the calibration curve for the device.

In the early experiments on this method it was found that the counting rate obtained with an absorber placed in the brass holder used for the mica-agar sandwiches and with the holder mounted centrally on the specimen plate agreed to an accuracy of $\pm$ 0.2% with the counting rate obtained with the

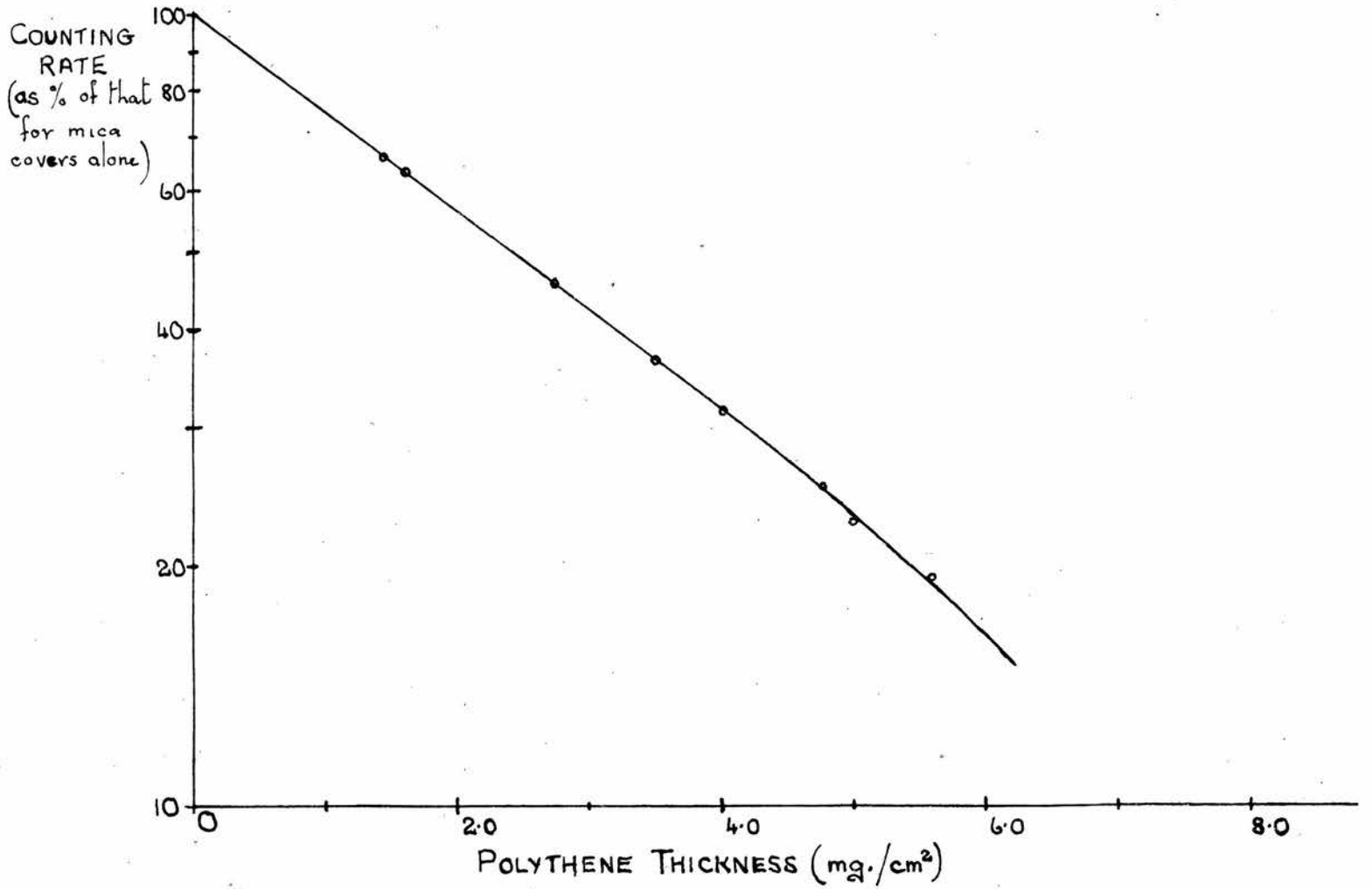

FIG. 4. Calibration curve showing how counting rate of system decreases as thickness of polythene layer enclosed in mica covers increases.

absorber merely placed on the specimen plate. The absorbers used in this test ranged from 1.5 mg./cm.^{2} to 9.0 mg./cm.^{2}. It follows that a calibration curve obtained for mica-agar sandwiches merely placed on the specimen plate will also hold for sandwiches mounted in the holder and placed on the plate.

It was decided to carry out trial experiments first with various solid materials replacing the agar gel layer in a mica-agar sandwich. Since the thickness of the absorbers could be found directly, calibration curves for the materials could thus be obtained. Two sheets of mica each of 2.0 mg./cm.^{2} thickness were selected as the covers and to ensure that these could be accurately replaced in the same position on the specimen plate, small ink circles were made around the portion placed over the aperture of the specimen plate. The counting rate with the mica covers on the specimen plate was determined, an absorber of known thickness was placed between the mica covers and the counting rate again determined. Readings were taken with absorbers of polythene, polystyrene, cellophane, mica and aluminium ranging in thickness from 1.0 to 5.5 mg./cm.^{2}. The calibration curve obtained with polythene (Fig. 4) is approximately exponential but there is a small increase in slope with thickness beyond 4.0 mg./cm.^{2}. The half-value layers obtained with the five absorber

TABLE 1

HALF-VALUE LAYERS WITH BETA-RAY THICKNESS GAUGE FOR MATERIALS INSIDE MICA COVERS

Thickness of Single Mica Cover = 2.0 mg./cm.^{2}

Half-value layer reduces counting rate (with mica covers alone) by 50%.

Material	Half-value Layer mg./cm.^{2}
Polythene	2.43 ± 0.03
Polystyrene	2.53 ± 0.05
Cellophane	2.52 ± 0.06
Mica	2.55 ± 0.03
Aluminium	2.58 ± 0.03

TABLE 2

CORRECTIONS FOR MICA COVERS.

If mica covers different from 2.0 mg./cm.^{2} are used to enclose polythene, readings of polythene thickness from calibration curve for 2.0 mg/cm.^{2} covers require correction.

Thickness from Calibration Curve mg./cm.^{2}	Correction mg./cm.^{2}	
	Cover (1.65 mg./cm.^{2})	Cover (2.35 mg./cm.^{2})
2.00	+ 0.02	- 0.04
3.00	+ 0.02	- 0.06
4.00	+ 0.03	- 0.08
5.00	+ 0.04	- 0.11
6.00	+ 0.05	- 0.13

materials (Table 1) show a change of 6.0% in going from polythene to aluminium, but there is a difference of only 4% between polythene and polystyrene. This suggests that the calibration curve for layers of agar gel will not differ by more than 4% from that for polythene in view of the fact that the electronic density of water (number of electrons per gm.) is intermediate between the electronic densities for polythene and polystyrene.

The calibration curve obtained for polythene is not greatly affected by using mica covers of thickness 1.65 mg./cm.^{2} or 2.35 mg./cm.^{2} in place of the 2.0 mg./cm.^{2} covers. Measurements were made with these two thicknesses of cover enclosing polythene absorbers. The ratio of counting rates obtained with the thinner covers for a given polythene sheet was slightly greater than the ratio obtained with the 2.0 mg./cm.^{2} covers, while the ratio obtained with the thicker covers was always less. From the results obtained with these covers, corrections were derived (Table 2) so that values of thickness read from the calibration curve for 2.0 mg./cm.^{2} covers could be adjusted to give the true values.

Direct Calibration of Gauge.

In view of the reported anomaly in the stopping power of water for α-particles it was thought that perhaps a similar anomaly might occur in respect of absorption curves obtained with soft β-radiation. The fact that these so-called absorption curves are determined by both scattering and absorption does not rule out the possibility of some anomaly existing. It was therefore decided to attempt a direct calibration of the gauge for mica-agar sandwiches. The plan was to prepare a fairly uniform sheet of sandwich, measure the thickness of the agar layer at a large number of points by assuming that the calibration curve for polythene held for water, and thus find the mean thickness of the agar layer. This value could then be compared with that obtained by weighing the sheet of sandwich with and without the agar layer present and the correction required in the assumed calibration curve could then be worked out.

Trials were carried out with small areas of sandwich roughly 2.5 x 2.5 cm. in area and it was found possible to reduce the variation in thickness of the layer of agar gel to within $\pm$ 15%. It was decided to measure the thickness with the β-ray gauge at nine points, the points being at the centres of the nine squares into which the sheet was geometrically divided. Measurements with various sheets

showed that there was negligible change in counting rate at any of these points over a period of ten minutes, and that therefore a sheet could be assayed by counting at these points for a period of 30 seconds each, allowing time for moving the sheet on the specimen plate.

There are however some pitfalls in this method. The small sheet of sandwich is cut from a large sheet and in the cutting process the perimeter of the small sheet is compressed so that in this region the layer of agar gel is reduced in thickness. Further, evaporation losses occur from the perimeter during the measurements with the β-ray gauge, and the rate of evaporation is not constant, being greatest immediately following the cutting and then decreasing rapidly. The β-ray determination of average thickness of the layer of agar gel corresponds to a sheet which is perfectly cut and free from evaporation losses so that all perimeter effects are negligible. The determination of the average thickness by weighing is affected by the perimeter effects and these must be corrected for to give the average thickness of a perfect sheet. The error made by neglecting this correction may amount to about 15%, and in fact in early experiments when this correction was deemed negligible, results were obtained which seemed to show that water had a much lower half-value layer

TABLE 3

DIRECT CALIBRATION OF BETA-RAY GAUGE

Sheet	Perimeter Correction as % of thickness	Agar Gel Thickness mg./cm²		% Error in Gauge
		β-ray Gauge	Weighing	
1	16.2	1.95	1.88	+ 3.6
2	14.5	2.43	2.45	- 0.8
3	12.7	2.29	2.23	+ 2.6
4	10.5	2.49	2.40	+ 3.6
5	12.0	5.06	5.18	- 2.4
6	14.0	5.12	5.40	- 5.5
7	10.5	5.20	4.94	+ 5.0
8	11.5	5.48	5.25	+ 4.2
Mean Value				+ 1.3

measured at six places and the error in the determination of the area was estimated at ± 2%. The square was then weighed at a noted time. The perimeter effects were then corrected for by the procedure detailed above, and the corrected weight of the square was found. As the mica sheets were of known thickness, the corrected thickness of the agar gel layer was thus found. The standard error in the corrected thickness was estimated at 3%, arising chiefly in the determination of the perimeter correction (2%) and the measurement of area (2%). The standard error in the measurement of thickness by the β-ray gauge was estimated at 2%.

In Table 3 the results are given for the eight sheets tested. In the first column is given the correction for the perimeter effects, and in the second and third columns the mean thicknesses derived by weighing and by the gauge. In the final column the percentage error in the gauge reading is given. The estimate of each error is subject to an error of ± 4%, due to the errors in the determinations of thickness. In the region of 2.3 mg./cm.^{2} there is the possibility of a small systematic error in the gauge of less than 3%, but viewing the results as a whole it seems reasonable to conclude that the polythene calibration curve is valid for the agar gel to an accuracy of ± 3%.

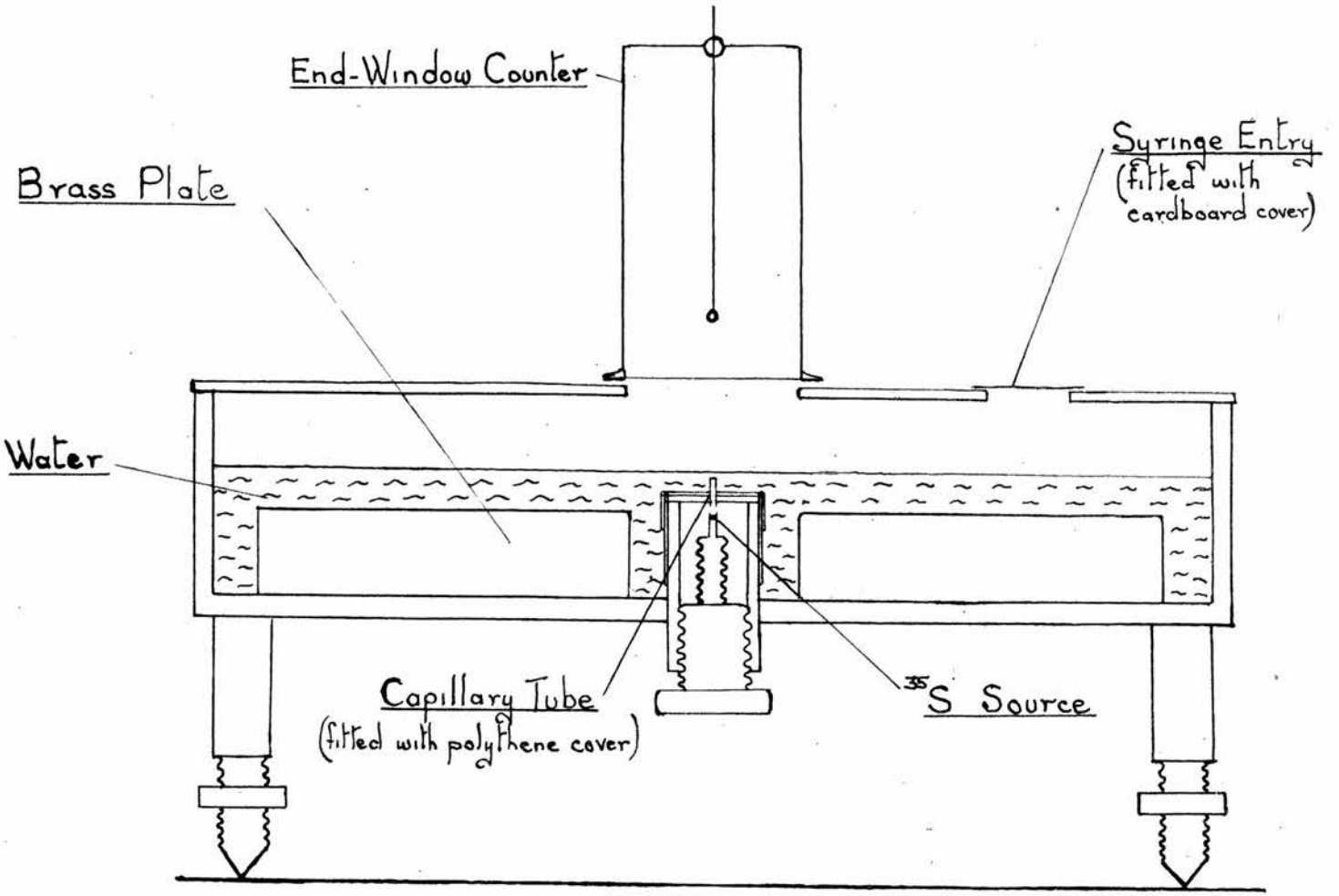

FIG. 5. Apparatus used to investigate absorption of ^{35}S β-radiation in water.

Wide Tank Experiment.

As the direct calibration of the gauge is a difficult procedure, an independent test was carried out to find if there was any difference in the absorption curves for polythene and water for ^{35}S β-radiation.

The principle in this experiment is to mount a capillary tube with a flat cover on top below the water surface in a large tank, place a ^{35}S source below the capillary tube and an end-window counter above, and determine the change in counting rate as the water level is altered. In such a system the change in level of water can be accurately controlled and measured by withdrawing or adding a weighed amount of water with a hypodermic syringe. The thickness of the water layer above the capillary tube can be reduced only to a certain level which depends on the degree of flatness and horizontality of the capillary top, but above this level an absorption curve can be determined. An absorption curve for polythene can then be derived by removing the water and placing polythene absorbers on the cap. By allowing for the zero level of water above the capillary tube in the water measurements, it is possible to compare the two curves and detect any significant difference between the two materials.

The wide tank used (Fig. 5) was of brass and was

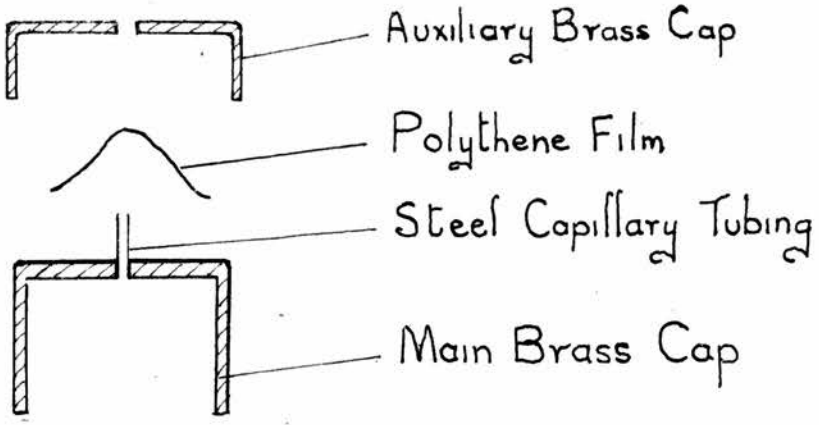

FIG.6. Components of Holder for Capillary Tube

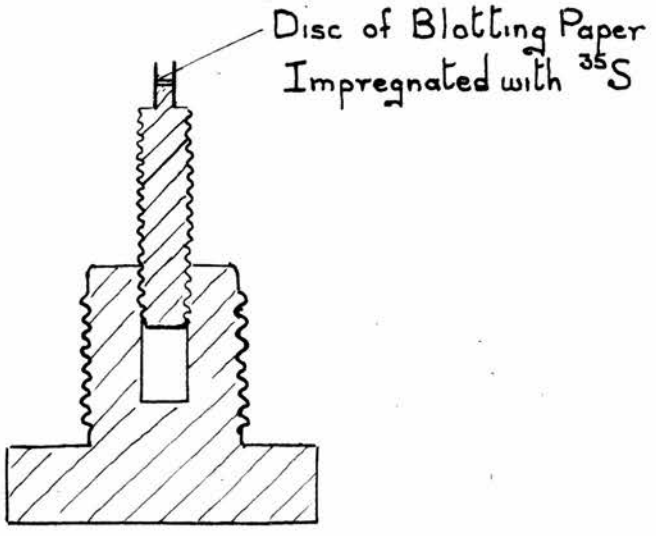

FIG. 7 ^{35}S Source

mounted on three levelling screws. Its internal diameter was 14.30 cm. and its depth 2.90 cm. At its centre was fitted a small hollow brass stem of diameter 1.25 cm. and the brass holder carrying the capillary tube was placed on this stem. The stem protruded 1.0 cm. below the base of the tank and was threaded so that a ^{35}S source mounted on a screw could be inserted below the capillary tube. The tank was fitted with a circular plate of brass, of diameter 13.0 cm. and height 1.25 cm. with a central hole of 2.50 cm. diameter, to reduce the total volume of water in the tank. A thin brass lid was screwed to the top of the tank and this had a central aperture of 2.54 mm. diameter above which the counter was placed. There was also a small hole, 1.27 cm. diameter, at 3.0 cm. from the edge of the lid through which a syringe could be introduced to withdraw or add water to the tank.

The brass holder (Fig. 6) which fitted on the central stem consisted of two main parts. The first was a brass cap of height 1.2 cm. and soldered into a central hole in its top surface was a 4.0 mm. length of surgical steel tubing of external diameter 0.8 mm. and internal diameter 0.5 mm. The second part was an auxiliary cap of brass with a small hole of 1.2 mm. diameter drilled at the centre of its top surface. It was 0.5 cm. high and was machined to fit closely

over the first cap. The auxiliary cap was used to hold down a cover of thin polythene over the steel capillary tubing. Before fitting the cover the top of the capillary tube was carefully ground flat. Then the top surface of the main brass cap was lightly smeared with Durofix adhesive. A piece of polythene sheet about 1.0 x 1.0 cm. in area and of 1.2 mg./cm.^{2} thickness was next placed to form a small tent over the capillary tube, the adhesive securing the base of the tent to the top surface of the main brass cap. The auxiliary brass cap was then pushed on to the main cap, this causing the polythene to be pulled down to form a taut skin over the capillary tube. The polythene cover over the top of the capillary tube was inspected with a microscope to detect any scars or pinholes. Usually three or four covers were fitted before a satisfactory one was found. With the auxiliary cap in position the length of capillary tubing above the holder was 1.5 mm.

The source of ^{35}S β-radiation (Fig. 7) was a small piece of blotting paper (14.0 mg./cm.^{2}) and was of approximately 1.0 mm. diameter. This piece of paper was placed in 1 millicurie of carrier-free ^{35}S solution in a standard Harwell isotope bottle, the solution was dried by an overhead lamp and the paper was removed. It was then fixed with a little adhesive in a small cavity 1.0 mm. deep at the top of a

thin brass rod. The rod was fitted to a screw and inserted in the stem of the brass tank so that the paper source was approximately 5.0 mm. below the top surface of the capillary tube.

The counter was an EHM2 tube with a mica end-window of 2.2 mg./cm.^{2} thickness and was mounted 1 mm. above the central aperture of the lid so that its window was 1.6 cm. above the top of the capillary tube. The syringe used had a capacity of 2.0 cc. and was fitted with a needle of 1.0 mm. external diameter. The weighings of the syringe were carried out on a quick-weighing Stanton chemical balance.

Before use the wide tank was carefully cleaned. Then the brass holder carrying the capillary tube was inserted on the stem and the source placed in position. The counting rate was then measured. After this the tank was flushed several times with distilled water. It was finally filled with distilled water containing a minute amount of Teepol, the concentration being 100 mg. per litre. The addition of this Teepol removed a troublesome tendency of the water surface to recede from the top of the capillary tube. Any bubbles of air on the water surface and on the brass were carefully removed.

Rough absorption curves were first taken by adjusting the water level above the capillary tube to about 12 mg./cm.^{2} thickness and reducing the level by

removing known quantities of water with the syringe. Since the area of the tank was 160.6 cm.^{2}, removal of 0.1 cc. of water produced a reduction of 0.622 mg./cm.^{2} in the water level. At a certain level there was a sharp bend in the absorption curve indicating that the water surface was being affected by the top surface of the capillary tube. The tank setting was then adjusted by means of the levelling screws so that this bend in the absorption curve occurred at the smallest possible level of water. The minimum value was found to occur at a water level corresponding to a uniform layer of 2.5 mg./cm.^{2}.

The zero level of the water was then fixed slightly above this at a thickness of 3.0 mg./cm.^{2} and the absorption curve was carefully determined by finding the reduction in counting rate brought about by increasing the level of the water by known amounts. The procedure followed was to weigh the syringe, containing about 2,0 cc. of water, in a small cardboard box, while at the same time determining the counting rate at the approximate zero level. A small quantity of water was then added to the tank, the divisions on the syringe stem being used as a guide and the exact amount being found by reweighing. The addition of the water was made slowly and no bubbles of air were formed. About 30 seconds after the addition a determination of the new counting rate was

FIG. 8. Absorption of ^{35}S β-radiation in water using wide tank. Zero level was taken at a mean thickness of water of 3.0 mg./cm.^{2}.

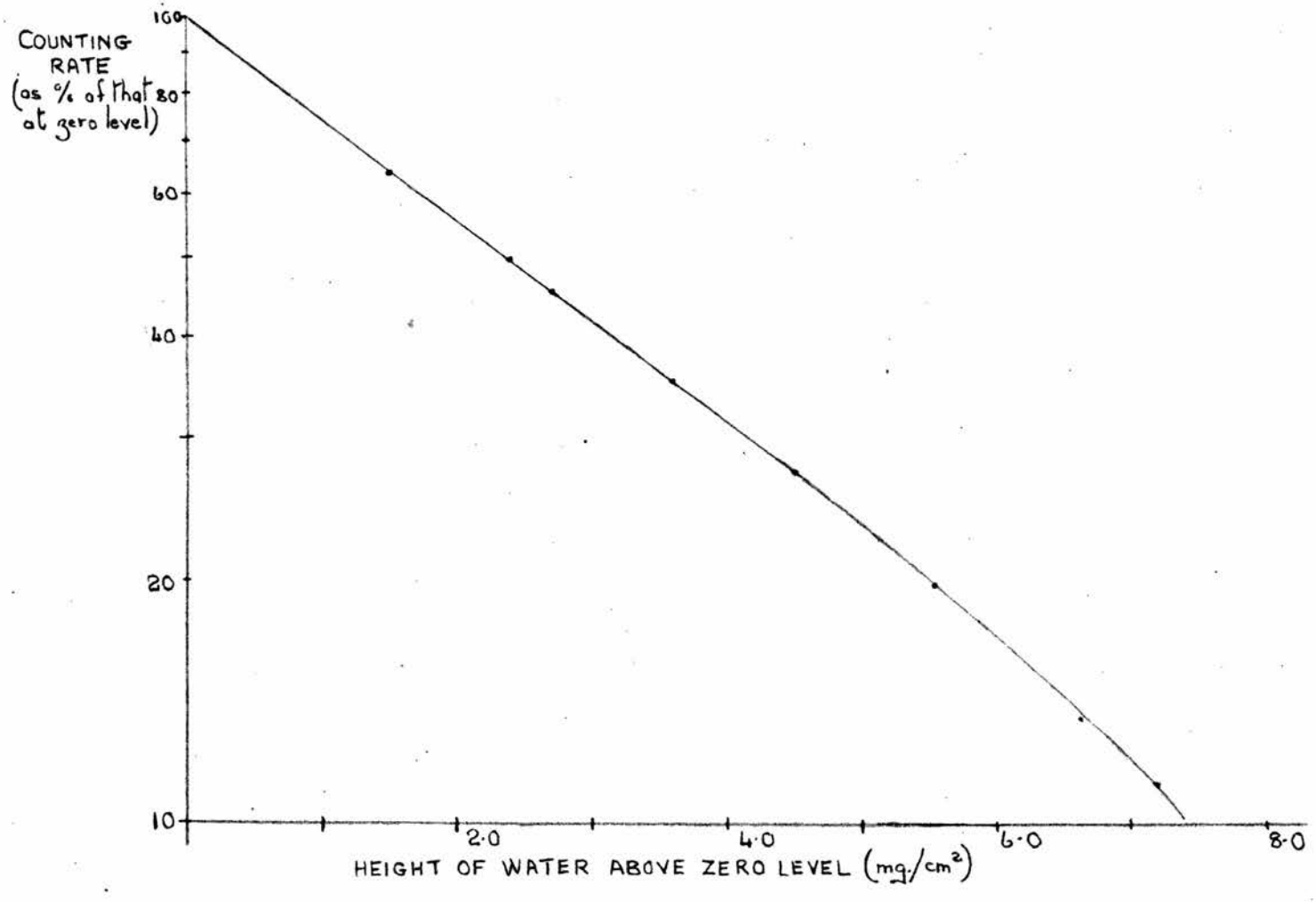

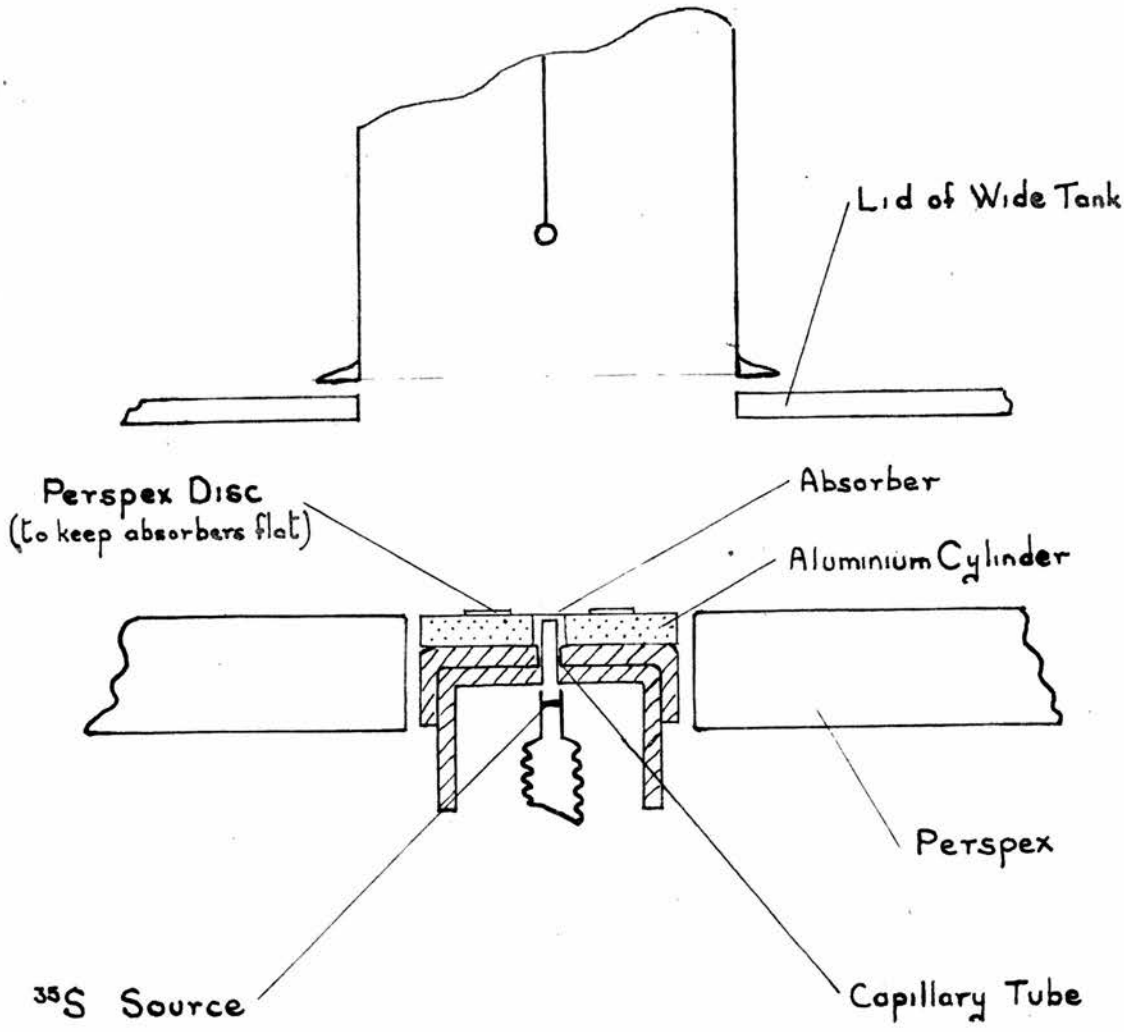

FIG. 9. Modifications to apparatus shown in Fig. 5 to investigate absorption of ^{35}S β-radiation in polythene and polystyrene.

made and the reduction in counting rate calculated. The syringe was then used to withdraw a quantity of water roughly equal to that which was added, the exact amount being determined by weighing, and the alteration in counting rate was found. From the quantity withdrawn, usually about 5% less than that added, the change in counting rate produced by a layer of the same thickness as was first added was calculated. The two changes in counting rate obtained by adding and removing water differed usually by less than 3% and the mean of the two changes was taken as the final value. By carrying out the determination in this way any steady change in the water level due to evaporation or alteration in temperature was corrected for. By using different alterations in level up to 7.2 mg./cm.^{2}, the absorption curve in water above the zero level was determined.

The absorption curve obtained (Fig. 8) is closely exponential with a half-value layer of 2.40 mg./cm.^{2} down to a thickness of 5 mg./cm.^{2}. Beyond this the curve begins to slope more steeply.

Absorption curves for polythene and polystyrene absorbers were next determined. The tank was drained and the polythene cap dried. A small aluminium cylinder (Fig. 9) with a central hole of 2.0 mm. was fitted on the brass holder carrying the

capillary tube. The surface of the cylinder was less than 0.5 mm. above the top of the capillary tube, so that absorbers placed on the cylinder were fairly close to the polythene cover on the capillary tube. The aluminium cylinder was surrounded by a disc of Perspex to simulate the conditions in the measurement of water absorption. The lid of the tank was kept in position as it was found that slightly different readings were obtained when it was removed.

In carrying out the measurements it was found desirable to use a small thin disc of Perspex with a central hole of 5 mm. diameter to keep the absorbers flat. It was also found that when a polystyrene absorber was placed in position for a short time and then removed the counting rate was often about 6% lower than its original value and that it slowly returned to this value in a period of about five to ten minutes. No explanation of this effect could be found other than that it was due in some way to electrostatic forces. The effect disappeared when a thin aluminium leaf (0.2 mg./cm.^{2}) was placed over the central aperture of the aluminium cylinder, and this leaf was retained during the rest of the measurements.

It was found that the absorption curves (Fig.10) for both polythene and polystyrene were both closely

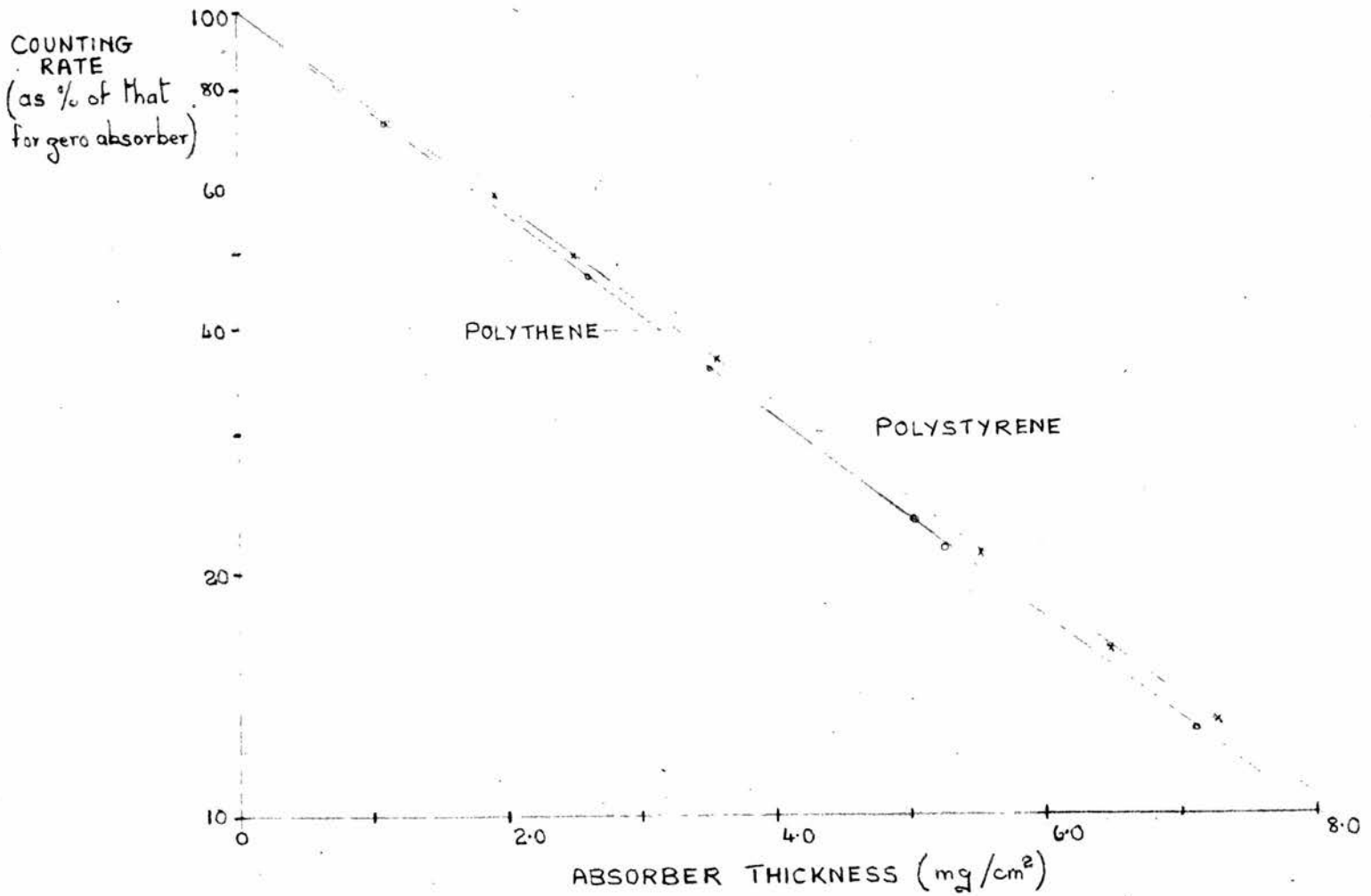

FIG. 10. Absorption of ^{35}S β-radiation in polythene and polystyrene using "wide tank" apparatus.

exponential up to 7.5 mg./cm.^{2}. The half-value layer for polythene was 2.37 mg./cm.^{2} while that for polystyrene was 2.50 mg./cm.^{2}. Before comparing the absorption curves in polythene and water it should be noted that in the water measurements the layer of water used as the zero level, although equivalent to a uniform layer of 3.0 mg./cm.^{2}, was probably not uniform above the aperture of the capillary tube. However, with a uniform layer one would expect that the same absorption curve as the experimental one would be obtained over the main portion with a possible difference in the region where the curve begins to bend down. It therefore seems reasonable to compare the water curve up to 4.5 mg./cm.^{2} thickness with the polythene curve in the region from 2.8 mg./cm.^{2} to 7.3 mg./cm.^{2}. Both curves are exponential in these regions, water giving a half-value layer of 2.40 mg./cm.^{2} and polythene 2.37 mg./cm.^{2}. Since the experimental error in both values is about 2%, it appears that to an accuracy of 3%, absorption in polythene and water are the same.

Discussion.

Although the geometry used in the above experiment is different from that in the β-ray thickness gauge, the half-value layer obtained, 2.37 mg./cm.^{2}, is fairly close to that found for polythene sheets

placed alone on the specimen plate (2.43 mg./cm.^{2}). It therefore seems probable that the absorption curve measured with the β-ray thickness gauge for polythene films inside mica covers will also hold for layers of the agar gel inside similar mica covers. The results of the experiment in which a direct calibration of the gauge was attempted lead to a similar conclusion. It was therefore decided to take the calibration curve for polythene as holding also for the agar gel in measuring the thicknesses of the agar gel layers in mica-agar sandwiches in the main experiment and allow for a possible error of ± 3% in the values of thickness obtained.

It may be added that the above apparatus used to compare the absorption of ^{35}S β-radiation in water and polythene can be modified to study the stopping power of liquids for α-particles. By using a source of ThC' α-particles in place of the ^{35}S source and using a movable proportional counter mounted on a vernier movement it appears possible to find the air equivalent of a small increment in thickness of the liquid level. Preliminary tests have already been carried out with such a system and with a few improvements in the apparatus, including a more accurately machined capillary tube, it is hoped to make precise measurements on stopping powers.

number of α-particles detected per unit time against the air pressure is usually made. The pressure required to cut off 50% of the α-particles is found and the thickness of air between the source and counter at this pressure is expressed in terms of standard air i.e. dry air at 15°C and a pressure of 76.0 cm. Hg. Another measurement is made with the absorber absent and the difference in the air thickness found is the air equivalent of the absorber.

A variable pressure apparatus of this type was built for the present investigation and several months were spent on its construction. It was found unsuitable however. Although evaporation losses from the mica-agar sandwiches used were made negligible by sealing the air gaps in the brass holder with a stiff grease, it was found occasionally that the layer of agar gel at the centre of the aperture of the brass holder increased in thickness when the air pressure was lowered. As an effect of this kind made exact measurement of the thickness of the agar gel during the α-particle measurements extremely difficult, the experiment was abandoned.

Instead it was decided to carry out the measurements of air equivalents with the mica-agar sandwich at atmospheric pressure and employ a system in which a movable source was used so that the distance between the counter and source was variable. Before

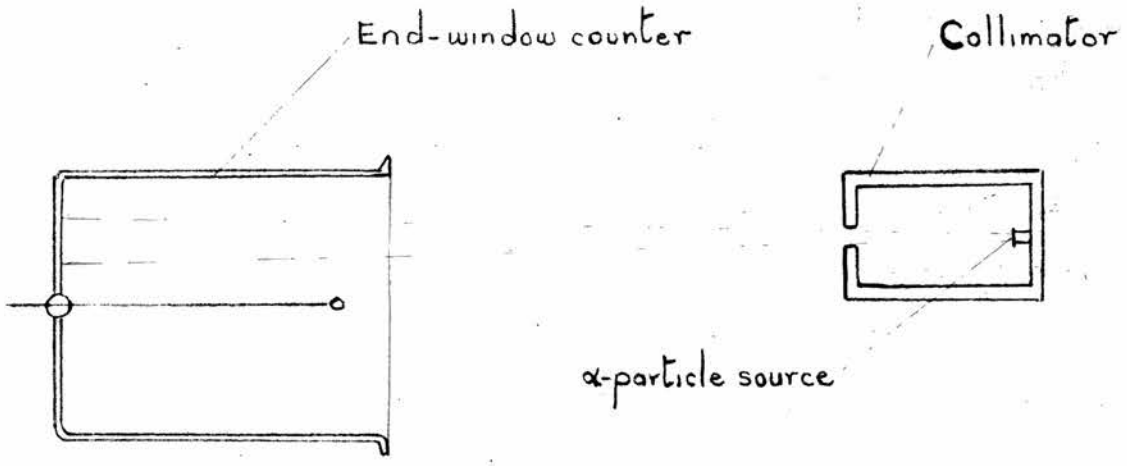
End-window counter
Collimator
α-particle source

FIG. 11

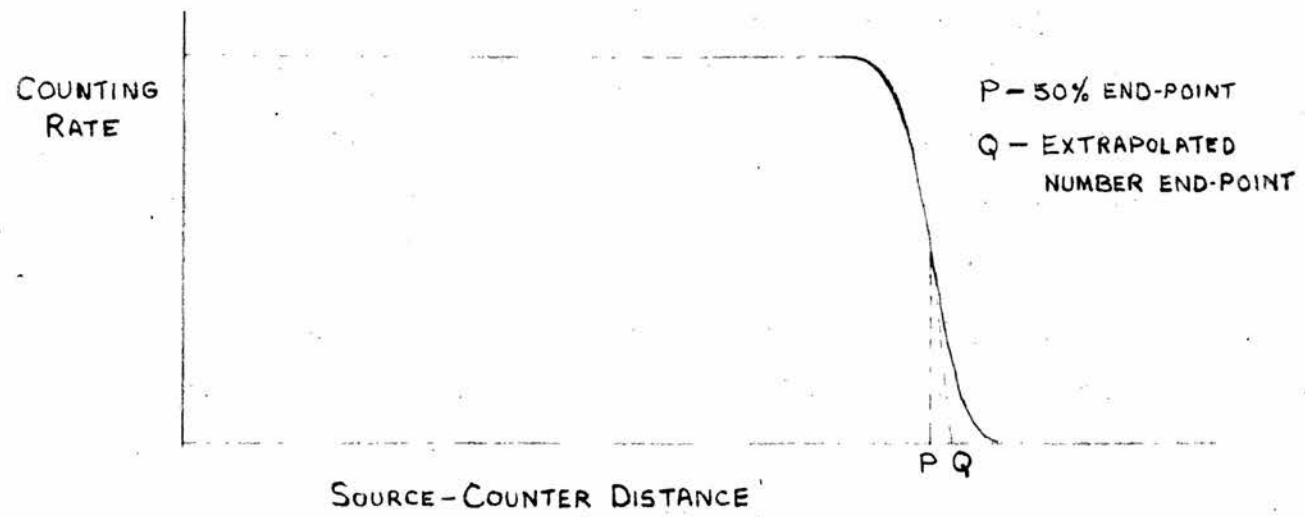
COUNTING RATE
P – 50% END-POINT
Q – EXTRAPOLATED NUMBER END-POINT
P Q
SOURCE – COUNTER DISTANCE

FIG. 12

considering the actual system used it is convenient to discuss briefly a simpler system. In this an α-particle source (Fig. 11) is fitted with a collimating system so that a fine cone of α-particles impinges on the end-window of a counter. If the distance between the source and counter is varied and the counting rate determined, then a number : distance curve of the conventional shape (Fig. 12) will be obtained. If an absorber is placed between the counter and source and a second number : distance curve is determined then the air equivalent is given by finding the spacing between the final parts of the curves, a correction being applied to give standard air conditions. Either the 50% end-point, the point at which the counting rate falls to half its initial value, or the extrapolated number end-point, the point at which the steepest tangent to the number : distance curve cuts the horizontal axis, may be used to find the spacing as long as the curves are of the same shape.

In the actual experimental system (Fig. 13) a counter with a small aperture was used with an uncollimated source, the counter having been constructed for the variable-pressure apparatus. The number : distance curve for such a system for the region where the distance between source and counter is large compared with the aperture of the counter

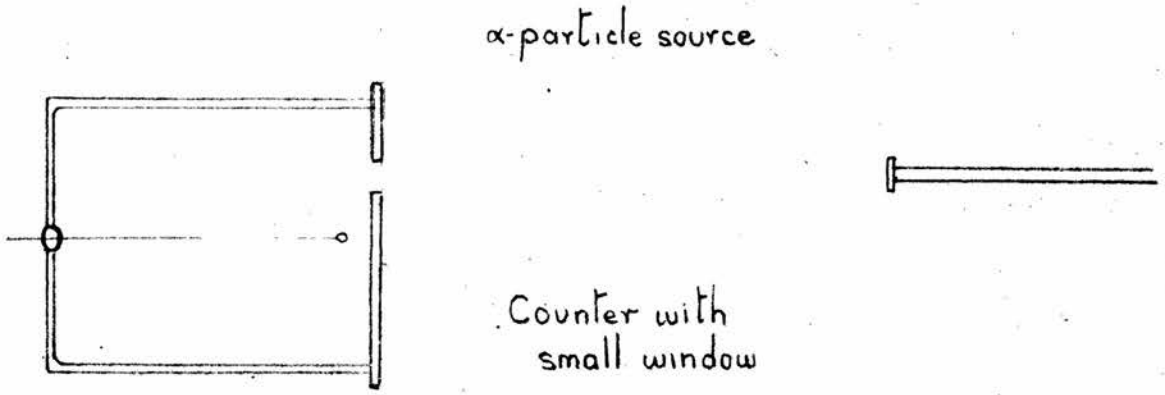
α-particle source
Counter with
small window

FIG. 13

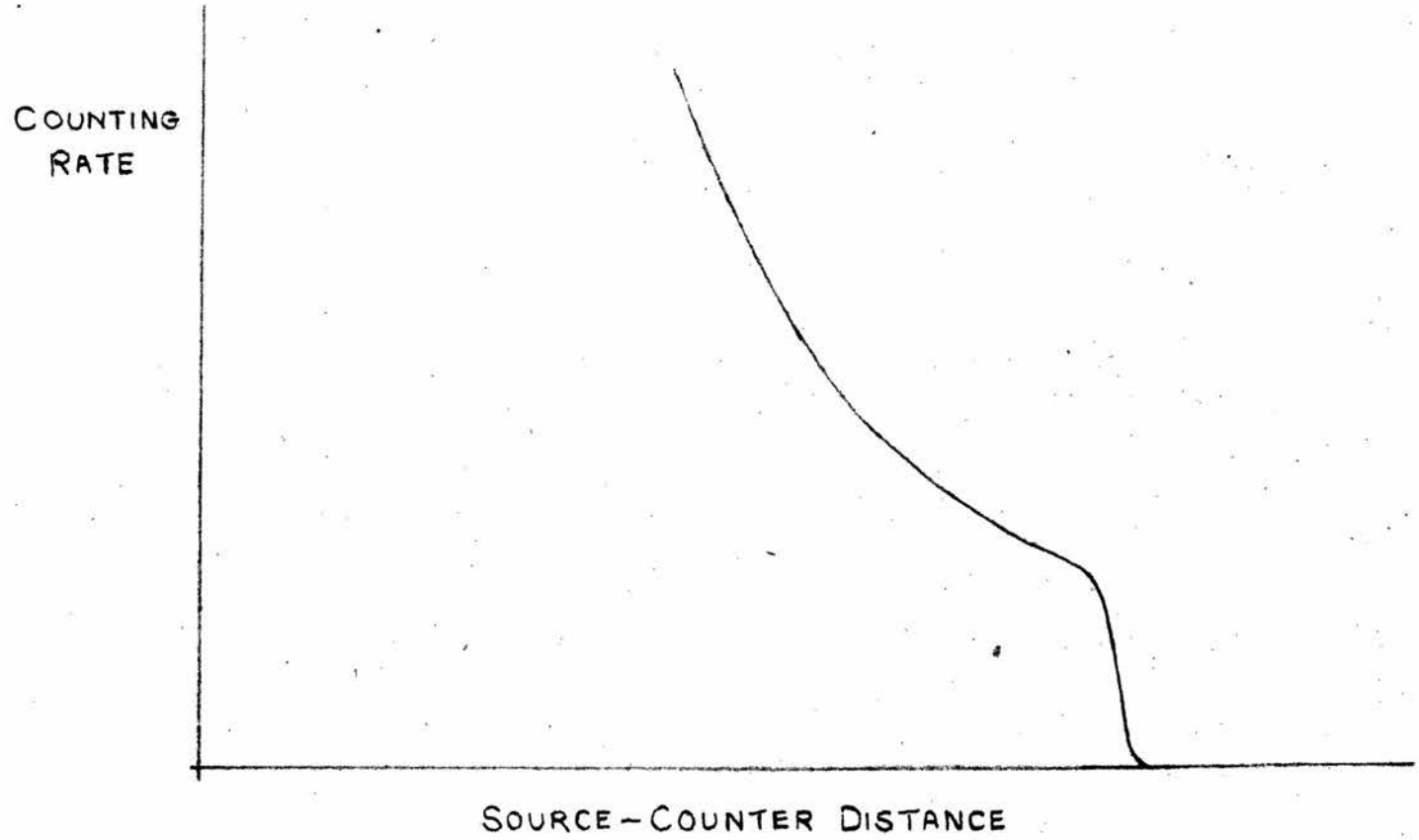
COUNTING
RATE
SOURCE – COUNTER DISTANCE

FIG. 14

and the width of the source is an inverse square curve with a final steep portion (Fig. 14). If, however, the number of α-particles detected per unit time for a given spacing of counter and source is expressed as a percentage of that which would be detected if no air layer were present between the source and counter, then a curve will be obtained of the same shape as the conventional number : distance curve. For convenience this kind of curve will be called a percentage number : distance curve. The percentage number of α-particles detected per unit time may be found by geometrical considerations, since, with no air present and for distances large compared with the aperture of the counter and the width of the source, the counting rate will be inversely proportional to the square of the distance between the counter and source. When an absorber is present, the percentage number may also be found by measuring the counting rate with and without the absorber present. This latter method was usually employed with a slight modification. If a button coated with thorium active deposit is used as a source of ThC' α-particles of energy 8.78 MeV, α-particles of energies below 6.08 MeV are also present. The percentage number of α-particles of energy 8.78 MeV may still be found by carrying out readings of counting rate first with the absorber

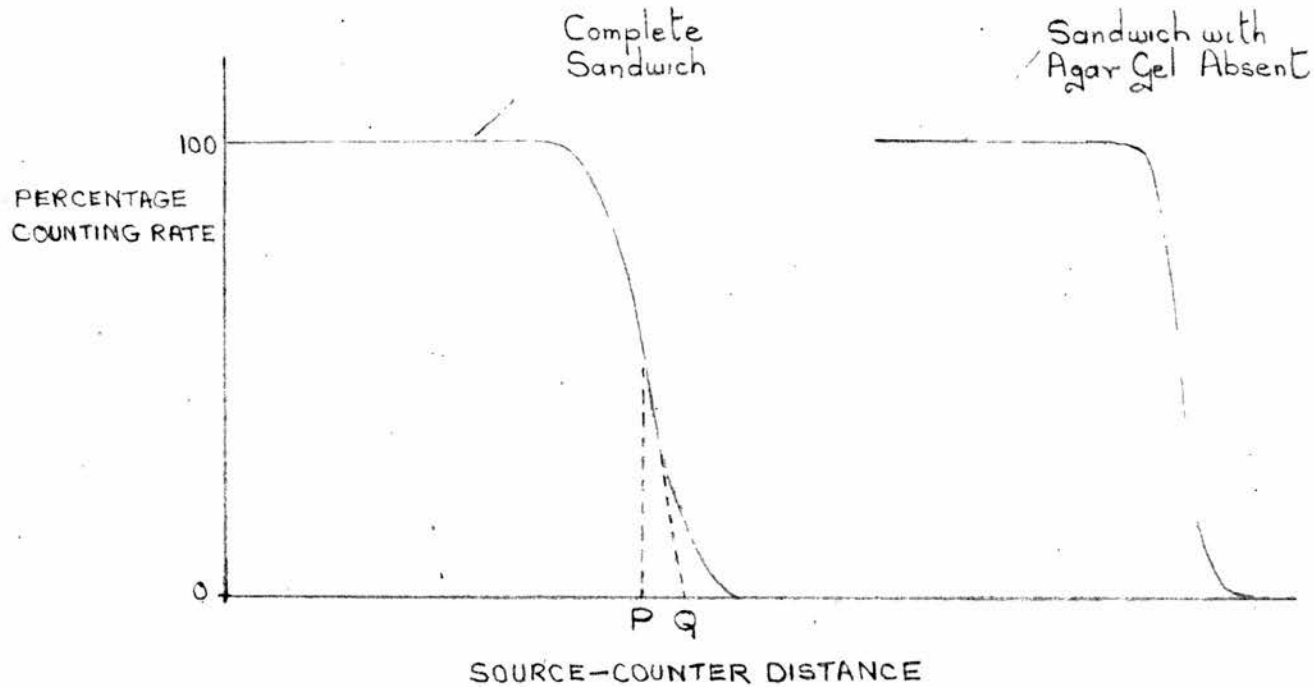

FIG. 15. Theoretical curves showing effect of non-uniformity of layer of agar gel in mica-agar sandwich.

under test and secondly with an absorber which is thinner but still sufficiently thick to screen off the α-particles of lower energy.

The method of determining the air equivalent of a layer of agar gel in a mica-agar sandwich consists then of finding the percentage number : distance curves for the sandwich with and without the agar present. If the curves obtained are of the same shape then it is immaterial whether the 50% end-points or the extrapolated number end-points are used in finding the air equivalent of the layer of agar gel. If on the other hand the layer of agar gel is not perfectly uniform over the region traversed by the α-particles while the layers of mica are, dissimilar curves will be obtained. If the variation in thickness is Gaussian a pair of curves as in Fig. 15 will be found with the curve for the complete sandwich having a final portion of less steepness. In this case the 50% end-points should be used to derive the air equivalent of the agar layer. Use of the extrapolated number end-points will lead to an underestimate. The distance PQ, the difference between the 50% end-point and the extrapolated number end-point, depends on the uniformity of the layer of agar gel. If the variance in range of the α-particle beam produced by this effect is σ_1^2 and that due to other causes such as ordinary straggling,

defects in the source and oblique traversal of the absorbing media by the α-particles is σ_2^2, then the total variance is

$$\sigma^2 = \sigma_1^2 + \sigma_2^2 \qquad (4).$$

The intercept PQ is then equal to $\sigma\sqrt{\frac{\pi}{2}}$. In the experiments only sandwiches giving a value of PQ less than double the standard value for ThC' α-particles in air were used. According to Bethe and Ashkin (14) this standard value is 0.11 cm.

So far the question of the effect of the variation in stopping power of mica with α-particle energy has not been discussed. In the measurement of the percentage number : distance curve for the empty sandwich, the mica covers should at the 50% end-point be traversed by α-particles of the same energy as in the measurement on the complete sandwich. Fortunately the variation in stopping power of mica with α-particle energy is small, a measurement of this being described later, and it is thus permissible to measure the percentage number : distance curve with the sandwich covers close together at the same position as the complete sandwich and apply a small correction to the air equivalent of the layer of agar gel derived using this curve to give the true air equivalent.

In compensation for the laboriousness of the above method compared with the method in which a

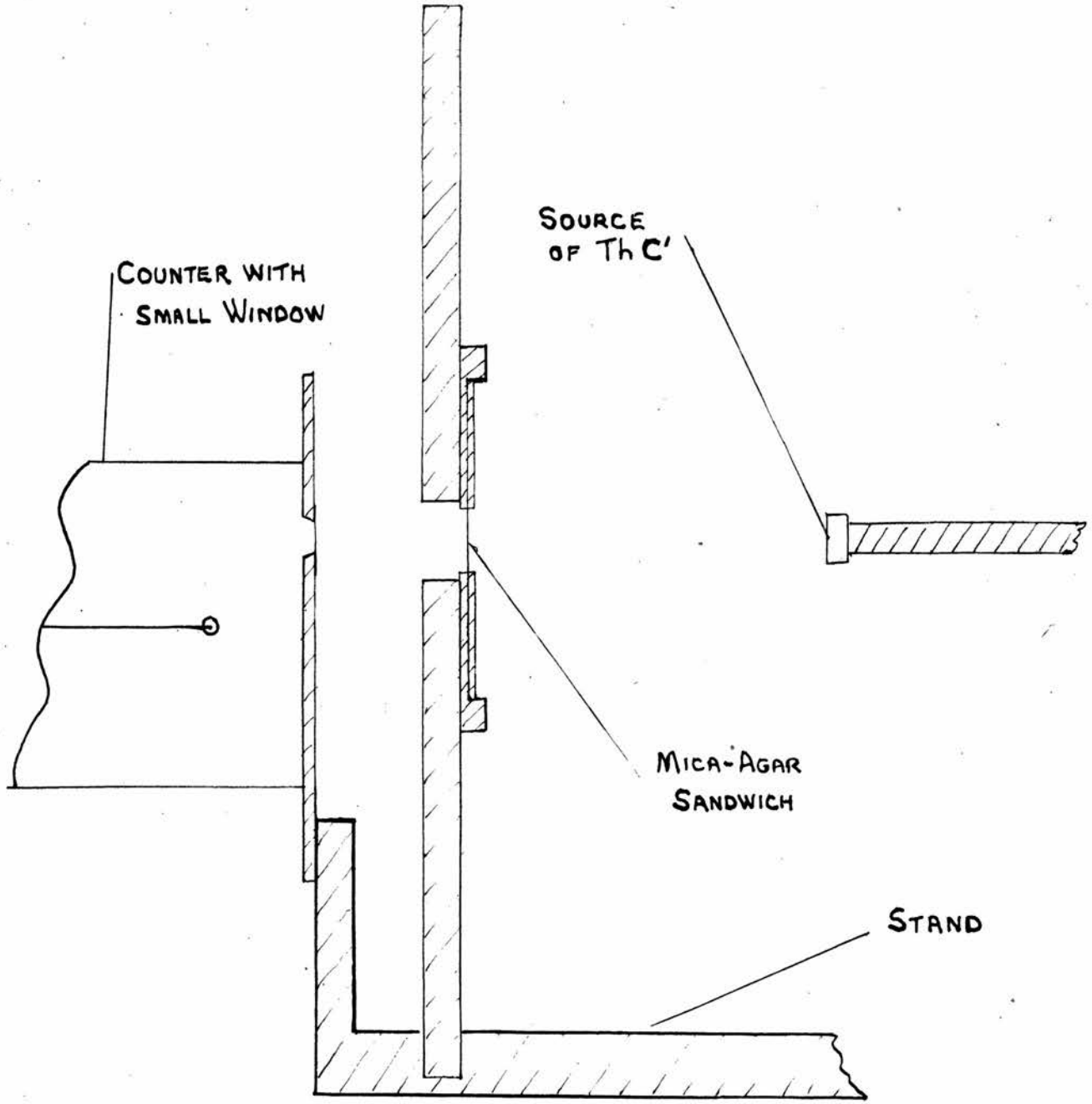

FIG. 16. Schematic diagram of variable distance apparatus.

collimated source and counter of large aperture is used, there is one advantage for the present problem in that it allows a smaller spacing between the source and the mica-agar sandwich to be used and thus permits measurements at higher α-particle energies.

Variable Distance Apparatus.

In the apparatus used, which will be referred to as the variable distance apparatus, a small counting stand of conventional design was employed (Fig. 16). A proportional counter with a window of 2.1 mm. diameter covered with thin mica was mounted with the centre of the window accurately set along the longitudinal axis of the system. The brass holder carrying the mica-agar sandwich was mounted on a brass plate with a central aperture of 6.0 mm. diameter, so that when the plate was inserted in a closely-fitting slot on the stand the centre of the mica-agar sandwich was accurately set on the longitudinal axis of the system and was at a distance of 1.23 cm. from the counter window. The source of thorium active deposit, 3.5 mm. in diameter, was mounted on a thick brass rod on the axis of the system and the rod was attached to a travelling microscope stand so that the distance of the source from the counter window could be varied and accurately

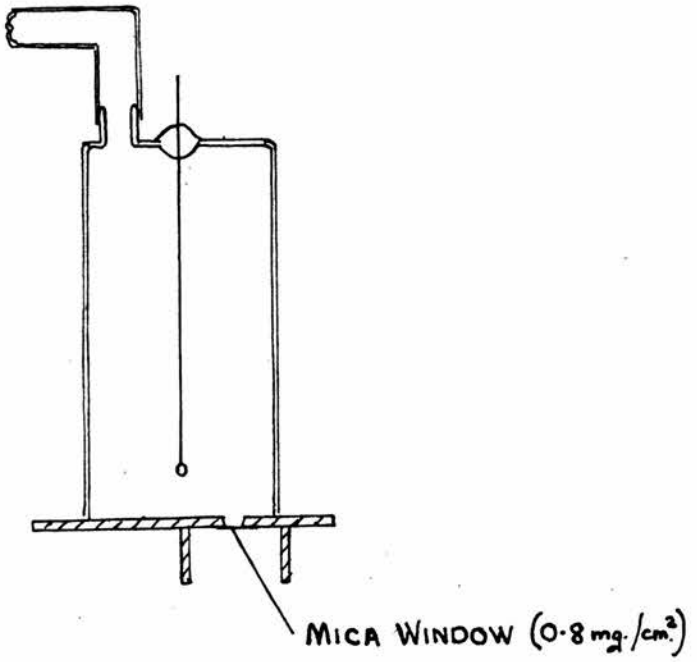

FIG. 17. Counter used in variable distance apparatus.

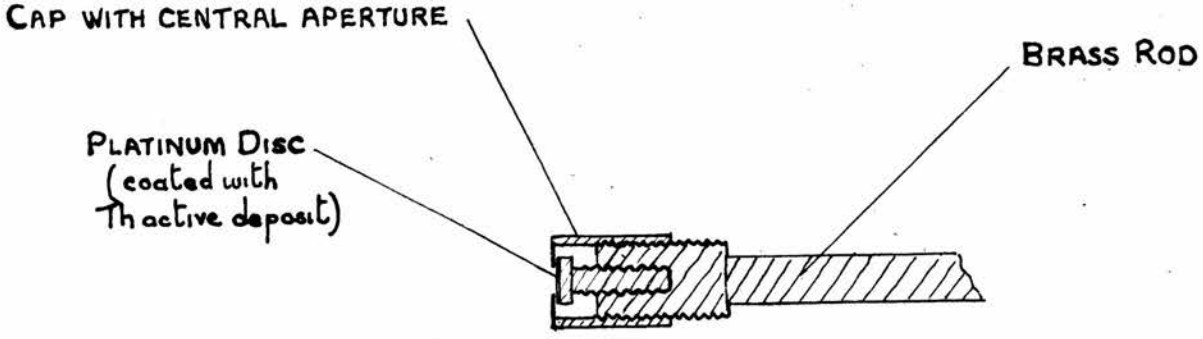

FIG. 18. Source used in variable distance apparatus.

measured. The brass plate carrying the mica-agar sandwich could be withdrawn and replaced by a similar plate carrying a mica absorber of air equivalent 1.6 cm. less than the sandwich under measurement, thus allowing the percentage number : distance curve to be measured.

Counter.

The counter (Fig. 17) was originally designed for a variable pressure system where a small thin window was required which could withstand a change in external pressure of one atmosphere. It was constructed from a defunct GM2 tube. The usual base was replaced by a thick brass base of 1.0 mm. thickness, which had a small aperture of 2.1 mm. diameter at a distance of 0.70 cm. from the axis of the tube. The lead filling stem at the top of the tube was fitted with a glass extension so that the counter could be readily attached to a filling line and sealed off after filling.

The aperture in the brass base of the counter was covered with very thin mica, which was sealed to the brass with Picein wax. Some difficulty was experienced in finding a suitably thin piece of mica which could withstand a change in external pressure of one atmosphere but success was eventually achieved and the final window is still in good order after

undergoing about two hundred reversals of external pressure of the order of one atmosphere. The window was 0.8 mg./cm.^{2} thick, being measured with the β-ray thickness gauge. A small cylinder was fitted to the base near the window so that a protective cap could be fitted when the counter was not in use. The counter filling was 6.6 cm. Hg of argon and 0.8 cm. Hg methyl alcohol.

The counter was used both as a Geiger-Muller counter and as a proportional counter. Its characteristic curve in the Geiger-Muller region was satisfactory, giving a plateau of 140 volts along which the slope was 0.05% per volt. The working voltage used was 1120 volts. When used as a proportional counter with a supply of 920 volts, a Type 200 power unit was used and the output pulses, after being amplified with a 1008B amplifier set at 26 db. attenuation of full amplification, were fed to a 1009B scaling unit where the discriminator was set at 5 volts. The tests on the proportional counter system are described later (p.108).

Source.

The source (Fig. 18) was a platinum disc soldered on top of a 4 B.A. screw. The disc was activated with thorium active deposit by exposing it in a conventional thorium pot. After activation

PRODUCTS FORMED IN THORIUM ACTIVE DEPOSIT

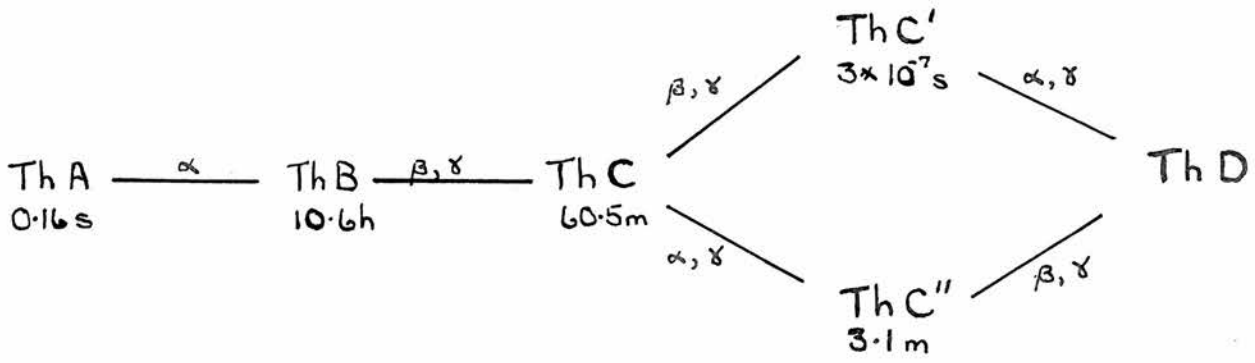

Apart from a very small amount of long range α-particles Th C' emits only α-particles of energy 8·78 MeV. Predominant α-particle groups from Th C are at 6·08 MeV (70%) and 6·04 (27%) with a small amount of lower energy.

FIG. 19

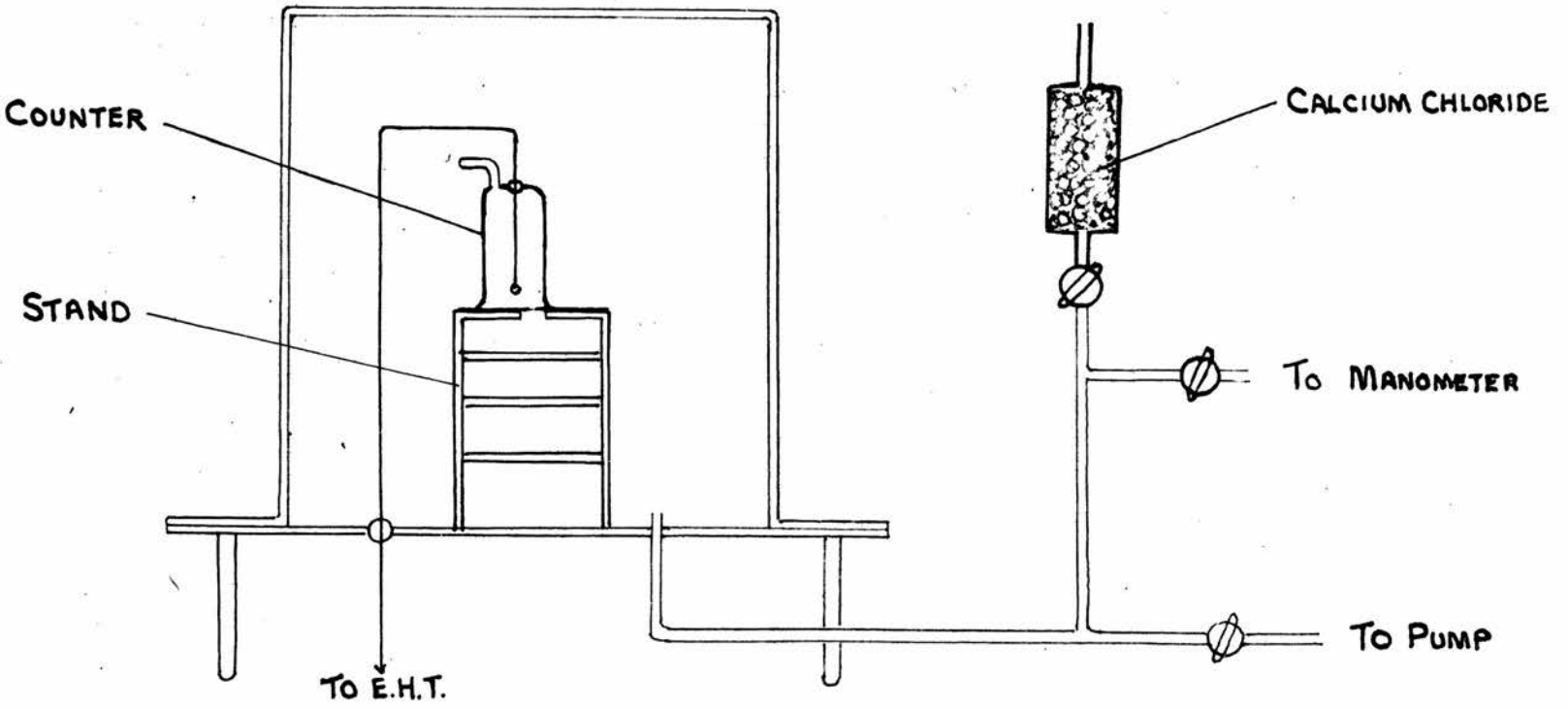

FIG. 20. Schematic diagram of variable pressure apparatus.

the screw was fitted in a thick brass rod and to cut off α-particles from the edges of the disc, a small cap with an aperture of 3.5 mm. was fitted over the screw. The α-particles used were those from ThC' which are of energy 8.78 MeV but there were also present a group of energy below 6.08 MeV due to ThC. As will be seen from the disintegration scheme for thorium active deposit, the decay in specific activity of ThC' is controlled by the half-lives of ThB and ThC and the time of activation of the source. The brass rod carrying the source was fitted to a travelling microscope stand equipped with a vernier device so that distances could be measured to 0.02 mm.

Variable Pressure Apparatus.

The variable pressure apparatus (Fig. 20), although originally designed for the main problem, was eventually employed for secondary purposes such as determining the variation in stopping power of mica with α-particle energy and testing the detector system used in the variable distance apparatus. It consisted of a small counter stand with the counter described above mounted on top. The stand was fitted with shelves so that various absorbers and sources could be placed at fixed distances from the counter. The counter stand was mounted in a large

brass chamber with a removable top, the chamber being connected to a filling line so that it could be filled with dry air at any desired pressure. A manometer was fitted to the filling line to read the difference between the chamber pressure and the external pressure.

Preliminary Tests.

The variable pressure system was used to test the general equipment. In some of these tests a small polonium source was used, the polonium being electrodeposited a few weeks before the tests on the centre of a small platinum disc. The minimum range of α-particle required for detection by the counter was measured for both types of operation i.e. in the Geiger-Muller and proportional counter regions. Counting rate : pressure curves were determined for both types of operation and compared. A determination of the variation in stopping power of mica with α-particle energy was also made.

In the first experiment with the counter used in the Geiger-Muller region the air thickness required to cut off 50% of the polonium α-particles was measured for two different spacings of source and counter, namely 4.407 cm. and 6.422 cm. There was a small detectable slope of the counting rate : pressure curves over the theoretically flat portion

FIG. 21. Comparison of counting rate : pressure curves for variable pressure system with Po source when counter used as (a) a Geiger-Muller counter and (b) a proportional counter.

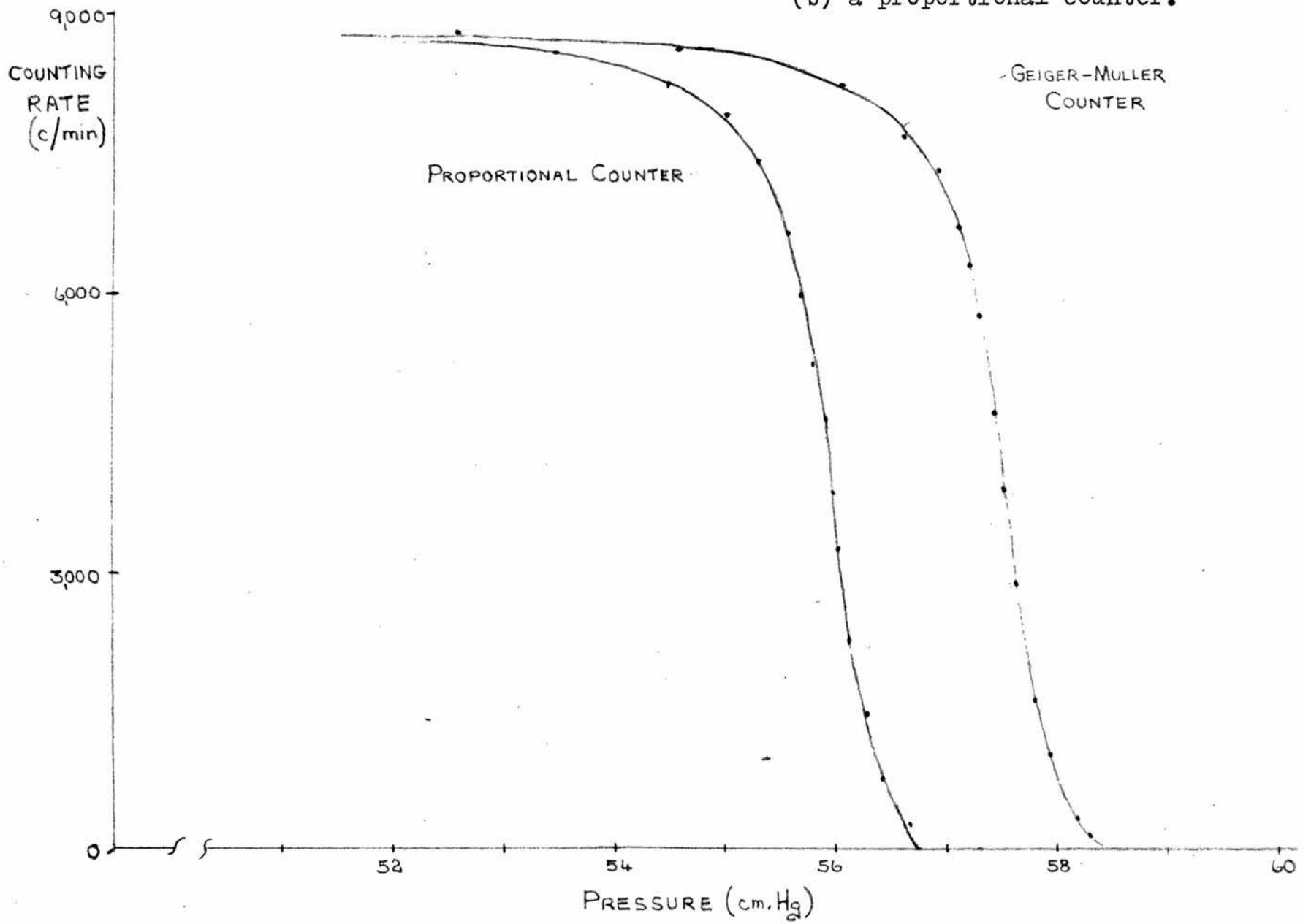

and the 50% end-point was taken as half-way down the final steep portion. The air thicknesses found agreed to within 0.2%, giving a mean of 3.25 cm. Using the mean range for Po α-particles found by Holloway and Livingston (16) of 3.842 cm. it was concluded that only α-particles of range greater than 0.59 cm. on entering the counter were detected.

Next the counting rate : pressure curves were measured with the Po source at a distance of 4.407 cm. from the counter when the counter was used first in the Geiger-Muller region and then as a proportional counter with the fixed settings of the equipment mentioned. Similar curves were obtained (Fig. 21) but there was a spacing between the curves corresponding to an air thickness of 1.7_4 mm. of standard air indicating that with the proportional counter an α-particle required to spend at least the final 1.7_4 mm. of its range in the counting volume of the counter to ensure detection. From the previous result it was concluded that an α-particle of range greater than 0.76 cm. on reaching the window of the proportional counter was detected.

The counting rate : pressure curve was then determined for a source of thorium active deposit. The source was placed at 5.0 cm. from the counter and was covered by a mica screen of about 4.0 cm. air equivalent. A similar curve to that for a Po source

FIG. 22. Counting rate ; pressure curve obtained with ThC' source in variable pressure system.

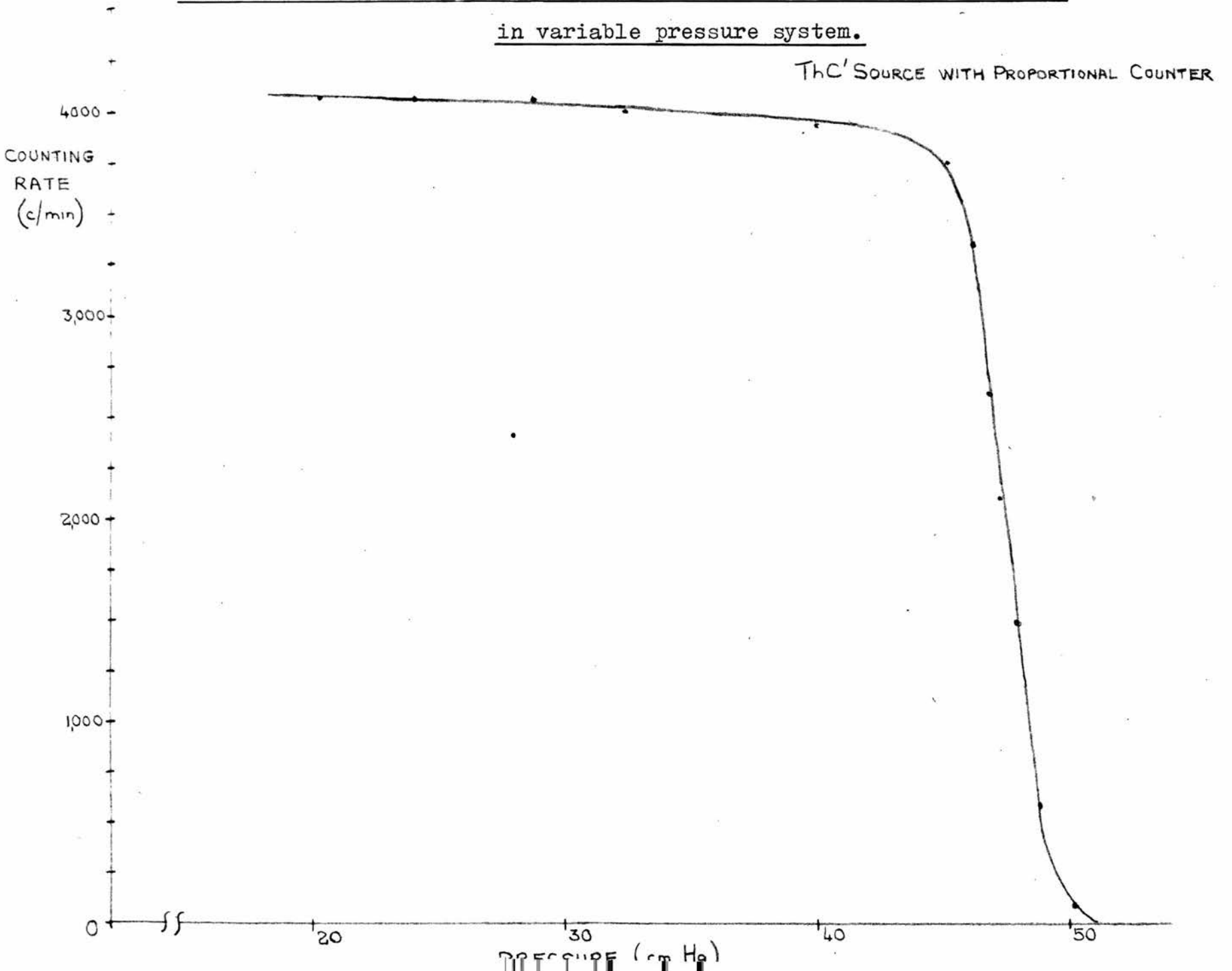

TABLE 4

VARIATION OF STOPPING POWER OF MICA WITH ALPHA-PARTICLE ENERGY.

Thickness of Mica = 1.88 mg./cm.^{2}

Air Equivalent at Mean Energy of 7.7 MeV = 1.36 cm.

Shelf	Energy of Alpha-Particle MeV			Decrease in Air Equivalent cm.	Stopping Power relative to that at 7.7 MeV
	Entry	Exit	Mean		
1	4.70	3.30	4.00	0.034	0.975
2	6.10	4.90	5.50	0.014	0.990
3	7.30	6.25	6.77	0.008	0.994
4	8.20	7.25	7.72	-	1.000

was found with a final portion of smaller steepness (Fig. 22). Again the theoretically flat portion was found to have a slight slope.

Apart from the slight slope in the theoretically flat portion of the counting rate : pressure curves it was concluded from the tests that the proportional counter system and the ThC' sources were satisfactory and could be used with confidence in the variable distance apparatus.

The variation in the stopping power of Bengal Ruby mica with α-particle energy was next measured with the variable pressure system. A thin sheet of mica, 1.87 mg./cm.^{2}, was placed in turn on four different shelves above a fixed source of ThC' and the displacements in the final parts of the counting rate : pressure curves were used to find the difference in air equivalent of the mica in the four positions. The actual air equivalent in any position was found from the known mean range of ThC' α-particles and the measured 50% end-points of the counting rate : pressure curves. The ranges of the α-particles on entering and leaving the mica were calculated and the mean energy of traversal found. The results (Table 4) indicate that there is little variation in stopping power with α-particle energy in the region of interest and that the simplification in the final method mentioned above (p.102) is permissible. The

experimental results of Bennett (2) though not extending to the lowest energy of α-particle used here, are in good agreement with the present results.

Preliminary Measurements with Variable Distance Apparatus.

In early measurements with the variable distance system using various absorbers and sources, it was found that a percentage number : distance curve was found of the expected type. However there was a slight slope in the theoretically flat portion which amounted to about 2.5% per cm. in the region just before the final steep slope. The slope decreased with distance from the final portion. A slight slope of this nature may result from several causes. There will always be a slight slope due to the back-scattering of α-particles from the source mounting. Defects in the source producing deviations from the ideal thin source will also tend to produce such an effect and a defect in the counter window such as an increase in thickness near the rim may play a part. In addition there must always be a decrease due to the scattering of α-particles from the narrow cone employed.

An effect of this nature in a variable distance apparatus of the present type is not serious. The theoretical 50% end-point of the percentage number :

distance curve is given by the point half-way down the final steep portion. There is a slight uncertainty, about 2%, in finding this point as the slope of the theoretically flat portion changes, but the effect is of no significance in determining the air equivalent of a layer of agar gel of the order of 2.0 cm. air equivalent.

To check that the apparatus was working satisfactorily a preliminary measurement was made of the difference in range of the α-particles from Po and ThC'. The apparatus was not enclosed and the air may have been slightly different from standard dry air but, from the general climatic conditions in the laboratory, it was assumed that the water vapour content of the air was negligible. Percentage number : distance curves were determined for both sources. The percentage number of α-particles detected per unit time was determined by multiplying each determination of counting rate by the square of the distance from the source to the counter, taking a reading 1.0 cm. from the final steep portion as 100%. Readings were made only of the last 1.4 cm. of the curve for the Po source and for the last 2.5 cm. of the ThC' curve. The points half-way down the final steep portion were taken as the theoretical 50% end-points. It was found that when the readings were corrected to standard air conditions the 50% end-

point for the Po source was 3.08 cm., agreeing perfectly with the previous determination made with the variable-pressure apparatus. For the ThC' source the 50% end-point was 7.79 cm., giving a difference in mean range of the two α-particles of 4.71 cm. The difference in mean range according to the data given by Holloway and Livingston (15) is 4.73 cm. It was concluded from the good agreement that the apparatus was functioning satisfactorily. Throughout the measurements, checks were made on the 50% end-point for ThC' α-particles. It was sometimes impossible to make a check on the actual sources used to measure the mica-agar sandwiches as the sources were too weak for the large distances used in the determination of the 50% end-point for the source alone. The measurements made however did not differ by more than $\pm$ 0.5% from the value found above.

Measurements of Stopping Power of Water.

In the final measurements of the stopping power of the agar gel, ten separate measurements were made. Mica-agar sandwiches were used with matched mica covers ranging from 1.65 to 2.3 mg./cm.^{2} and with layers of agar gel ranging from 1.9 to 3.7 mg./cm.^{2}.

The procedure in each experiment was first to measure the thicknesses of two large mica sheets with

FIG. 23. Percentage number : distance curves for sandwich with and without agar gel present.

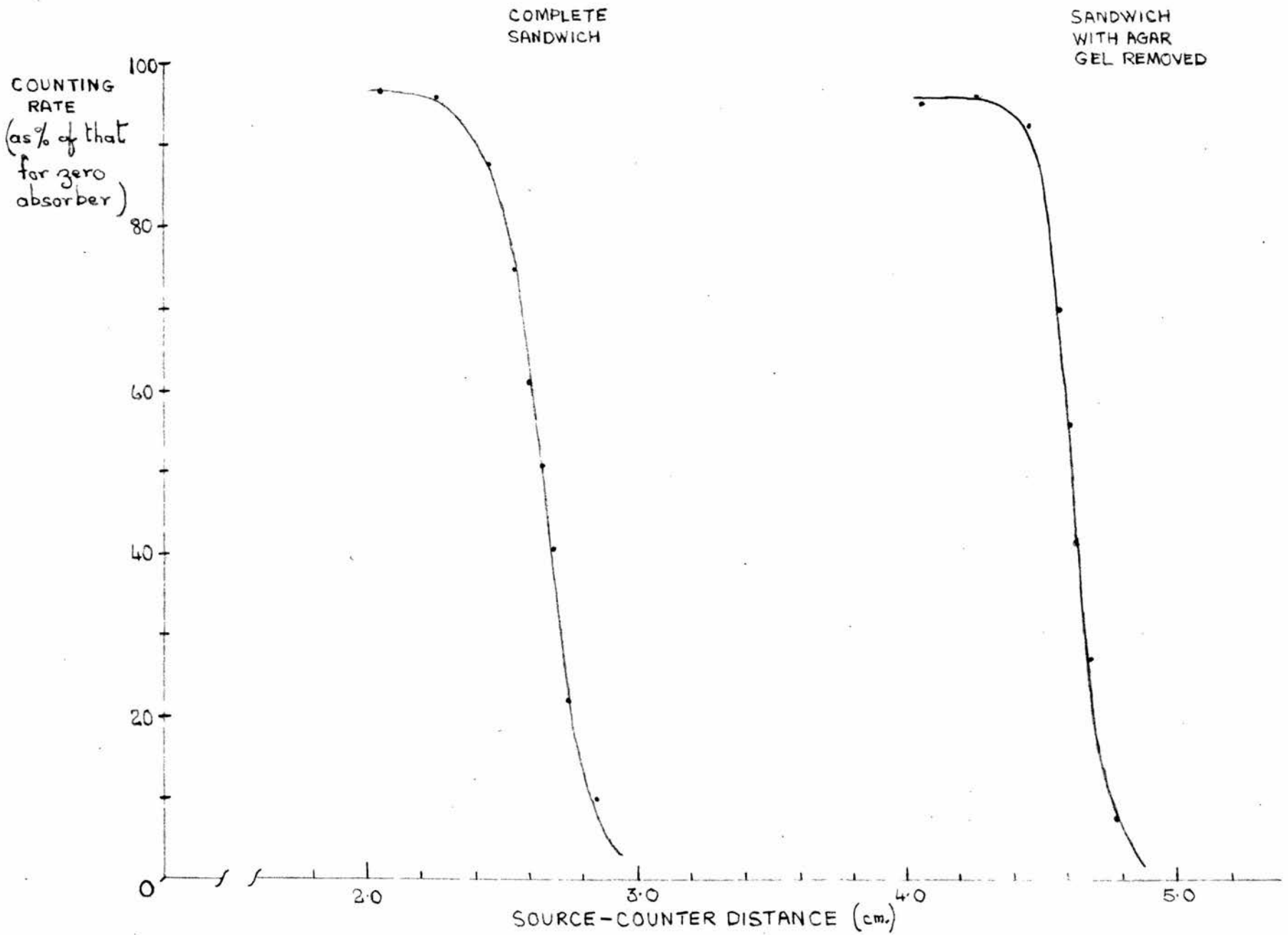

the β-ray thickness gauge. If the sheets were of equal and suitable thickness, they were used to make a large sheet of mica-agar sandwich. This was tested over the central region with the thickness gauge and if it was of suitable thickness, a small portion approximately 1.5 x 1.5 cm. in area was cut out and inserted in the brass holder. The holder was then placed on the specimen plate of the gauge and the counting rate determined.

The holder was next placed on the brass plate used in the variable distance apparatus. A quick determination was made of the approximate 50% end-point, the rough air equivalent was found and a second brass plate was fitted with a mica absorber of air equivalent approximately 1.6 cm. less than the mica-agar sandwich. An accurate determination of the 50% end-point followed in which alternate readings were taken with the two plates and the percentage number : distance curve was drawn. One advantage of this method compared with the method in which the percentage counting rate is found by geometrical considerations is that corrections for decay of the activity of the source become negligible. It will be seen from one of the experimental curves (Fig. 23) that the "horizontal" portion was at 96% indicating a slope of 2.5% per cm. near the last part of the curve. If the distance between the 50% end-

point and the extrapolated numbers end-point exceeded 2.0 mm. the experiment was abandoned and a new sandwich made. About one in three sandwiches were rejected on this score. At the end of the determination of the percentage number : distance curve, the holder containing the sandwich was transferred to the specimen plate of the thickness gauge and the counting rate determined. This reading was sometimes less than the previous reading, corrected for variations in the zero-absorber reading of the gauge, but the decrease on the average corresponded to a decrease in thickness of the agar gel layer of less than 2%. The mean of the two readings was taken as that corresponding to the time of measurement of the 50% end-point.

Next the top plate of the holder was gently prised up to open the sandwich. The fragments of agar gel adhering to the mica covers were wiped off with a piece of filter paper and the covers were dried under a lamp to remove traces of moisture. The top plate was then replaced in the holder to form an empty sandwich and the measurements detailed above were repeated for this. A reading on the β-ray thickness gauge was made before and after a determination of the 50% end-point.

The readings of the β-ray thickness gauge for the empty and complete sandwiches, duly corrected for

any shift in the zero-absorber counting rate, were used to derive the thickness of the agar gel layer, the calibration curve for polythene being employed. A correction was made where the covers differed significantly from 2.0 mg./cm.^{2}.

The temperature and pressure of the air were separately measured for the two determinations of the 50% end-point, and the latter were corrected to give the values in standard air i.e. at a temperature of 15°C and a pressure of 76.0 cm. Hg. The difference in the two end-points was taken as the air equivalent of the layer of agar gel, after a few minor corrections were made.

The first correction was that for the variation in stopping power of mica with α-particle energy. A correction was made in the 50% end-point for the empty sandwich to give the 50% end-point obtained with mica covers traversed by α-particles of the same energy as in the determination for the complete sandwich. The correction required was small and caused a change in the air equivalent of the agar layer by amounts varying from 0.3 to 0.6% in the ten measurements made. The next correction was for the water vapour content of the air. At a relative humidity of 100% at a temperature of 24°C, the temperature at which most of the experiments were carried out, the decrease in stopping power of 1 cm.

of air compared with 1 cm. of dry air is 0.7%. As no measurements were made of the relative humidity of the air, it was decided to assume 50% relative humidity and make the appropriate correction.

The effect of oblique traversal of the mica-agar sandwich was considered. For the closest spacing of counter and source employed namely 2.0 cm., a calculation of the average increase in path length in the sandwich shows that it is 0.2% greater than for traversal at 90°. The 50% end-point for the complete sandwich was corrected for this effect. The maximum correction in the air equivalent of the agar layer on this account was 0.5%. Finally the displacement of air by the sandwich required a correction of 0.1% in the air equivalent of the agar layer.

The air equivalent of the layer of agar gel, corrected for these effects, and the measured mass thickness were used to find the stopping factor f for the agar gel i.e. the thickness of agar gel in mg./cm.^{2} equivalent to 1 cm. of standard air. At an α-particle energy of 6 MeV the stopping factor for an agar gel containing 2.5% of agar is 0.075% greater than the stopping factor for pure water, assuming no anomaly in the stopping power of liquid water. Even with a supposed anomaly for liquid water of 15%, the difference in stopping factors is

0.45%. It follows that there is negligible error in taking the two stopping factors as equal.

The molecular stopping of liquid water i.e. the stopping power of one molecule relative to that of the average atom of standard air is

$$s = \frac{1000dM}{fA_o} \qquad (5)$$

where d is the density of standard air (1.226×10^{-3} gm./cc.), M is the molecular weight of water, and A is the atomic weight of the average atom of air (14.56). This equation was used to find the molecular stopping power of liquid water.

The energy of the α-particles on entering and leaving the layer of agar gel was worked out from the known range of ThC' α-particles in air and the mean energy of traversal was calculated.

As a check on the measurement of stopping power for liquid water, the 50% end-point of the empty sandwich was used to find the stopping factor for mica i.e. the thickness in mg./cm.^{2} equivalent to 1 cm. of air. The actual 50% end-point for the ThC' source with only air between the source and counter was not always measured, but the mean of the determinations made was used in those experiments where the source was too weak to make a separate determination.

TABLE 5

STOPPING POWER OF LIQUID WATER.

EXPT	THICKNESS OF SINGLE MICA COVER mg./cm²	THICKNESS OF AGAR GEL mg./cm²	AIR EQUIVALENT OF AGAR GEL cm.	STOPPING FACTOR mg./cm² of agar gel equivalent to 1 cm. of air	MOLECULAR STOPPING POWER OF WATER	ALPHA-PARTICLE ENERGY IN AGAR GEL MeV		
						ENTRY	EXIT	MEAN
1	1.65	2.87	2.745	1.046	1.45	6.95	4.65	5.80
2	1.65	3.71	3.590	1.034	1.47	7.55	4.65	6.10
3	1.69	2.13	2.095	1.017	1.49	6.50	4.70	5.60
4	2.28	1.91	1.880	1.016	1.49	6.65	5.05	5.85
5	2.00	2.40	2.300	1.043	1.46	6.80	4.90	5.85
6	2.23	2.07	2.000	1.035	1.47	6.70	5.00	5.85
7	1.77	3.36	3.295	1.020	1.49	7.40	4.70	6.05
8	1.71	3.15	3.030	1.040	1.46	7.20	4.70	5.95
9	1.88	3.10	3.040	1.020	1.49	7.25	4.80	6.02
10	1.93	2.49	2.370	1.051	1.44	6.80	4.85	5.82
Mean Values					1.47			5.89

Results.

The results of all ten experiments are displayed in Table 5. The values deduced for the molecular stopping power of liquid water show very little variation. The mean energies of traversal of the α-particles are all fairly close to the mean value of 5.9 MeV although there is a large variation in the entry and exit energies for the various sandwiches.

The mean value of the molecular stopping power of liquid water is 1.47 at a mean α-particle energy of 5.9 MeV. In assessing the error in this determination, it appears that the main source of error may lie in the measurements of thickness with the β-ray thickness gauge. Use of the calibration curve for polythene may produce an error of $\pm$ 3%. The individual measurements of stopping power show very little variation from their mean and an allowance of 1% appears adequate to cover the possibility of systematic errors in the determination of air equivalents. It may be added that use of the extrapolated number end-point instead of the 50% end-point in the determination of air equivalents reduces the mean value of stopping power by 2.0%.

It is concluded that the experimental error in the determination is 3.5% and that therefore the stopping power of one molecule of liquid water

TABLE 6

STOPPING POWER OF MICA.

Experiment	Mica Thickness mg./cm.^{2}	Air Equivalent cm.	Stopping Factor mg./cm.^{2} equivalent to 1 cm. of air	Alpha-particle Energy MeV		
				Entry	Exit	Mean
1	3.30	2.32	1.42	5.65	3.45	4.55
2	3.30	2.32	1.42	5.65	3.45	4.55
3	3.38	2.39	1.41	5.75	3.45	4.60
4	4.56	3.22	1.42	6.45	3.45	4.95
5	4.00	2.89	1.38	6.15	3.45	4.80
6	4.45	3.14	1.42	6.35	3.40	4.87
7	3.53	2.51	1.41	5.80	3.40	4.60
8	3.41	2.46	1.39	5.75	3.40	4.57
9	3.76	2.64	1.42	5.95	3.40	4.67
10	3.85	2.77	1.39	6.05	3.40	4.72
Mean Values			1.41			4.70

relative to that of the average atom of air at an α-particle energy of 5.9 MeV is

$$\underline{s = 1.47 \pm 0.05} \qquad (6).$$

In Table 6 the determinations made of the stopping power of mica are reported. At a mean energy of traversal of 4.7 MeV the thickness of mica equivalent to 1 cm. of standard air is 1.41 mg./cm.^{2}. From the data given by Bennett (2) the value for Green Madras mica is 1.45 mg./cm.^{2} at the same energy. Bennett found however that there is a variation in stopping power of about $\pm$ 2% among samples of this kind of mica and concluded that there would probably be larger differences among micas of the same general type but of different origins. No significance can therefore be attached to the small difference of 3% in the present value from that given by Bennett. The results given are only a rough check on the functioning of the apparatus, ruling out the possibility of errors greater than 5%. More conclusive evidence is provided by the satisfactory result for the difference in range of the α-particles from ThC' and Po.

Discussion.

In the tables of stopping powers given by Wilkins (16), the values of "differential" stopping powers are based on the semi-theoretical calculations

made by Livingston and Bethe (17), small adjustments being made to cover the corrections suggested by Hirschfelder and Magee (18) and by Warshaw (19). The physical constants used in the calculation are derived from the ranges of various α-particles in the gases. From the tables the atomic stopping power of hydrogen at 5.9 MeV is 0.205 and that of oxygen is 1.056 so that if the Bragg law is valid the molecular stopping power of liquid water at 5.9 MeV is

$$s = 1.47 \pm 0.04 \qquad (7)$$

when an error of 3% is assigned. The value is the same as the present experimental result.

According to Gray (1) from a review of the experimental data on the ranges of α-particles in oxygen and hydrogen, the integral molecular stopping power of liquid water, assuming no departure from the Bragg law is 1.51 for α-particles of energy 5.3 MeV and 1.49 for those of energy 7.7 MeV. A small difference would be expected in the values of the "differential" and integral stopping powers at an α-particle energy of 5.9 MeV, but this is unlikely to exceed $\pm$ 2%. It is concluded that as the above values exceed the experimental value by 3% at most and this lies within the limits of error of the experimental result that there is no evidence for any significant failure of the Bragg law.

Phelps, Heubner and Hutchinson (5) have used the experimental results on stopping powers of various liquid gases and organic compounds for protons at a mean energy of 270 MeV obtained by Thompson (21) and the equation given by Livingston and Bethe with a small correction factor given by Walske (22) to calculate the stopping powers of different atoms at an α-particle energy of 5.9 MeV. They take account of the small effects of chemical binding found by Thompson. If we take the atomic stopping power of a hydrogen atom with a saturated binding in a carbon compound, namely 0.204, and that of an oxygen atom in the liquid gas, 1.075 and use the Bragg law to compute the molecular stopping power of liquid water we find

$$s = 1.48 \pm 0.03 \qquad (8).$$

The excellent agreement with the present experimental result shows that the stopping powers of hydrogen and oxygen atoms are substantially the same in water as in the liquid gases and various solid materials used by Thompson.

It is difficult to reconcile the above experimental result $s = 1.47$ at an α-particle energy of 5.9 MeV with that of 1.71 found by Appleyard (8) at 4.5 MeV unless there is a large increase of stopping power for a fairly small decrease in energy of the α-particle, an event which does not seem very

probable. The present method could possibly be used to investigate the variation in stopping power of liquid water with α-particle energy but the sandwich would require to have much thinner mica covers and a thinner layer of agar gel.

Conclusion.

It is concluded that at an α-particle energy of 5.9 MeV the stopping power of one molecule of liquid water relative to that of the average atom of air is

$$s = 1.47 \pm 0.05.$$

This value is in close agreement with the values derived from the atomic stopping powers of hydrogen and oxygen in the gaseous state and it is concluded that at an α-particle energy of 5.9 MeV the Bragg law is valid to an accuracy of 4% for liquid water.

REFERENCES.

(1) Gray L.H., Proc. Camb. Phil. Soc. 40, 72, (1944).

(2) Bennett W.E., Proc. Roy. Soc. A 155, 419, (1936).

(3) Wilkinson D.H., Proc. Camb. Phil. Soc. 44, 114, (1948).

(4) Ellis R.H. (Jr.), Rossi H.H., and Failla G., Phys. Rev. 86, 562, (1952).

(5) Phelps J., Heubner W.F., and Hutchinson F., Phys. Rev. 95, 441, (1954).

(6) Michl W., Sitzber. Akad. Wiss. Wien Kl. 123, 1965, (1914).

(7) Philipp K., Z. Phys. 17, 23, (1923).

(8) Appleyard R.K., Proc. Camb. Phil. Soc. 47, 443, (1951).

(9) De Carvalho H.G., and Yagoda H., Phys. Rev. 88, 273, (1952).

(10) Ellis R.H. (Jr.), Rossi H.H., and Failla G., Phys. Rev. 97, 1043, (1955).

(11) Förster M., Ann. Phys. Lpz. 27, 373, (1936).

(12) Appleyard R.K., Thesis, Cambridge University, (1949).

(13) Platzman R.L., Symposium on Radiobiology (1952), Chapter 9, (John Wiley and Sons Inc.).

(14) Bethe H.A., and Ashkin J., Experimental Nuclear Physics (1953) Vol. I Part II (J. Wiley and Sons Inc.).

(15) Holloway M.G., and Livingston M.S., Phys. Rev. 54, 18, (1938).

(16) Wilkins J.J., Atomic Energy Research Establishment Report G/R 664 (1951).

(17) Livingston M.S., and Bethe H.A., Rev. Mod. Phys. 9, 261 (1937).

(18) Hirschfelder J.G., and Magee J.L., Phys. Rev. 73, 207, (1948).

(19) Warshaw R., Phys. Rev. 76, 1759, (1949).

(20) Thompson T.J., University of California Radiation Laboratory Report UCRL - 1910, (1952).

(21) Walske M.C., Phys. Rev. 88, 1283, (1952).